Aus der Abteilung für Zahnerhaltung und Präventivzahnmedizin der Charité Centrum 03 für Zahn-, Mund- und Kieferheilkunde, der Medizinischen Fakultät Charité - Universitätsmedizin Berlin

DISSERTATION

Structural characterization of interaction zone between Glass Ionomer Cement and enamel and dentine in human teeth

Strukturelle Charakterisierung der Wechselwirkungszone zwischen Glasionomer Zement und Schmelz und Dentin in menschlichen Zähnen

zur Erlangung des akademischen Grades

Doctor medicinae dentariae (Dr. med. dent.)

vorgelegt der Medizinischen Fakultät

Charité – Universitätsmedizin Berlin

von

Hawshan Abdulrahman Mustafa

aus Kurdistan-Irak

Datum der Promotion: 25.11.2022

Table of Contents

List of Figures

List of Tables

List of Abbreviations

2D	Two dimensions
3D	Three dimensions
Al	Aluminum
Ca	Calcium
CLSM	Confocal laser scanning microscopy
COOH	Carboxylic acid
CPD	Critical point dryer
D	Dentine
E	Enamel
EDJ	Enamel-dentine junction
EDX	Energy dispersive X-ray chemical mapping
F	Fluoride
GIC	Glass ionomer cements
HAP	Hydroxyapatite
IIL	Interaction interphase layer
La	Lanthanum
Mg	Magnesium
M	Month
μCT	X-ray computed micro-tomography
Na	Sodium
P	Phosphate
PAA	Polyacrylic acid
PCE-CT	Phase contrast enhanced micro-computed tomography
SEM	Scanning electron microscopy
Si	Silicon
Sr	Strontium
TA	Tartaric acid
W	Week

Abstract English

Objectives: Glass ionomer cements (GIC) are biomaterials with one particular advantage for dentistry: their self-adherence to both dentine and enamel in teeth. Although brittle, GICs have multiple merits that entail remarkable endurance on the tooth substrates through long-term chemical interactions. To quantify these effects, this in vitro study characterizes the structure of the interaction zone between a conventional restorative GIC and tooth tissues using 2D and 3D techniques, with increasing water storage times.

Methods: caries free human molars were restored with a conventional GIC (Ketac Fil Plus, 3M, Neuss, Germany) in class I cavities without cavity conditioning. Thereafter, each sample was sliced to expose internal surfaces, followed by storage at room temperature in water containing 0.5% chloramine-T for 1 week, 3 months, 6 months, 9 months and 18 months. Samples were imaged down to the micrometer length scale using different techniques: light/optical microscopy, scanning electron microscopy (SEM) with energy dispersive X-ray chemical mapping (EDX) in two dimensions (2D) and by confocal laser scanning microscopy (CLSM), X-ray computed microtomography (μCT)**,** and phase-contrast-enhanced μCT (PCE-CT) in a synchrotron radiation facility in three dimensions (3D). Additional replicas were prepared and compared to direct sample imaging by SEM, to reveal the GIC-tooth substrate interfaces.

Results: All 2D and 3D techniques revealed increasing chemical and density changes in both GIC and dentine with increasing time, quantified both at the base and at the outer surface of the cavity. In many regions, both mixed and cohesive cracks were observed in GIC. In dentine, the greatest changes over time were observed at the interface closer to the pulp. Little change was observed in enamel over time. Many samples exhibited an interaction interphase layer (IIL) at the interface between GIC and both dentine and enamel. The IIL was more acid resistant than both GIC and the tooth hard tissue near it, appearing speckled. Various ions diffuse across the IIL region: Ca and P from tooth tissues impregnate the GIC, whereas F, Sr, Al and La from the GIC were identified in the tooth substrates. Pores in GIC, particularly near the GIC-dentine interface, often contain spherical bodies consisting mainly of Si.

Conclusions: between GIC and the dental hard tissues, a good attachment was almost always observed. An IIL that formed at the interface was resistant to acid etching. Through complementary 2D and 3D materials characterization techniques, attributes of the IIL were

quantified. Water storage of up to 18 months revealed both an active IIL and maturation of spherical bodies, suggestive of a long-term, chemically reactive GIC.

Abstract Deutsch

Einleitung: Glasionomerzemente (GIZ) sind Biomaterialien mit einem besonderen Vorteil für die Zahnmedizin: Sie haften sowohl am Dentin als auch am Zahnschmelz in den Zähnen. Obwohl sie relativ spröde Materialien sind, haben GIZ mehrere Vorteile, die eine außergewöhnliche Langlebigkeit der Restaurationen durch langfristige chemische Wechselwirkungen mit den Zahnhartsubstraten mit sich bringen. Um diese Effekte zu quantifizieren, wurde in dieser in-vitro-Studie die Struktur der Wechselwirkungszone zwischen einem konventionellen restaurativen GIZ und dem Zahngewebe in Abhängigkeit von unterschiedlichen Aufbewahrungszeiten in Wasser durch 2D- und 3D-Techniken charakterisiert.

Methoden: Kariesfreie menschliche Molaren wurden mit einem konventionellen GIZ (Ketac Fil Plus 3M) in der Klasse I Kavitäten behandelt. Danach wurde jede Probe in Scheiben geschnitten, um innere Oberflächen freizulegen, und anschließend 1 Woche, 3, 6, 9 und 18 Monate bei Raumtemperatur in Wasser mit 0,5% Chloramin-T gelagert. Die Proben wurden unter Verwendung verschiedener Methoden hochaufgelöst im Mikrometerbereich abgebildet. Dazu zählen: Lichtmikroscopie, Rasterelektronenmikroskopie mit energiedispersiver Röntgenspektroskopie und konfokale Laser-Scanning-Mikroskopie, Röntgen-Mikro-Computertomography und Röntgen-Phasenkontrast verstärkte. Zusätzlich wurden vergleichbare Proben und Replikate hergestellt, um GIZ-Zahn-Substrat-Grenzflächen zu vergleichen.

Ergebnisse: Alle 2D- und 3D-Techniken ergaben, mit zunehmender Zeit chemische und Dichteänderungen in beiden GIZ und Dentin zu erhöhen, quantifizierten sowohl an der Basis als auch an der äußeren Oberfläche der Kavität. In vielen Regionen wurden bei GIZ sowohl gemischte als auch kohäsive Risse beobachtet. Im Dentin wurden die größten zeitlichen Veränderungen an der Grenzfläche näher an der Pulpa beobachtet. Im Laufe der Zeit wurde nur eine geringe Veränderung des Zahnschmelzes beobachtet. Viele Proben zeigten eine Interaktions-Interphasenschicht (IIS) an der Grenzfläche zwischen GIZ und sowohl Dentin als auch Schmelz. Die IIS war säurebeständiger als das GIZ und das Zahnhartgewebe in der Nähe und schien gesprenkelt zu sein. Verschiedene Ionen diffundieren über die IIS-Region: Ca und P aus Zahngeweben imprägnieren den GIZ, während F, Sr, Al und La aus GIZ in den Zahnsubstraten

identifiziert wurden. Poren im GIZ, insbesondere in der Nähe der GIZ-Dentin-Grenzfläche, enthalten häufig kugelförmige Körper, die hauptsächlich aus Si bestehen.

Schlussfolgerung: Zwischen GIZ und den zahnärztlichen Hartgeweben wurde fast immer eine gute Anhaftung beobachtet. Eine IIS, die sich an der Grenzfläche bildete, war resistent gegen Säureätzung. Durch komplementäre 2D- und 3D-Materialcharakterisierungstechniken wurden Attribute der IIS quantifiziert. Wasserlagerung bis zu 18 Monate ergaben sowohl eine aktive IIS als auch die Reifung von kugelförmigen Körpern suggerieren eine langfristige, chemische Reaktion von GIZ mit den Zahnhartsubstanzen.

1. Introduction

Teeth are important for the cutting of food during the digestion process and are designed to function as intact robust structures. Once damaged, however, e.g. due to caries, the loss of tooth structure leads to compromised performance. Yet nowadays, such teeth are not doomed, rather, they can be treated and brought into function during routine dental management. The treating dentist uses restorative materials that can comprise metals, polymers, cements, ceramics or composites. Such materials, when adapted to the remaining healthy tooth tissue reproduce the natural function and aesthetics of the affected parts (1-4). How well this is achieved remains a challenge for dentistry. In this thesis, I focused on one group of material used for tooth decay restoration, namely, glass ionomer cements (GIC).

1.1 Anatomy of tooth substrates

Teeth are composed of hard tissues (enamel, dentine and cementum) with an inner, vital soft core known as 'pulp tissue', which is highly innervated with an elaborate blood supply. Tooth tissues have a complex developmental fate, with enamel originating from cells of the ectoderm, whereas dentine and cementum are of mesenchymal origin (2). The following summarizes the main attributes of each tissue.

1.1.1 Enamel

Dental enamel is the hardest tissue in the human body and forms one of the main tissues in the crown of the tooth. The thickness of enamel varies considerably. Beneath the cusps or incisal aspects of the tooth, this tissue may exceed 2.5 mm in thickness, whereas near the margins of the crown in cervical areas of the tooth it becomes thin and knifelike (3, 4). Enamel is composed mainly of mineral, with minor contributions of organic phases and water. The mineral part is 96% by weight and composed of bundles of crystalline hydroxyapatite $[Ca_{10}(PO4)_6(OH)_2]$ with impurities such as Mg^{2+}, F^- and carbonate (5). The remainder of enamel is organic, comprised of groups of proteins (1% wt.) and water (3% wt.).

The crystal's orientation patterns inside prisms confer the enamel's high strength. These prisms extend from the enamel-dentine junction (EDJ) and run perpendicular to the surface, and contribute to an increased resistance of enamel against breaking forces (6, 7, 8). Although enamel is very hard, non-vital and resistant to wear and breakage, the surface integrity may be lost due to exposure to different forces and erosive compounds in the oral cavity (e.g., mastication, abrasion,

erosion, attrition as well as from traumatic dental techniques). Irrespective of the reasons for the loss of enamel structure (e.g. caries, erosion, tooth wear, etc.) it cannot currently be restored into its original prismatic structure (3, 4). The loss of enamel may lead to exposing the underlying dentine. In such circumstances, enamel no longer acts as a protective layer covering dentine and protecting it from thermal insults during eating, drinking or bacterial infiltration (6, 9).

1.1.2 Dentine

Dentine is the major tissue of the tooth. It supports enamel in the crown of tooth and is surrounded by cementum in the roots. It is composed of 70% inorganic carbonated apatite nanocrystals, similar in composition to the mineral in enamel, and 20% organic protein, mainly collagen fibrils, in addition to about 10% water. Dentine is significantly more porous than enamel, tubular in structure and is formed during the genesis of the tooth by odontoblasts (2). Dentine is a viscoelastic material and acts as a stress absorber in the tooth, and it subsequently deforms during mastication in order to prevent any enamel fracture (2, 10, 11, 12). In particular, the narrow region underneath the EDJ has a cushioning effect and protects the whole tooth structure from cracking (13). The strength of dentine is due to its composite structure and organic matrix. This matrix of collagen fibrils makes dentine stronger than enamel in terms of compressive, tensile and flexural strength. The hardness of dentine is due to the presence of nanocrystals with calcium salts, which confers dentine with both toughness and strength (10, 12). With time, dentine forms new layers, which have been classified into the primary, secondary and tertiary dentine. In the root, dentine is covered by cementum, which is a bone-like structure connected to the alveolar bone through periodontal ligaments (3).

1.2 Glass Ionomer Cement

"GIC is an acid-base dental biomaterial consisting of a degradable fluoro-aluminosilicate glass powder, a polymeric acid dissolved in water and tartaric acid (14). GIC has been used successfully in many dental applications. As a liner, it can be used to replace calcium hydroxide and other similar base materials in all cavities under class I and II composite restorations (15). It is considered as an alternative sealing material replacing mineral trioxide aggregate (MTA) due to reduced crown discoloration (16). GIC is used for perio-restoration in root caries: when reinforced with hydroxyapatite it enhances fibroblast proliferation and attachment (17). Additionally, GIC buffers bacterial acidic byproducts and it totally inhibits the growth of *S. mutans* and *S. sanguinis* (18).

Endodontically, GIC is used for cementation of glass fiber posts and showed similar push-out bond strength tests when compared with resin-modified glass ionomer cements and self-adhesive resin cement with a similar depth of dentine penetration (19, 20). When used to bond orthodontic brackets to tooth surfaces, it leads to significantly less white spot formation on enamel when compared with diacrylate orthodontic cements (21). An important application is the use as a fissure sealant to prevent caries in situations where drying of the tooth and moisture control are a problem. Although the effect of fluoride is still controversial, GIC is particularly useful for patients with high-risk caries as it releases fluoride (22, 23, 24). The consensus on caries management has led to the recommendation that GIC is used in atraumatic restorative treatment for the management of caries on smooth tooth surfaces (e.g. class five restoration) as a restoration in primary and even in permanent dentition (25, 26). In a 1-year randomized controlled trial, atraumatic restorative treatment was compared to standard dental care and was found to be more cost effective (27). Indeed, GIC-based dental materials are associated with lower secondary caries (28). GIC was even advocated as a bulk fill material in the cavity, due to minimum shrinkage and excellent surface attachment (29). However, GIC lacks color stability and is not as strong as metallic restorations. Indeed, evidence shows that GIC is brittle, has a compromised wear resistance and cracks easily, due to its low flexural strength (30)" (52). Further GIC-based products include additive resins, fillers, and acids that have established a class of dental materials known as "resin modified GIC" (31).

1.2.1 Conventional glass ionomer cements

Conventional GIC was developed and introduced into practice by Wilson and Kent in 1969 (30). It has been used in medicine for bone cements, bandages, splint materials and casting, and has found wide use in dentistry as a restorative and luting material (32). The first dental glass ionomer cement invented was described as an acid-base translucent material capable of leaching ions. The cement was formed as a result of mixing a leachable glass with an aqueous solution of homopolymers or copolymers (33). Generally, the composition of modern commercial GICs is similar to the early developed conventional GIC. They additionally contain fluoride and comprise a glass base of fluoro-aluminosilicate glass, PAA, water and tartaric acid (1).

1.2.2 Hybrid GICs

Unlike conventional glass ionomer cements, where an acid-base reaction stabilizes the cement, some modified GICs need additional polymerization to reach a full setting (31). These cements

are known as resin modified GICs (RMGIC) or hybrid (dual cure setting) materials. The dual setting reaction improves the physical and aesthetic properties of RMGICs when compared with conventional GICs. They generally reduce shrinkage and increase color instability (30). RMGICs can be light activated and they set due to the presence of light-initiated cross-linking. They contain an addition of 2-hydroxyethyl methacrylate (HEMA) (34).

1.3 Composition of GIC

1.3.1 Glass

Glass is the basic part of the cement, and has an amorphous microcrystalline structure (28, 30). Glasses used in GIC preparation are of aluminosilicate origin. They are very reactive and release ions when exposed to acids (31). Glasses are produced by mixing and melting different elements for specific times based on the type and melting degrees of the included elements (31). Basically, the glass is formed from different oxides. Some are called network formers such as silicon oxides, which are the backbone of the glass composition. Additionally, network modifiers change the glass network, and these include Ca^{2+}, Sr^{2+}, Mg^{2+}, Na^+, and K^+. However, some oxides (such as aluminum oxides) remain in a state between network formers and modifiers and are known as intermediate oxides. Intermediate oxides can bind with modifiers and act as network formers (35).

The first aluminosilicate glass that was used for making cement during the invention of GIC was G200, with the following composition: (SiO_2, Al_2O_3, AlF_3, CaF_2, NaF, $AlPO_4$). G200 is high in alumina and silica, and gives the glass a high basicity (28). The two most used glass systems in GIC are: ($SiO_2 \cdot Al_2O_3 \cdot CaO$ and $SiO_2 \cdot Al_2O_3 \cdot CaF_2$). These simple glass compositions became the source of further glass developments which involve incorporating or changing the ratio of different ions that ultimately change the GIC properties (31, 36). For example, calcium is substituted partially or totally by ions - e.g. by strontium, which increases the cement's radiopacity and fluoride release (30, 37). Further, F^- incorporation disrupts the glass networks and enhances the leaching of ions (28).

1.3.2 Polyacrylic acid (PAA)

PAA is formed by free radical polymerization of monomers in an aqueous solution in which a chain transfer agent and an initiator such as ammonium persulfate are present (36). PAA has features of both polymers and electrolytes and can be considered as a class of polyelectrolytes. The importance of PAA comes from the charged polymer chain groups of (COOH), which make

PAA functional in GIC preparation and soluble in water (28). Additionally, carboxylic groups of PAA are responsible for the crosslinking of the cement ions with the calcium in the tooth substrates (38). A range of (11,000- 52,000 Dalton) PAA's molecular weight is used to produce cements with the best physical properties (39, 40). The use of high concentrations of PAA in cements provides better mechanical properties, higher compressive strength and flexural strength with more a stable cement matrix, and thus higher resistance against hydrolyzing factors (28). However, using high molecular weight PAA increases the viscosity of the acid, which makes it difficult to mix with the glass particles during cement preparation (40).

1.3.3 Tartaric acid (TA)

Incorporation of TA is considered as one of the most important steps in GIC development (28). Tartaric acid shortens the GIC setting time without affecting or increasing the working time, while increasing the mechanical properties of the set cement (36). TA enhances leaching of ions, by forming complexes with the metal ions to slow down the reaction with polyanions for a short time. This increases the availability of cations in the matrix for further glass ionomer reactions (41). Prosser et al. (42) have examined the role of TA in GIC using NMR spectroscopy and reported an effect of increased working time of the cement. TA delayed the early premature binding of cations and polyanion chains in the cement matrix.

1.4 Hardening and Setting of GIC

As the glass powder and PAA are mixed, an acid base reaction occurs to harden the GIC, in which the glass acts as a proton receiver and the PAA acts as a proton donor (43). Crisp and Wilson (44) summarized the chemistry of GIC setting in the following stages.

1.4.1 Glass decomposition

During the first stage protons (H^+) from the carboxyl group attack the glass particles, resulting in leaching of Na^+, Ca^{2+}, F^-, PO_4^{3-}, and Al^{3+} ions into the aqueous matrix (43). This process is not uniform and occurs mostly in calcium rich sites in the glass since these regions are more basic (45). Both glass degradation and cross linking of polyacids increase the pH and the viscosity of the cement (30, 44).

1.4.2 Gel formation

In a second stage, the released ions precipitate as insoluble polyacrylates. Metallic salt bridges form between Al^{3+}, Ca^{2+}, F^- and free (COO^-) groups of the PAA, increasing the cross linking of polycarboxylate chains and ultimately leading to setting. The cross linking density delays the metal

ion movement towards the PAA carboxyl sites, which results in an incomplete neutralization reaction (43). Initial gelation and hardening of the cement within 4-10 minutes of mixing is due to the calcium polyacrylate formation, which is followed by aluminum salt formation that require longer (48 hours) (45, 46). During the initial setting phase of the cement, the pH of the matrix increases and orthosilicic acid on the glass surfaces is converted to silica gel that supports binding of the glass particles to the matrix (47).

1.4.3 GIC Maturation

In a final stage, after formation of polyacrylate complexes and silica gel, a permanent maturation stage sets in that results in an increase in the compressive strength of GIC (48). During this stage, mobile Al^{3+} ions cross link the $COOH^-$ groups of the remaining acid, where they act as network formers that help in further cross linking and maturation (49, 50).

1.5 Merits of GICs

Glass ionomer cements have some advantages and disadvantages when compared to other restorative materials.

1.5.1 Advantages

1. GIC requires 2.6 – 6.25 minutes to become a hard material, while other cements invented before GIC required a long time to set. (31). Clinicians favour this GIC property to avoid dislodgement and creeping of the material after placement in the oral cavity.

2. GIC is biocompatible in various ways. It is a pulpal-friendly material. Unlike other dental restoratives, during setting it releases low heat and produces no monomers (32). Furthermore, the PAA molecules are large enough to enter the dentinal tubules to reduce sensitivity after use (51).

3. GIC successfully adheres to teeth, metals (32) and bone tissues with no additional preconditioning (31).

4. GIC adheres to wet tooth structures and seals the gaps in the GIC-tooth interfaces in moist environments (32). This property is of particular importance in patients where drying and control of the cavity during restoration is impossible (52).

5. GICs are used to fix orthodontic brackets on the tooth surface (31) as a possible fluoride-releasing replacement of orthodontic bonding agents. They leave fewer white spot lesions on enamel when brackets are removed (21).

6. GIC is antibacterial due to presence of multiple ions incorporated, including F^-, Sr^{2+}, Ag^+, and Zn^{2+}. These ions are capable of bacterial growth inhibition (28, 31).

7. GIC induces remineralization of dental tissues that have lost apatite due to caries. This then helps in preventing secondary caries (53). Depending on the surrounding environment, GIC releases and recharges F^- continuously. A dynamic ion transport from a high concentration region to a low concentration region occurs (32). Fluoride recharge is very helpful in oral health prevention as F^-, at a level of 1 μg/mL, promotes tooth substrate remineralization (53, 54).

8. GIC can be used under very simple, sub-optimal treatment conditions (e.g. in schools, or in field settings in 3rd world countries); it requires no adhesives to attach to the tooth substrate, and can be cleaned manually without the need of electrical dental drills, anesthesia or ideal illumination conditions (52).

9. Because GIC is antibacterial and it can be inserted in bulk in low compliance populations (e.g. non-cooperative kids), it is an ideal material for atraumatic restorative treatment, especially for the management of caries and restorations in primary teeth (52).

1.5.2 Disadvantages

Despite its many advantages, GIC is not free from limitations and drawbacks:

1. The reliability of GIC for load sustaining is limited. It cannot be used in high stress bearing areas as a restoration material because of the low fracture toughness and compromised flexural strength (30).

2. In acidic environments, GIC undergoes surface erosion (30). Freshly set GIC is more prone to erosion than old cements, as the precipitation of various ions is slow to reach a stable form, so that certain ions, especially Al^{+3}, remain soluble. This affects the durability of the cement after placement (55).

3. Compared to composite materials, GIC has a poor color stability (32).

4. GIC is sensitive to moisture, and calls for surface coverage (by varnish) to prevent dissolution by water. This is of special concern in conventional GIC, in which water is necessary for the continuous hardness and maturation process of the material (55).

1.6 Attachment between GIC and tooth substrates

Successful restorative dental materials are assessed by their attachment to the tooth cavity walls and their stability over time. GIC attachment to hydroxyapatite (HAP), which is present in dentine and enamel, is permanent (56). However, to achieve a good attachment, the cleanness of tooth substrate surfaces, wettability of tooth structures and transformation of the attachment area from soft and gel like to a hard state are essential (57).

GIC has self-adhesive properties (28). The GIC-tooth attachment is the result of chemical bonding between COO^- groups of PAA and the Ca^{+2} of the enamel and dentine. However, GIC can slightly demineralize the dentine surface and provide porous dentine structure. This increases the retention area for the freshly applied cement and enhances the adhesion of GIC to the tooth structure (51). The attachment of GIC to dentine is due to the reaction between PAA molecules and organic collagen inside the dentine, which is either hydrogen or metallic bonding (47), whereas the bondage of GIC to the enamel is a true chemical ion exchange between hydroxyapatite and PAA molecules (25, 58). Ellis et al., (56) studied the effect of PAA on HAP substrates and found that PAA formed a layer on the HAP surface due to the dissolution and adsorption of PAA into HAP substrate structure. The GIC-HAP attachment was examined using X-ray photoelectron spectroscopy, and found to be a pure chemical bond between GIC and HAP, where phosphate (PO_4^{3-}) of the tooth substrate was replaced by the carboxyl groups of PAA that reacted with Ca^{+2} to form ionic bonds (59).

"Recent evidence has shown that in spite of compromised properties, several clinical meta-analysis works favor GIC-based materials for cervical restorations, where they showed excellent often superior longevity as compared with other treatment alternatives (60, 61). The main advantage of this material over the alternatives lies in the interaction with the tooth substrate. GIC attaches to the underlying dentine or enamel by one or several mechanisms. These include: GIC-tooth interlocking - it has been proposed that GIC eliminates the smear layer and partially erodes the substrate surfaces providing mechanical retention; adsorption - this mechanism assumes that

chemical bonds (ionic, hydrogen) or forces (Van der Waals) act together; and diffusion - various authors propose that mobile ions exchange at the GIC-tooth transition zone where an "interphase" of gradual transition between the two material phases is formed (55). In this in vitro study, this transition zone is called the interaction interphase layer (IIL).

With time, after GIC application, chemical bonds are formed between carboxyl groups (COO$^-$) in the GIC and the tooth substrate hydroxyapatite mineral particles comprising calcium and phosphate (29). Any etched, detached ions (calcium and phosphate) from the tooth are trapped in the unreacted GIC cement and form a distinct zone/layer at GIC-tooth interphase. This interphase comprises a layer of hybrid composition, and typically appears less dense and more transparent than both the adjacent tooth substrate and GIC bulk. It contains calcium, phosphate, aluminum, fluoride, and silica depending on the composition and on GIC interaction with the substrates (62). The interphase interaction layer between GIC and tooth substrates has been given various, often confusing terms (25) including "interfacial layer", "distinct zone of interaction", "demineralized dentine", "acid-base resistant layer", "mineral infiltration zone", "absorption layer", "hybrid layer", "interdiffusion zone", and "intermediate layer" (52). The GIC sealing and its interphase with tooth substrates have been characterized using polarized-light microscopy (63, 64), scanning electron microscopy (SEM) (65,66), transmission electron microscopy (TEM) (67, 68), confocal laser scanning microscopy (CLSM) (69, 70), micro-computed tomography (μCT) (71, 72), X-ray photoelectron spectroscopy (XPS) (63, 64, 73, 74), energy-dispersive X-ray spectrometry (EDX) (75, 76), Fourier transform infrared spectroscopy (FTIR) (74, 77), Raman spectroscopy (78, 79, 80), and electron probe microanalysis (81, 82)" (52). There also remains uncertainty regarding the precise location of the interaction interphase layer related to dentine. While some authors believe that it resides within the smear layer, others believe it may be located on/within the surface of the demineralized dentine (83). Thus, this work was needed to determine the relationship between tooth substrates and GIC, as well as the location and morphology of the interphase layer.

1.7 Aims and Objectives

The aim of the current in vitro study was to characterize the structural morphology of the interaction zone between GIC, enamel and dentine in human teeth, and to describe how it changes over time. Various gaps exist in our knowledge regarding the interactions of GIC with tooth substrates. Combining multiple modern microscopy techniques paves the way to integrate information both from the sample surface and from internal structures. The problem is complicated by the fact that GIC maturation is a continuous process, as the material remains chemically active for extended periods. Thus, there is a need to examine the interactions of GIC with the tooth substrates over months following placement. In this in vitro work I focused on:

1. Examination of structural changes over time in samples with GIC-tooth interfaces. Each sample served as its own control to circumvent biological sample variability.
2. Utilization of low and high contrast 3D optical and X-ray techniques. The samples were kept hydrated to preserve them as closely as possible to the clinical reality during the study.
3. Implementation of high resolution 2D electron and confocal laser techniques to map the GIC-tooth interface changes at submicron resolution.
4. Analysis of the GIC-tooth interface in multiple samples of up to 9 months and comparing them with newly prepared samples to quantify dynamic changes over time.

Hypothesis

In this study I tested the following hypotheses:

Hypothesis 1. The GIC-enamel and GIC-dentine interfaces change composition in a similar manner over time.

Hypothesis 2. The different contrast and different storage conditions are essential parameters for the interpretation of 2D and 3D characterization techniques in studies of GIC-tooth interface analysis.

2 Materials and methods

2.1 Sample preparation

Healthy extracted intact molar teeth with no signs of caries were collected under an ethics-approved protocol (EA4/102/14) by the Ethical Review Committee of the Charité-Universitätsmedizin Berlin, Germany. The teeth were stored in water containing 0.5% chloramine-T until they were needed for experiments (Fig. 1). Class one cavities were prepared using high-speed dental headpieces and drills under constant water irrigation. The cavities were 3-5 mm deep to include both enamel and dentine. Each was washed, air dried and restored with a conventional GIC (Ketac Fil Plus, 3M, Neuss, Germany) without use of any further cavity conditioner. Immediately after standard mixing for 10 seconds within the designated mixing capsule (SDI Ultramat, Australia), the cement was injected into the cavities. The restored teeth were left in air at room temperature for one hour, followed by water storage for 24 hours before longitudinal cutting to expose the internal geometry. Using 2 vertical cuts by means of a water-cooled diamond blade (Exakt, impressum, Norderstedt, Germany), the GIC margins and interfaces with both dentine and enamel were exposed. The cut samples were stored in a water solution containing 0.5% Chloramine-T in plastic tubes for 0-7 days, 3 months, 6 months, 9 months and 18 months on a shaker in an incubator (Orbital Shaker-Incubator ES-20, Biosan SIA, Latvia) using 50r/min at 37°C. The cut samples were imaged with a Keyence microscope and by X-ray Computed microtomography (µCT) without surface polishing to avoid the creation of artifacts. Prior to imaging with other techniques, the samples were first ground using silicon carbide paper grit P4000 (MICROCUT, RA11, USA) for 1 minute followed by polishing using a diamond suspension (Dia Complet Poly water based, ATM GMBH, Great Britain) with grain sizes of 3, 1 and 0.25µm for 3, 6 and 9 minutes, respectively. The samples were cleaned in an ultrasonic bath for 30 seconds after each polishing step to remove debris and any particles left on the sample surfaces.

Additional samples were prepared to (1) compare the GIC-tooth interface imaged using SEM-EDX with images by synchrotron radiation following dehydration, and (2) to check the GIC-tooth interface using replicas. The replicas were prepared by making impressions of the polished samples following acid etching with 17% phosphoric acid for 30 seconds followed by water rinsing and air drying. Imprints of the etched surfaces were then created using addition-curing silicone-based impression material (Honigum light, DMG, Hamburg, Germany). The impressions were then cast with Stycast 1266 Epoxy resin and allowed to set for 24 hours. The replicas were then

coated with carbon using a carbon coater (Blazers union, MED 010, Weimar, Germany) and imaged using backscattered SEM-Phenom.

Table 1 The number of samples tested by: optical microscope Keyence (A), X-ray computed microtomography (μCT) (B)**,** confocal laser scanning microscopy (CLSM) (C), phase-contrast-enhanced micro-computed tomography with synchrotron radiation (PCE-CT) (D), and scanning electron microscope with energy dispersive X-ray analysis (SEM-EDX) (E). W= week, M= month, Samples not tested (-).

	1 W	3 M	6 M	9 M	18 M
A	5	5	5	5	-
B	5	5	5	5	-
C	5	5	5	5	20
D	3	3	-	-	3
E	12	9	9	-	9

Additionally, to examine the effects of freshly applied GIC on the dentine prior to cement hardening, six dentine discs of 2 mm thickness were prepared. At least one was used as a control without GIC treatment. The dentine discs were polished using silicon carbide paper (P4000) for 2 minutes and diamond suspension (1 μm) as a final polishing stage for 3 minutes. The discs were placed in an ultrasonic bath for 1 minute in between and after each polishing step. GIC was prepared according to manufacturer instructions and directly applied to the polished dentine surfaces. After 60 seconds of GIC application, an air-water jet was used to remove the GIC completely from the disc surfaces. A control disc was cleaned in the same manner. Dentine discs were dried under ambient conditions. One additional disc was tested for 120 seconds, though removal of the set GIC from the dentine surface was difficult.
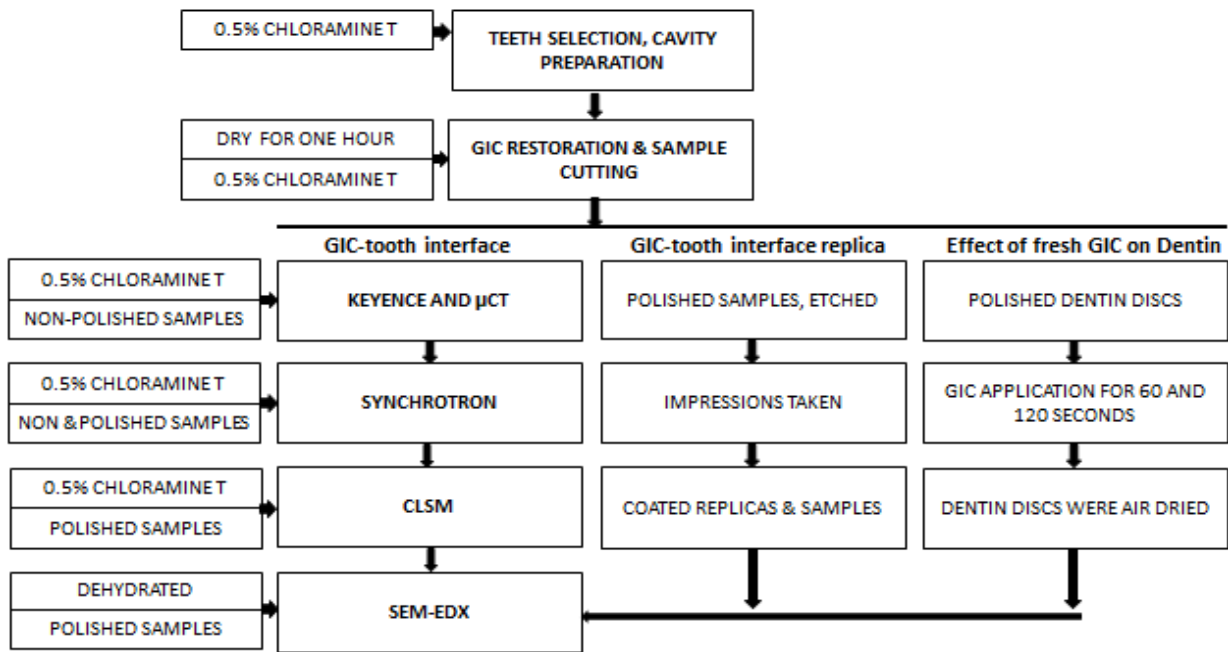
Figure 1 Schematic diagram of sample selection and all experiments included in this study.

2.2 Characterization techniques

Samples were divided into four groups, according to the storage time in water (0-7 days, 3 months, 6 months and ≥9 months). Each sample was imaged as described in the following section, in the sequence listed in Table 1. The order and comparisons between methods were defined so as to observe changes occurring during storage under moist conditions (all samples stored in water containing 0.5% chloramine-T). For SEM-EDX analysis, and as a final step, the samples were dehydrated in a graded series of ethanol, with some of the samples treated by critical point drying.

2.2.1 Light/optical Keyence Microscope

The cut non-polished samples were imaged with a multi-focus, high-resolution Keyence microscope (VHX-S550E, KEYENCE CORPORATION, Japan) using a x200 objective lens. Each sample was placed on the microscope stage, where an illumination source was directed at the sample. Multi focus imaging and stitching helped collect sharp images of the surface of each sample (Fig. 2a).

2.2.2 X-ray Computed microtomography (μCT) and synchrotron radiation phase-contrast-enhanced micro-computed tomography (PCE-CT)

Both lab-based μCT (Skyscan 1172, Bruker-microCT, Kontich, Belgium) and PCE-CT from a synchrotron radiation imaging beamline (BAMline, BESSY, Berlin, Germany) were used to scan the cut, non-polished samples. Prior to scanning, the samples were assembled in the center of PVA tubes (Micro tube 2 ml, Sarstedt, Numbrecht, Germany) using styropore supports, sandwiched between 2 wet sponges at both ends of the tubes to keep the samples in a humid environment. This approach was adopted to minimize stresses on the interfaces and to prevent dehydration during scanning leading to shrinkage/delamination.

μCT scans were obtained at 4 μm pixel size, using a source energy of 80 kV and 125 μA, an 0.5 mm aluminum filter, 360° scans and 0.3° rotation steps. The measurement time per scan was approximately 2 and a half hours for each sample. The scans were reconstructed with NRecon (Version 1.7.0.3, Bruker microCT, Kontich, Belgium) and visualized in 2D and 3D using ImageJ (ImageJ 1.52d, National Institute of Health, USA) and CTVox (Version 3.3.0 r1403, Bruker microCT, Kontich, Belgium).

A higher resolution imaging technique, i.e., phase-contrast-enhanced micro-computed tomography, was used to scan the GIC-tooth interface regions in 3 groups. Group 1 consisted of 3 old samples (18 months) scanned with all other techniques used in this study. The rest of the samples (n= 3 in each group), i.e., group 2 (1 week) and group 3 (3 months), were newly prepared and imaged by PCE-CT.

Samples were scanned on the imaging beamline BAMline, using inline propagation-based contrast microtomography. An X-ray photon energy of 30 keV with an effective pixel size of 4.35 μm was used. To enhance the visibility, PCE-CT scans were obtained using a sample to detector distance of (45) mm. Each sample was mounted on the high resolution rotation stage and a total of 1,800 radiographic projections were recorded during 400 ms exposure times while the sample was rotating continuously by 360 degrees. Following normalization and reconstruction by NRecon, the GIC, dentine and enamel were analyzed using ImageJ by creating line plots as well as a study of changes in these structures.

2.2.3 Confocal Laser Scanning Microscopy (CLSM)

The CLSM has an adjustable focal plane and uses a tunable laser source of one of several wavelengths (colors) to image different depths beneath the sample surface. Both dry and wet samples can be scanned with this technique, though in this study only wet samples were examined. To identify the restoration tooth interface, samples were polished as described in the sample preparation section. Each sample was fixed on transparent microscopic slides (Plexiglas, patho service) using double sided tape. All samples were kept moist during CLSM scanning by immersion and by use of chloramine-T on moist tissues.

The samples were scanned with a CLSM (LSM 700, Zeiss, Jena, Germany) using 10X, 20X and 50X objective lenses in reflection mode, in conjunction with 405-nm laser excitation, without using fluorescent probes or synthetic dyes. The CLSM images were captured into images sized 2048x2048 pixels. Z-stacks with 1 μm z-step optical sectioning of different regions of GIC-dentine and enamel interfaces were collected. The images and stacks were further analyzed using ImageJ.

2.2.4 Scanning Electron Microscopy (SEM) and Energy Dispersive X-ray analysis (EDX) analysis

The scanning electron microscope creates and focuses electrons to produce images of structures at the micro and sub-micrometer levels. A beam of electrons is directed at the sample surface and reflected electrons (high energy for backscatter images) create high resolution images. Many modern SEM instruments can operate in a low or high vacuum or environment where moist samples can be scanned. Different detectors can be built inside the SEM to give different analyses and information. Superficial information of the sample is collected when a secondary electron detector is used, while deeper surface information is collected when a backscattered electron detector is utilized. Depending on the detectors, SEM can map the surface structures when an EDX X-ray detector is installed. Chemical analysis of material structure (organic and non-organic) is possible with EDX, through emission of characteristic X-rays for each element illuminated by the electron beam. However, many biological sample materials require a thin coating layer with a conductive material such as gold or carbon to prevent electron charging and surface damages.

SEM-EDX sample scanning

The last scan in each sample was mapped for X-ray fluorescence by electron excitation. The polished samples were dehydrated in a series of ethanol concentrations (25%, 50%, 75%, 96%, and 100%) exchanged once per day. Thereafter, the 1-week and 3-month samples were placed in a desiccator using silica gel for 48 hours, and the 6- and 18-month samples were placed in a critical point dryer (CPD) (BALTEC CPD 030, Weimar EM-Service oHG, Weimar, Germany). Before the CPD dehydration, samples were further treated with acetone and ethanol as 50:50, 96:4 and 100:0 acetone:ethanol for 1 day each. The SEM-EDX samples were not coated, except the resin replicas made from the samples in the GIC-tooth interface study. Two SEM microscopes were used to study the dehydrated samples. A Phenom XL (Thermo Fisher Scientific, Eindhoven, The Netherlands) in low-vacuum mode was used for backscatter, secondary electron imaging and side view imaging using the Topo B detector. EDX mapping was performed together with backscatter electron imaging in high-vacuum (~10^{-4} mbar) in a CamScan MaXim (Electronen-Opti-Service GmbH, Dortmund, Germany). The Phenom XL SEM with a Cerium Hexaboride cathode (CeB6) source provides a better signal-to-noise ratio and better visibility than the older generation detectors of the CamScan SEM. A Bruker spectrometer (QUANTAX EDS XFlash 6130, Bruker Nano GmbH, Berlin, Germany) was used for elemental mapping in the electron microscope using 20 kV acceleration voltage at a working distance of ~ 31 mm. Point scans of the GIC-tooth interfaces and the maps of the region of interest were collected using a dwell time of 256 µs and a line average of 6 with a 1 µm spot size. All data were processed using Esprit 2.0 (Bruker QTX, Berlin, Germany).

2.3 Quantification of change in GIC

Changes in the GIC color and contrast in a thick region at the dentinal and at the outer GIC restoration were quantified by measuring several lines (n= 10) drawn (300 µm) away from the filling margins inwards (100-250 µm). These allowed comparison of both sides of the restoration. Figure 2 shows typical regions of interest for analysis used for quantification in both 2D techniques (optical and SEM microscope photos) and 3D techniques (µCT and PCE-CT in synchrotron samples).
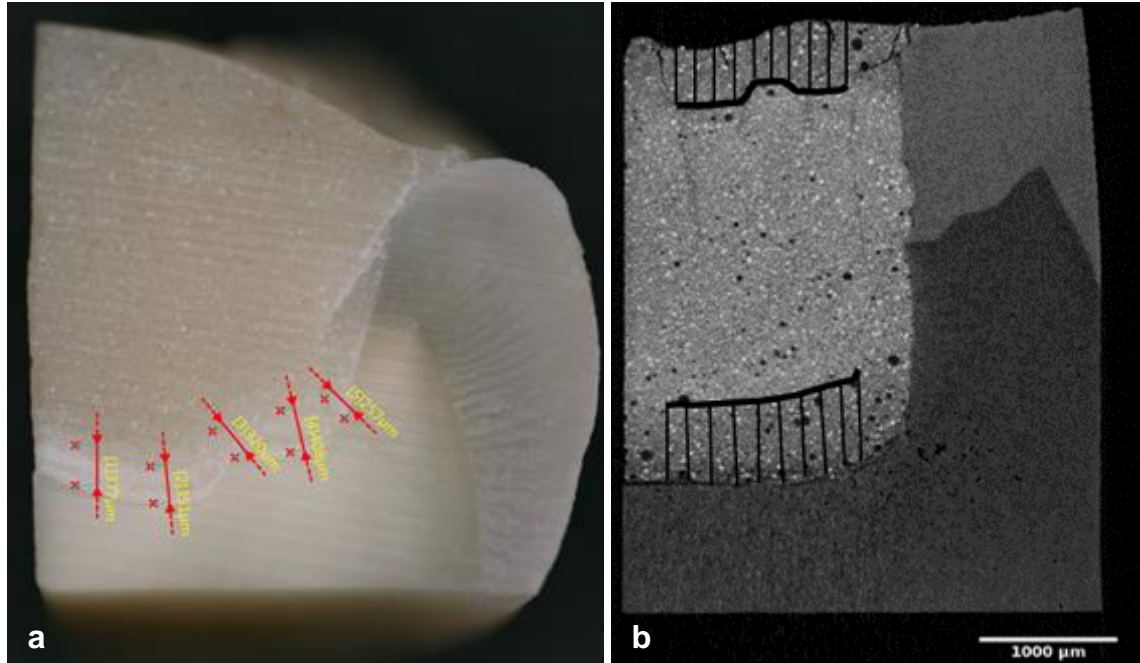
Figure 2 Light microscope and µCT images of typical structural changes observed in the GIC contrasts, concentrated at the dentinal GIC restoration (a). Measurement of GIC contrast changes in thickness (µm) by drawing 10 lines and averaging them to have the mean (b).

Keyence can take sharp images of the whole sample by stitching images over a wide area without resolution dislodgement. Direct measurements of the sample surface directly after the image is taken are also possible (Fig. 2a).

The mean of the lines in each sample as well as in each time point are measured in distances from the restoration margin and recorded. The repeated measurements of means in the 3 samples from each group were averaged.

2.4 Statistical analysis

In addition to the raw data, means are reported for different time points determined between samples, as well as between time points and different restoration locations. The change in thickness (µm) over time at the outer and dentinal GIC restoration was calculated and fitted with linear regression lines using Microsoft Excel. A polynomial regression analysis was performed using (SciDAVis 2.3.0) to study the density change in dental tooth substrates, enamel and dentine.

3 Results

The results of both the 2D and 3D techniques utilized in this study in order to evaluate the early initial effects of GIC and how it reacts on tooth substrates - namely, enamel and dentine - over time will be presented in this chapter.

3.1 Early effects of GIC on dentine surface

The GIC eroded the dentine surface and changed the peritubular dentine composition in seconds. It etched the dentinal tubule orifices and led to further opening of the tubules.
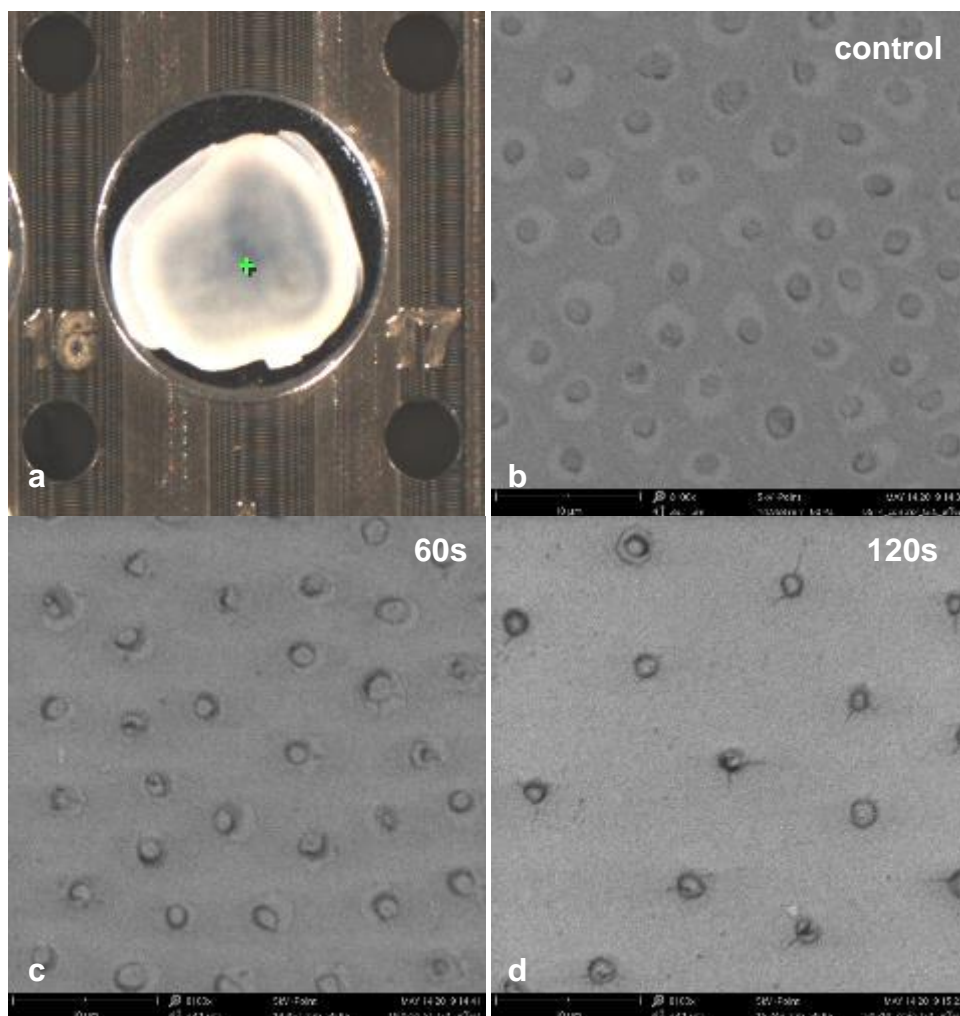
Figure 3 Effect of the fresh GIC applied on dentine. Dentine disc, optical image of the region of interest (a), SEM images of control (b), 60 second GIC application effect (c), 120 second GIC application effect (d). GIC has the ability to erode the dentine surface, open dentinal tubules and etch the odontoblastic processes inside dentinal tubules. Bars represent 10 μm in b, c, d.

When GIC was applied for 120 seconds, the dentine surface was totally etched, the peritubular dentine morphology was significantly changed, and cracks appeared (as seen in Fig. 3.d). The bleaching effect of freshly applied GIC was clearly seen. Most of the dentinal tubule orifices and odontoblastic process remnants, which are seen as smoothed round structures inside tubules, were etched. In contrast, the control disc has a homogenous topography and most of the dentine tubules were not patent (Fig. 3.b), peritubular dentine was well demarcated, and odontoblastic processes etching were not quite visible.

3.2 Direct observations at the GIC-tooth interface

3.2.1 Optical microscopy

The quality of the images from GIC-tooth samples was clear and sharp, and most of the structures were visible in both GIC and tooth substrates without using a fluorescent probe or dyes. In general, most of the samples revealed changes in contrast thickness at the dentinal and at the outer GIC restoration (Fig. 4). The 9-month samples showed further GIC dissolution signs, as they were eroded at the interface with dentine.

Moreover, after 9 months of immersion, dentine had a higher contrast than other time point samples at the GIC-dentine interface (Fig. 4.d). Pores and cracks of different size and length were seen in all the samples. Pores were spread at various locations of the GIC with no pattern. Cracks were seen, but less at the first two time points when compared to the last two time points, and especially at the edges, where the sample (GIC-dentine) was cut, or at the occlusal surface where the GIC-enamel was in contact with the outer environment.
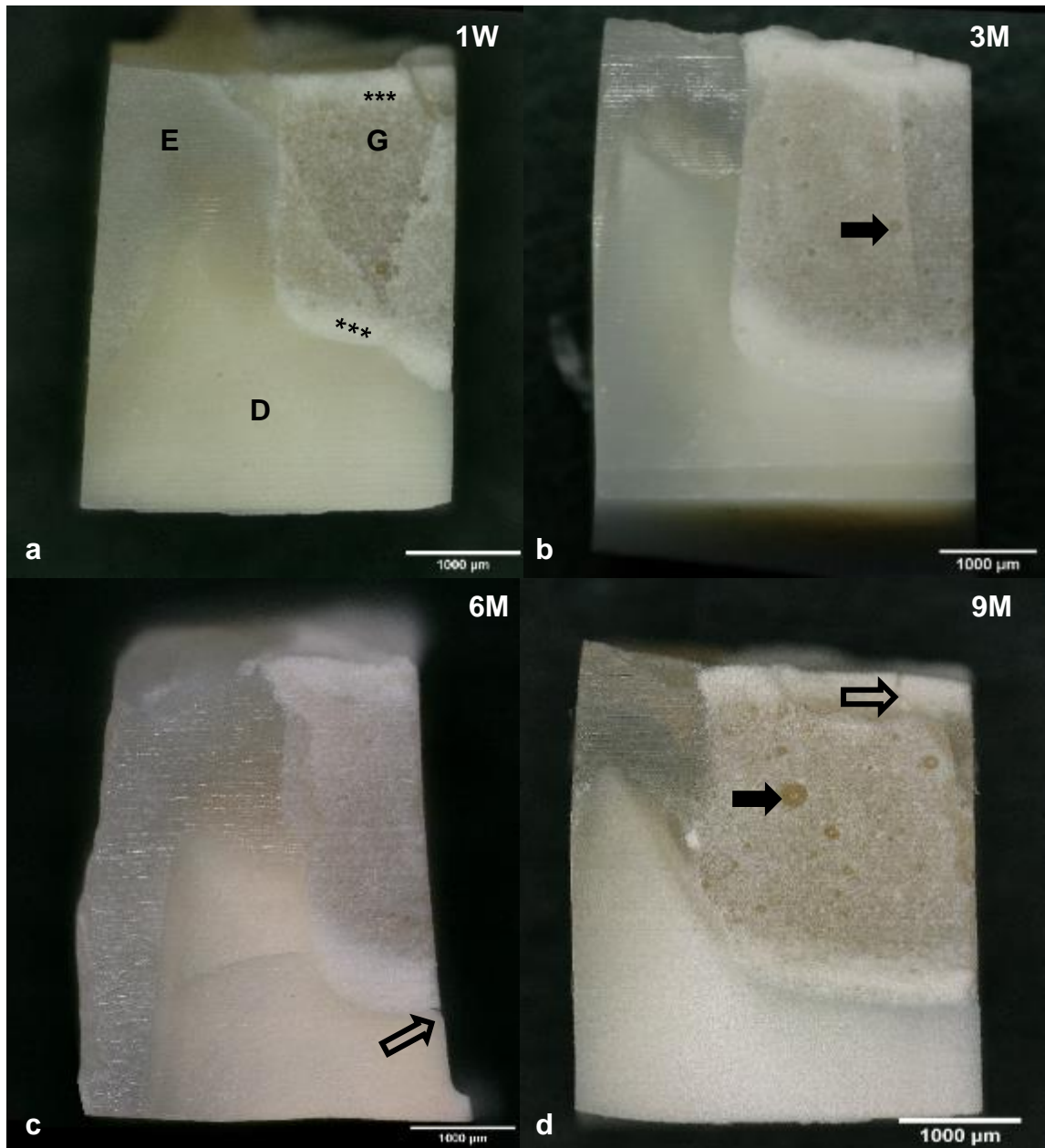
Figure 4 GIC-tooth samples from the same tooth examined at different time points show visible changes in GIC (contrast thickness, asterisk) close to the dentine at the dentinal and at the outer GIC restoration: 1 week (a), 3 months (b), 6 months (c), and 9 months (d). GIC (G), enamel (E), dentine (D), Pore (arrow), cracks (empty arrow). Bars represent 1000 μm.

Change in the outer or dentinal GIC restoration

The contrast change in thickness at both the outer and dentinal GIC restorations were measured. Dentinal GIC restoration, where it is in contact with the dentine cavity floor, exhibited more contrast change in thickness (μm) than the outer of the GIC. The outer GIC restoration showed

less change than the dentinal GIC restoration at every time point, as seen below in Table 2 and confirmed by the statistical linear regression (Fig. 5).

Table 2 Thickness of contrast change in the outer and dentinal GIC (µm) from optical microscope images at different time points.

	1 week	3 months	6 months	9 months
Outer GIC (µm)	112	390	294	452
Dentinal GIC (µm)	319	548	444	483

It is worth mentioning that outer GIC was in contact with air during early sample preparation for 60 minutes and then stored in water containing 0.5% chloramine-T for the rest of the study.
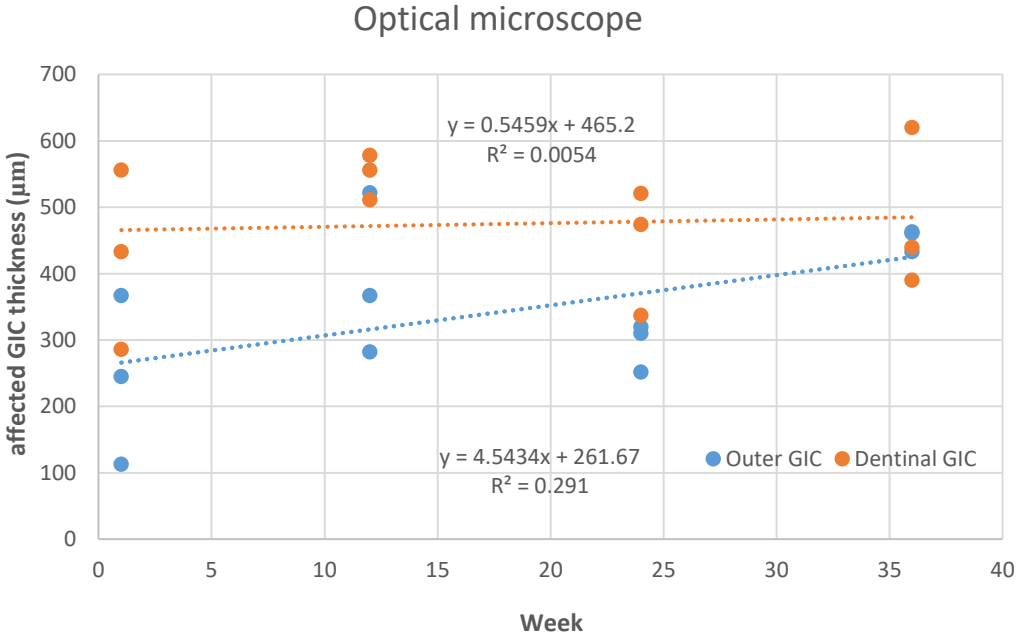
Figure 5 Linear regression (R) of GIC thickness contrast change with time at the outer GIC restoration (R= 0.54) and at the dentinal GIC restoration (R= 0.073).

3.2.2 Micro Computed Tomography (μCT)

μCT revealed the changes in dentinal GIC at the base of the restoration and in the outer GIC, where it is in contact with enamel and with the outer environment in all the samples, as shown in Figure 6.Those regions showed different contrast than the rest of the GIC restoration. This GIC change in density or contrast (in thickness) particularly occurred at the dentinal GIC, and increased with time to reach the lower part of the dentine in the vertical wall (axial wall) of the cavity close to the EDJ, whereas GIC density changes in enamel were seen only at the outer GIC restoration far away from the EDJ. This change increased with time. The dentinal GIC displayed more thickness change than the outer GIC, and the results are shown in Table 4.
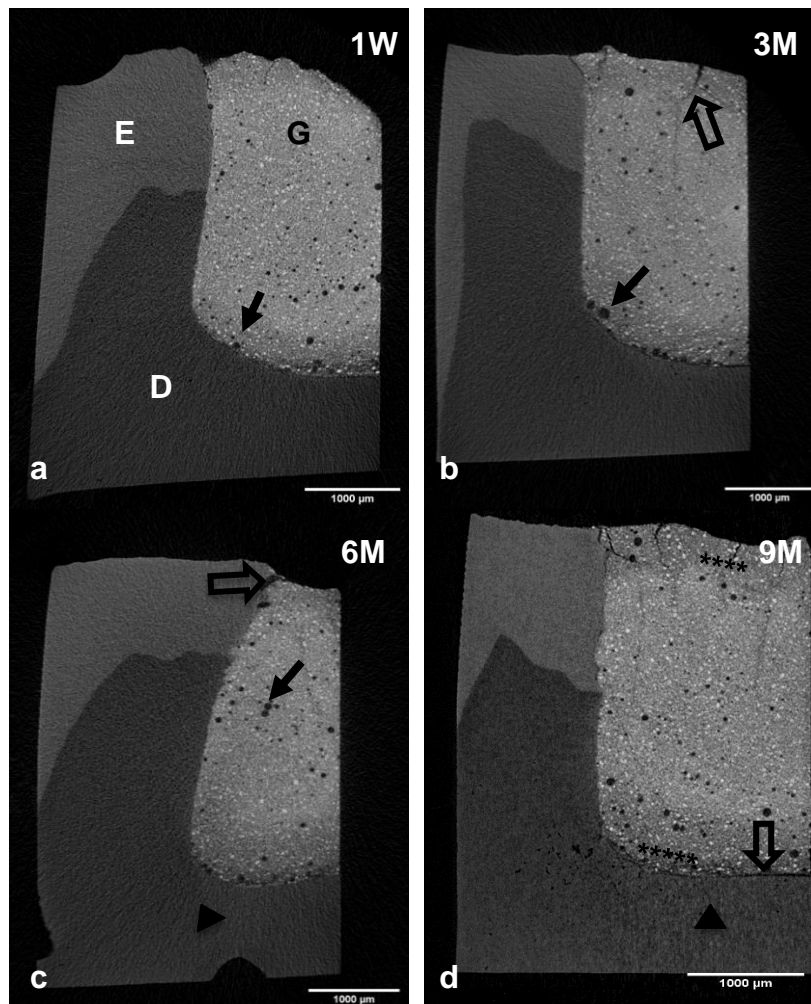
Figure 6 Different samples from the same tooth. Water immersion of: 1 week a), 3 months b), 6 months c), and 9 months d). Voids present in all samples (arrow) with cracks (empty arrow) inside GIC or at GIC-tooth interfaces and density change in GIC (asterisks) and dentine (arrowhead). No interaction layer is seen at the interface. GIC (G), enamel (E), dentine (D). Scale bars= 1000 μm.

Furthermore, the pores and cracks were clearly seen. The pores were spread all over the GIC in a nonhomogeneous shape and manner. The pores were seen in the GIC in contact with both enamel and dentine, but mostly present in the part usually close to the GIC-dentine interface at the base of the cavity. This region showed signs of corrosion, some of the material particles were removed or washed off with time, and this can be seen clearly in the 9 month samples (Fig. 6.d).

Although the GIC-tooth samples were stored in a moist environment throughout the study and during imaging, the GIC parts revealed cracks of different shapes and patterns. Cracks were not limited to the outer GIC in contact with water, or to the top of the restoration only. They were also seen at the dentinal GIC too, especially after 6 months or more of immersion time. Figure 6b-d shows cracks at the cutting edges where GIC meets both dentine and enamel. There were different horizontal cracks at the dentinal GIC restoration and vertical ones at the outer GIC restoration. Those cracks were pertained in GIC only.

The µCT study revealed no tissue cracking at any time points. However, it showed obvious density changes in pulpal dentine where it is in contact with dentinal GIC at the bottom of the cavity. The dentinal change appeared 3 months after immersion, and increased with time. The change was more evident in the regions close to the dental pulp horns (funnel shape) than other parts of the dentine (Fig. 6.c). This might have a relation with the dentinal tubules direction as the pattern of contrast change follows the tubules direction.

Similarly, density changes in thickness (µm) in dentine happened at the axial walls of the cavities (axial dentine). They were more evident after 6 months of immersion. In comparison to the pulpal dentine, there was significantly less change in the axial dentine (Fig. 7). Table 3 shows the results of several 6 and 9 month immersed samples where changes in density at both pulpal and axial dentine tissues are compared.

Table 3 Layer thickness [means (standard deviations) in µm] showing changes in dentine density at the pulpal and axial cavity walls in three teeth samples after 6 and 9 months' (M) immersion.

Regions	Sample 1		Sample 2		Sample 3	
	6M	9M	6M	9M	6M	9M
Pulpal dentine	150 (42)	80 (18)	134 (12)	179 (40)	422 (100)	380 (43)
Axial dentine	80 (14)	35 (4.8)	35 (5.09)	108 (34)	132 (30)	60 (9)
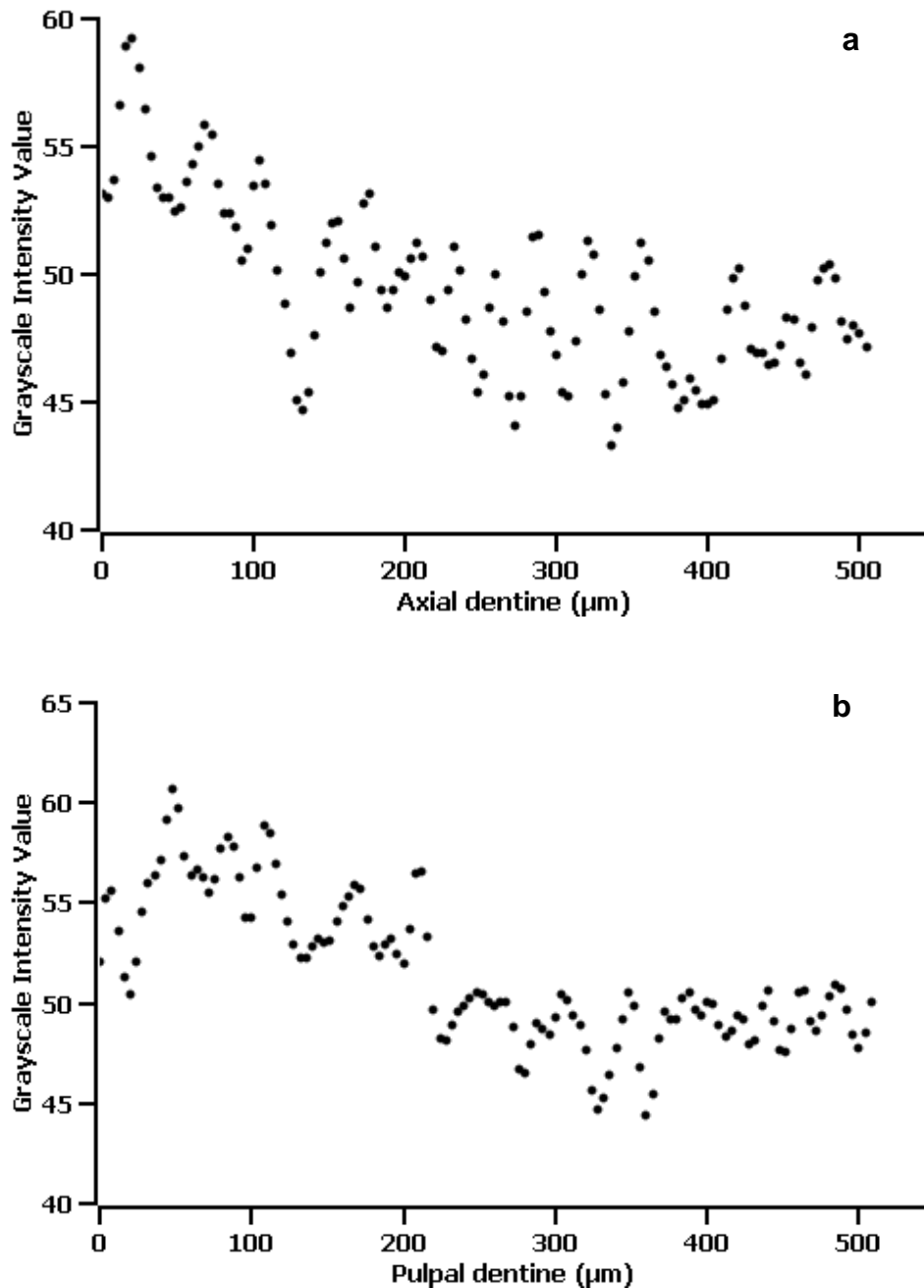
Figure 7 Density changes of dentine in contact with GIC after 9 months' immersion. The axial dentine close to the EDJ (a) showed less density change (120 μm), as compared to the pulpal dentine (b) with higher density change (220 μm). Zero in the x-axis indicates the GIC-dentine interface.

Change in the outer or dentinal GIC restoration

Similar to Keyence, μCT showed more density change in thickness at the dentinal than the outer GIC restoration. The results are presented in Table 4 and supported by statistical linear regression (Fig. 8).

Table 4 Thickness of contrast change in the outer and dentinal GIC (μm) from μCT images at different time points.

	1 week	3 months	6 months	9 months
Outer GIC (μm)	329	429	378	390
Dentinal GIC (μm)	440	578	600	726
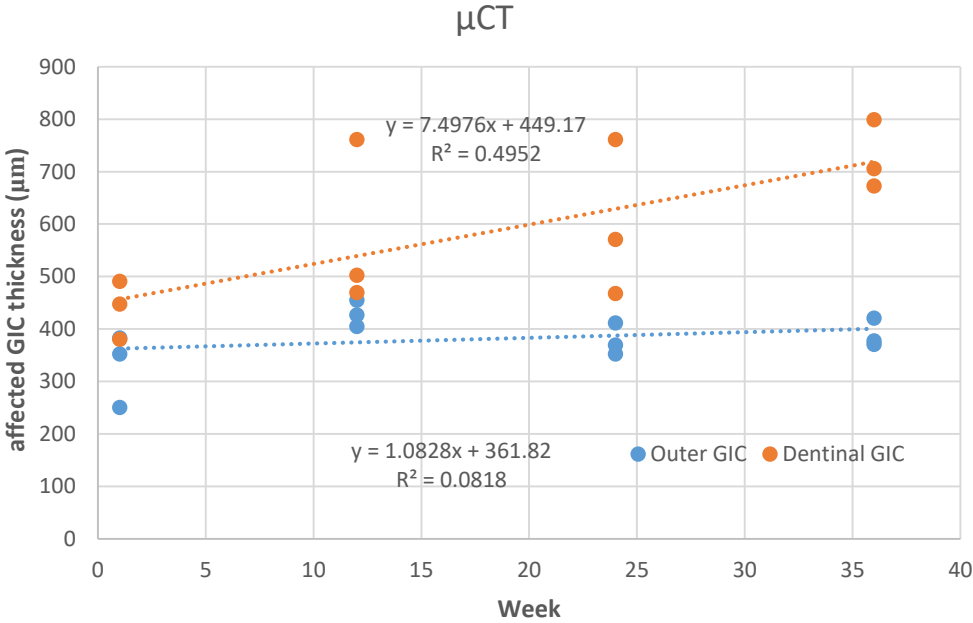
Figure 8 Linear regression (R) of GIC thickness contrast change with time at the outer GIC restoration: R= 0.29 and at the dentinal GIC restoration: R= 0.70.

3.2.3 PCE-CT with synchrotron radiation

Samples in each group revealed the density (in thickness) change in the outer and dentinal GIC restoration. The change was seen slightly in 1 week samples, and increased from the 3 month samples to the 18 month samples, where GIC appeared washed out at the pulpal region. See Figure 9f.

Although the GIC density change was minimal in 1 week immersion samples, PCE-CT clearly revealed the external and internal change at the outer and dentinal GIC restoration. Figure 10 shows the effect of water containing chloramine-T on the GIC surface - both the outer and side of the restoration are color coded in the regions of direct contact with water. The dentinal GIC

restoration also has the same color of outside surfaces. The same features were seen in both 3 months and 18 month samples, as in Figure 11. The changes of GIC density at the outer and dentinal GIC restoration obtained from PCE-CT data are displayed in Table 5.
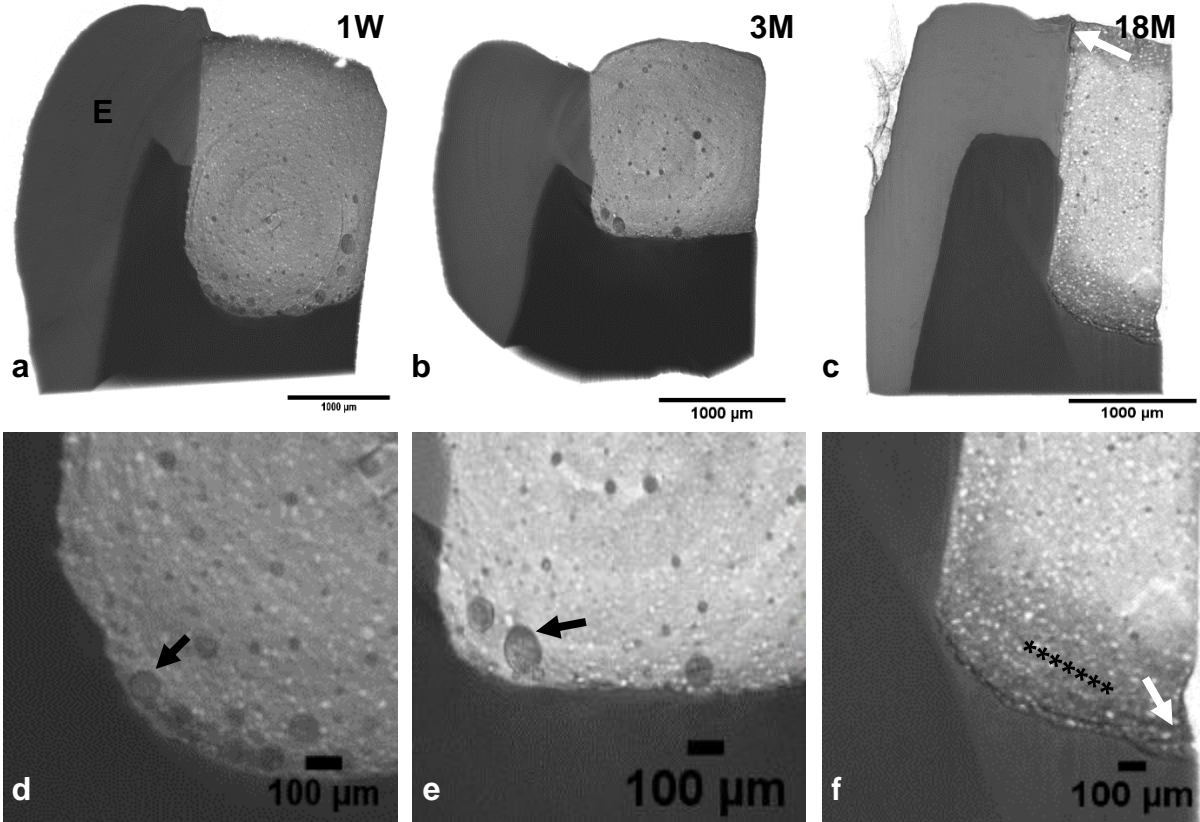
Figure 9 One week, 3 months and 18 month samples scanned using PCE-CT in synchrotron. Thickness change in GIC phase contrast density at the outer and dentinal GIC restoration, and pores and cracks (arrows), were seen in all groups. The 18 months sample cracked at the base cohesively and showed high contrast change (asterisk) in GIC. Scale bars a, b, c= 1000 µm, d, e, f= 100 µm.

Table 5 Thickness of contrast change in the outer and dentinal GIC (µm) from PCE-CT images at different time points.

	1 week	3 months	18 months
Outer GIC (µm)	349	192	451
Dentinal GIC (µm)	521	480	443
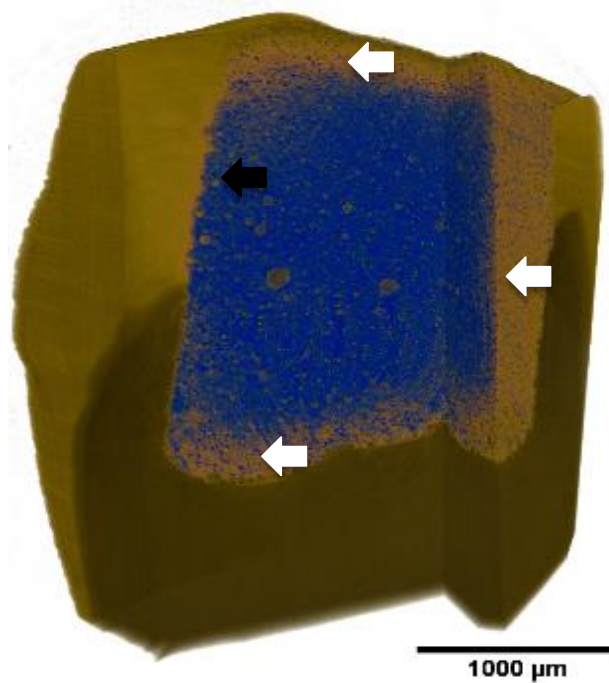
Figure 10 One week sample examined with PCE-CT, effect of GIC exposure to water on the external surface and pulpal dentine internally (white arrows). GIC in contact with enamel is not changed (black arrow). Pores of different sizes are seen. Dentine change is not visible. Scale bar= 1000 μm.

Besides the change in GIC contrast/density, dentine was changed in the regions in contact with GIC. The change occurred often in the pulpal wall in comparison to the axial dentine wall. The width of the dentine density change in the pulpal wall was higher than the axial wall. The pulpal dentine change was not constant throughout the cavity base as regions close to the pulp horns showed a higher dentinal change. Figure 11 shows the change in dentine density from the surface to the last point of the axial wall in an 18 months immersed sample. A rim- or layer-like structure is seen at the GIC-dentine interfaces at both pulpal and axial walls, externally. Internally the dentinal change was varied in depth from the GIC interface, especially at and in the vicinity of the pulpal horns. The change of dentine in density at the pulp horn region exhibited a funnel shape. This funnel shape disappeared when the sample was checked far away from the pulp horn.

Using intensity histograms of the grey value data in each group, changes in GIC and tooth substrates were obtained. PCE-CT visualized the changes in dentine density, however it was not successful in picturing the changes in the GIC-enamel interface. None of the enamel or the GIC in contact with it illustrated changes that can be seen in all 1 week and 3 months groups, except the 18 months group, where GIC was changed in areas attached to dentine, enamel and in direct contact with water containing chloramine-T (Figs. 11, 12).
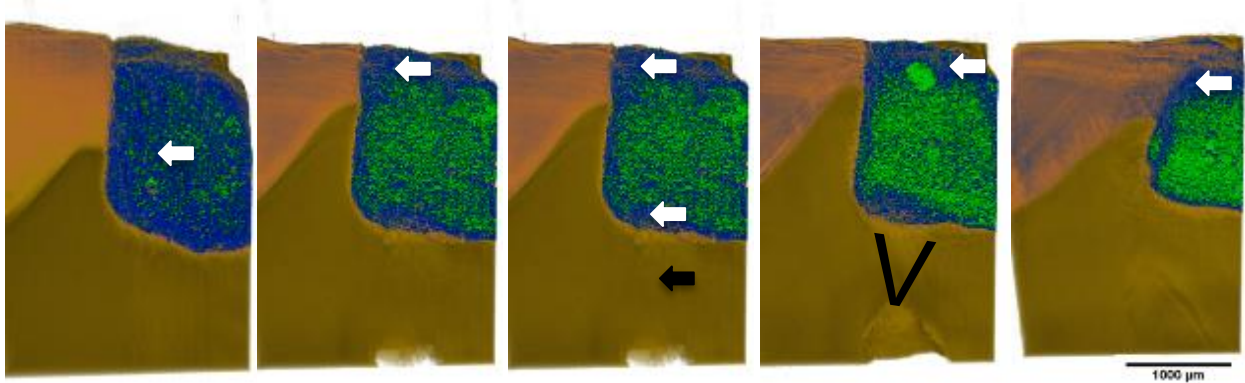
Figure 11 PCE-CT image of the same sample immersed for 18M shows the density change in GIC and dentine. GIC changed externally and internally (white arrows). Dentine changed differently, a layer-like structure at the interface with GIC and a funnel shape like change (black arrow and V letter) close to the pulp horn. Scale bar= 1000 μm.

The changes of GIC contrast thickness in contact with dentine and the outer surface were revealed and proved again using density profiles and statistical linear regression lines. Among all the time point samples, the 18 months immersed group showed the highest value; 18months>3 months>1 week (as shown in Figures 13, 14, 15). GIC change was always higher at the GIC-dentine than the GIC-enamel interfaces.
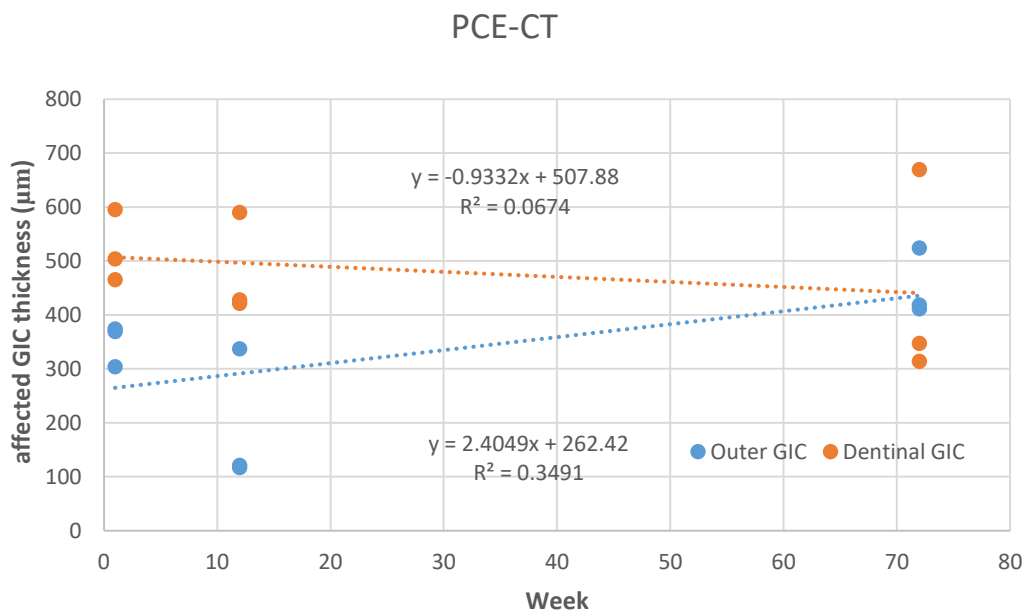

Figure 12 Linear regression (R) of GIC thickness contrast change with time at the outer GIC restoration: R= 0.48 and at the dentinal GIC restoration: R= 0.28.
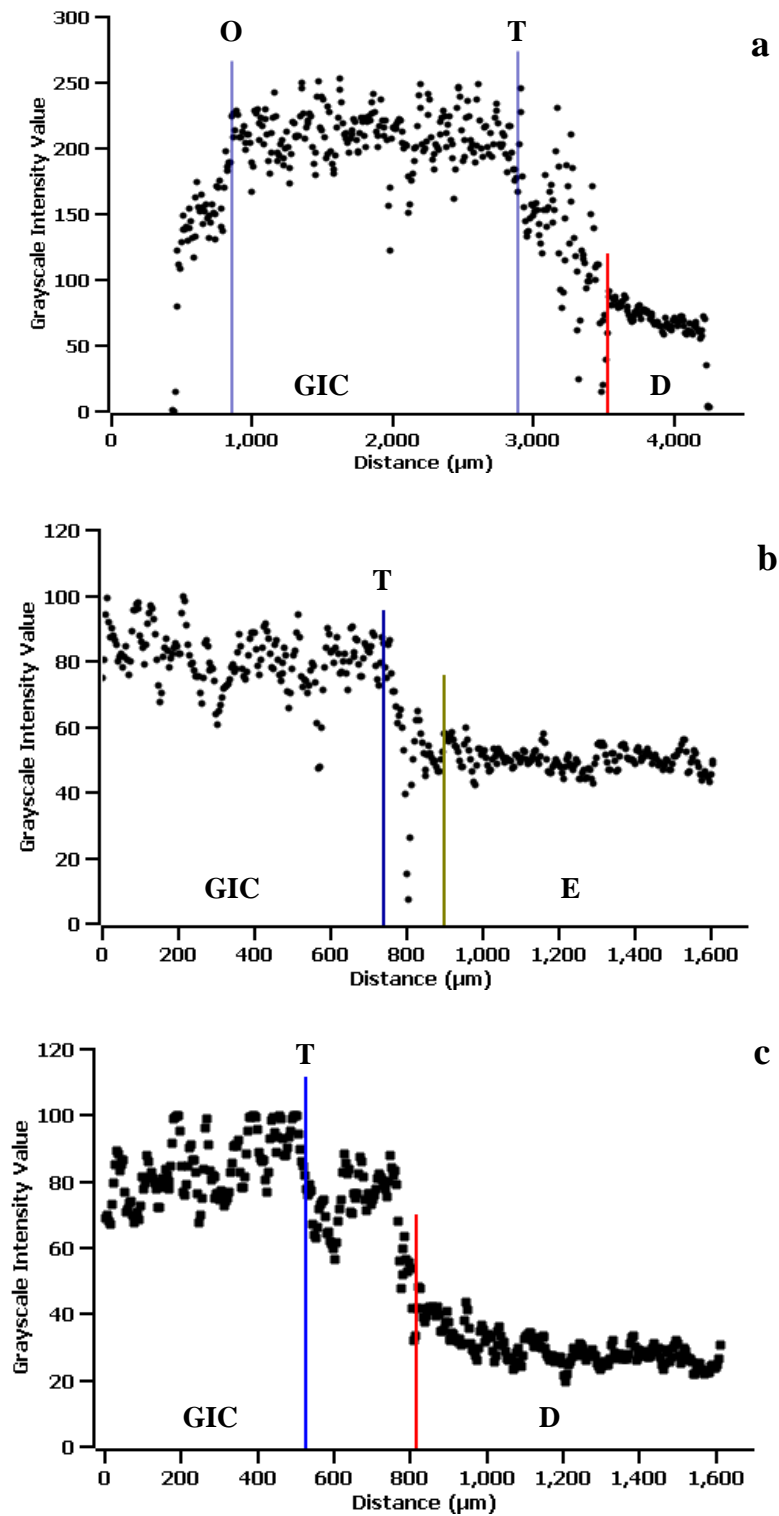
Figure 13 Density profiles of tooth substrates in contact with GIC: Dentine (a), enamel (b), and axial dentine (c) after 18 months' immersion. Red lines indicate dentine and enamel interfaces with GIC. Blue lines represent the change in GIC toward tooth substrates (t) or outer environment (o). Tooth substrate changes occurred mostly at the GIC-dentine interface rather than the GIC-enamel interface.

Additionally, dentine density change was examined, and it was maximal in 18 months and then 3 month samples. 1 week samples displayed slight density change in dentine, with no signs of change in enamel. Enamel change was only seen in 18 months immersed samples, which was about 80μm at the interface with GIC (Fig. 13.b).
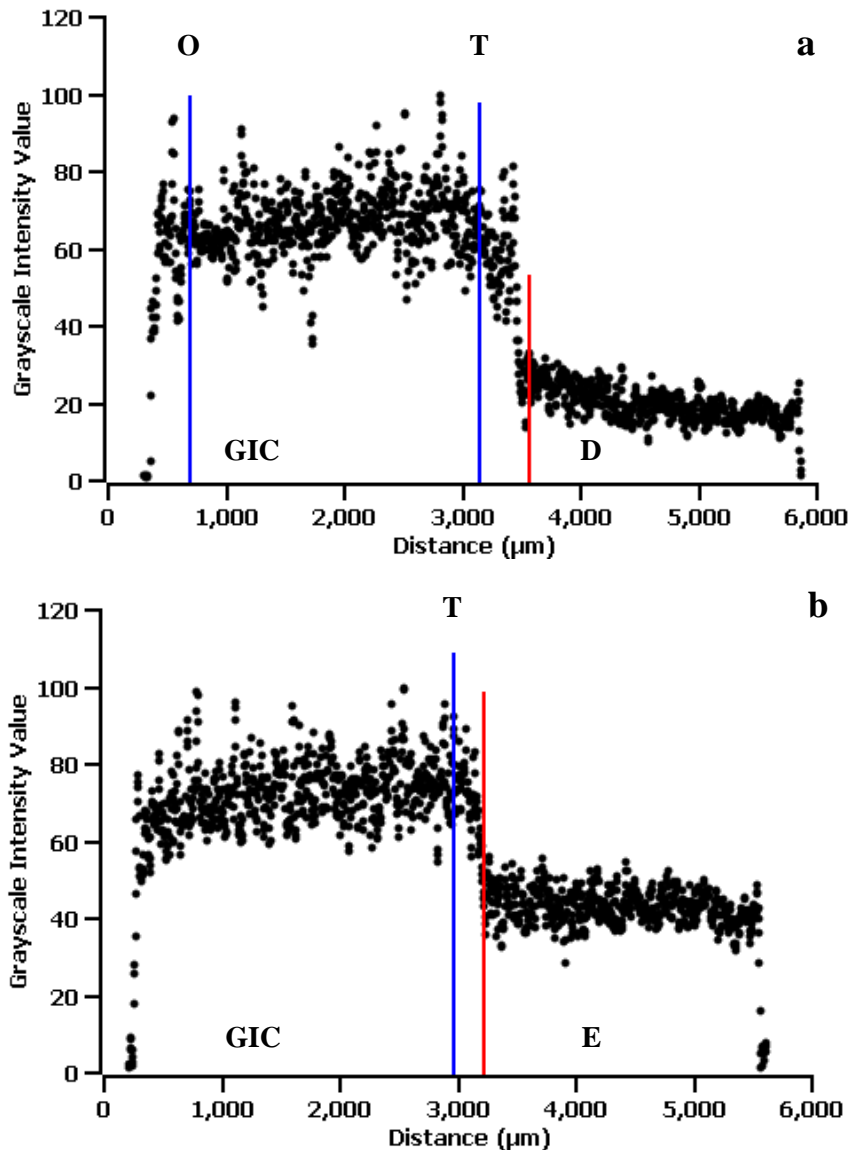
Figure 14 Density profiles of tooth substrates in contact with GIC: dentine (a) and enamel (b) after 3 months' immersion. Red lines indicate dentine and enamel interfaces with GIC. Blue lines represent the change in GIC toward tooth substrates (t) or outer environment (o). GIC changes at the GIC-tooth interfaces are clearly seen. Tooth substrate changes occurred only at the GIC-dentine interface.

Furthermore, PCE-CT indicated the higher dentinal density change of the pulpal wall in comparison to the axial wall (as shown in Figure 13a and c). Both dentine and GIC changes in density at the pulpal wall were higher than the vertical wall.

Density changes in tooth substrates were always higher in dentine in comparison to both axial dentine and enamel. Polynomial linear regression lines from the graphs in Figures 13-15 revealed the following: dentine polynomial fit (R^2) at 18, 3 months and 1 week were $R^2 = 0.785$ (axial dentine was 0.771), 0.698 and 0.737, respectively. Whereas subsequently enamel polynomial fit (R^2) at 18, 3 months and 1 week were $= 0.683$, 0.545 and 0.586.
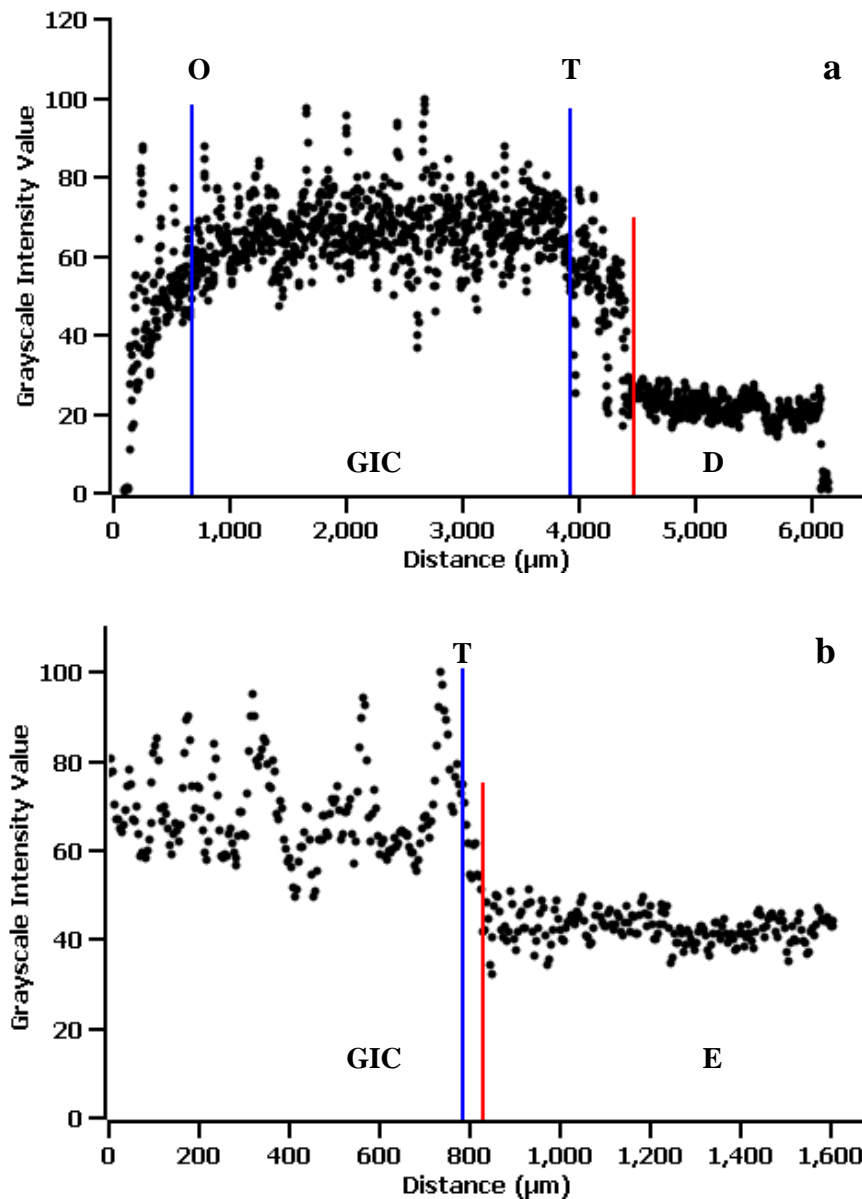
Figure 15 Density profiles of tooth substrates in contact with GIC: dentine (a) and enamel (b) after 1 week immersion. Red lines indicate dentine and enamel interfaces with GIC. Blue lines represent the change in GIC toward tooth substrates (t) or outer environment (o). GIC changes at the GIC-tooth interfaces are clearly seen. Tooth substrate changes occurred only slightly at the GIC-dentine interface.

3.2.4 Confocal Laser Scanning Microscopy (CLSM)

In most of the samples throughout the study, enamel preserved an intact and continuous interface with GIC. It was well integrated and revealed no cracking either at the interface or in the tissue itself in the CLSM study too. Changes in enamel were barely seen, whereas dentine change at the interface with GIC was observed from the first weeks of immersion (Fig. 16).
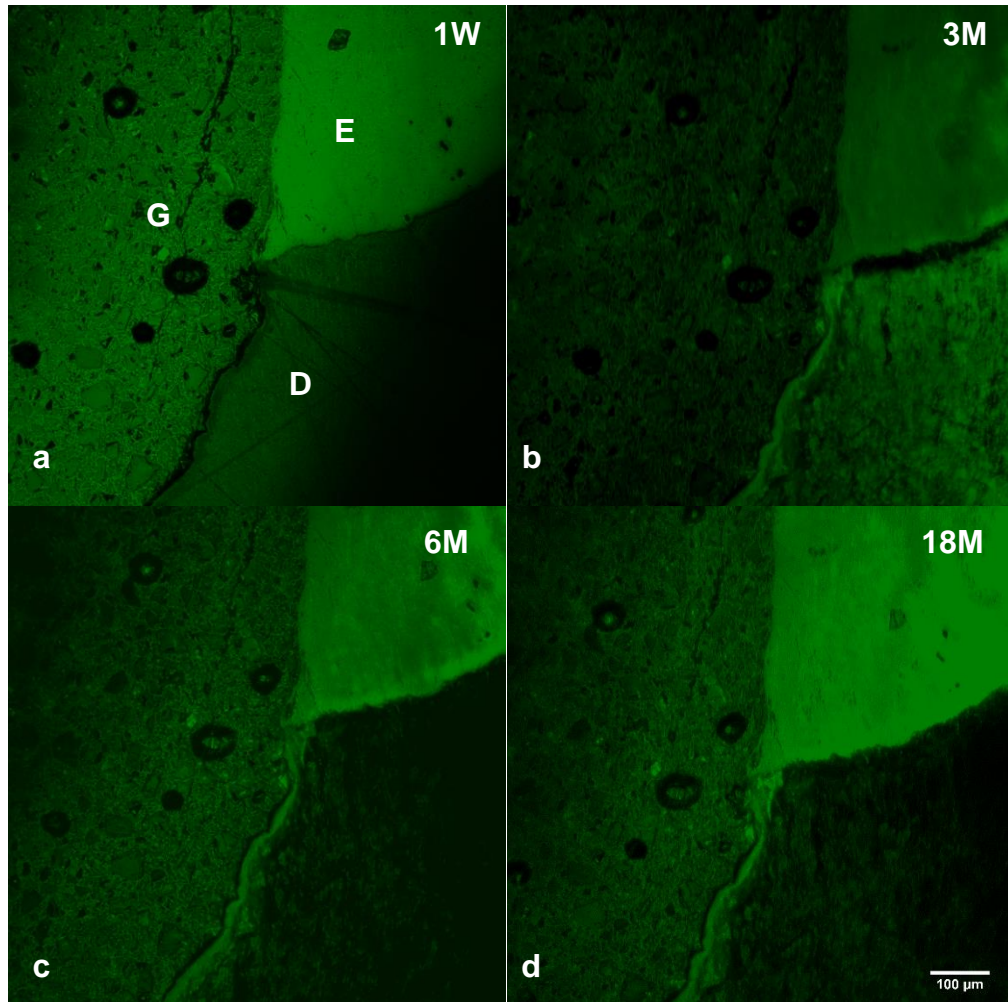
Figure 16 CLSM images revealed changes over weeks and months in the dentine at the interface with GIC after 1 week (a). After 3 months' immersion (b), dentine change disappeared and a well-defined structure or layer (interaction interphase) appeared at the GIC-dentine interface for the rest of the study, after 6 months (c), 18 months (d). Enamel revealed no signs of change and attached well to the GIC. Pores of different size are seen inside GIC. GIC (G), enamel (E), dentine (D). Scale bars= 100 μm.

The change in dentine was apparent after one week of immersion in water, which eventually formed the "interaction interphase layer" (IIL). Three months after immersion, the IIL became a well-distinguished structure that had a brighter reflection than the surrounding GIC and dentine tissue. This was obviously seen afterwards at 6, 9 and 18 months. This interaction interphase layer

was intact with no disruption (not fragmented) from the EDJ point to the bottom of the cavity where the sample was cut (Figs. 16 and 17.a).
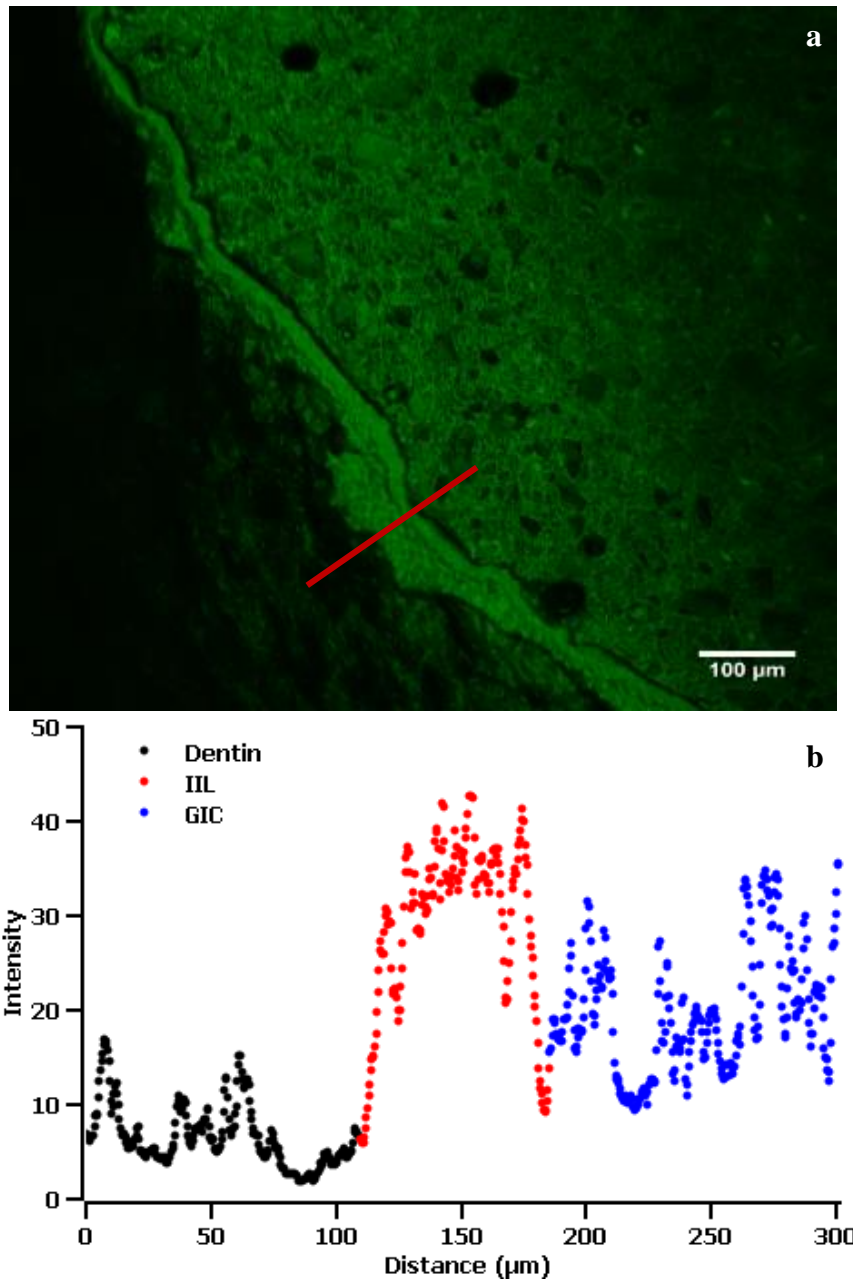
Figure 17 CLSM shows the interaction interphase layer (IIL) at the GIC-dentine interface, which is intact and not fragmented (a), and the histogram (b) of the layer density (red) that has higher intensity than neighboring structures (dentine= black and GIC= blue). Scale bars= 100 μm.

Measurement of the grey values from the IIL displayed a higher value of intensity (reflection) than surrounding structures, namely dentine and GIC, as seen in Figure 17.b. It had a prickled surface (speckled) appearance and looked like a separate structure during CLSM sample analysis. Similarly, other samples showed the IIL formation. However, they were not as intact as the IIL shown in Figure 17, and at some points they were interrupted and looked like delicate structures

formed between the etched dentine and GIC. They appeared as a thin layer, which experienced tension forces that ripped them off and ruptured (Fig. 18).
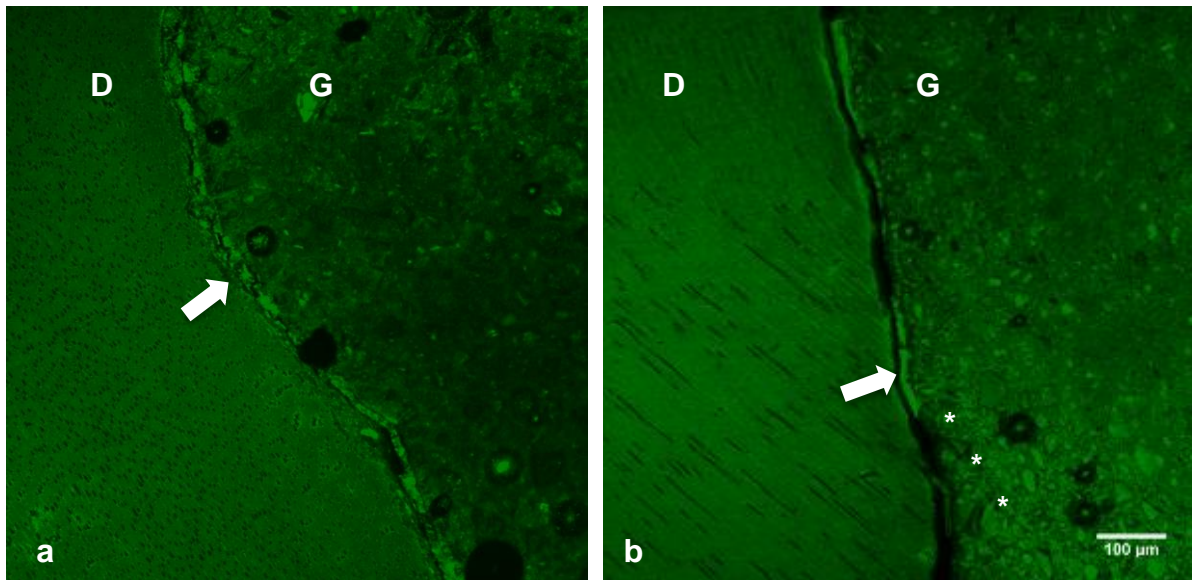
Figure 18 CLSM image shows formation of the brittle and disrupted (arrows) interaction interphase layer between GIC and dentine in an 18 months sample (a, b). The dentinal GIC restoration is changed in appearance in comparison to other GIC parts (asterisk, b). Dentine (D), GIC (G). Scale bar= 100 µm.

Since the samples were stored in a moist environment during the CLSM examination, the cracks in GIC were minimal. GIC was attached firmly to both enamel and dentine. However, there were few cohesive and mixed cracks that appeared at the interface with tooth substrates. Like other techniques, CLSM also showed the GIC change at the dentinal region to the outer GIC restoration. It appeared as a washed out region with brighter scattering 200-400 µm in length away from the interface (Fig. 18.b).

3.2.5 Scanning Electron Microscopy (SEM)

Imaging with SEM and EDX required sample dehydration. The dehydration process, either by using silica gel in a desiccator or CPD, cracked the samples similarly at various locations. Cracking at the GIC-tooth interface was called adhesive, while at the bulk of GIC or tooth substrates it was called cohesive. In region where GIC was partially (adhesive or cohesive) cracked it was called mixed cracking. The number and type of cracks are documented in Table 6. Cracks occurred as follows: cohesive>mixed>adhesive cracks.

Table 6 The crack forms (adhesive, mixed and cohesive) in GIC-tooth samples per time period (1 week, 3, 6, and 18 months). GIC cracks were mostly cohesive. Enamel (E with numbers) cracked cohesively in many samples, whereas dentine (D) never cracked cohesively.

Cracks	1 Week		3 Months		6 Months		18 Months		Total
	D	E	D	E	D	E	D	E	DE
Adhesive	4	-	2	-	4	-	6	1	17
Mixed	10	-	7	1	7	-	9	1	35
Cohesive	8	8 E5	6	8 E8	9	8 E5	6	7 E2	60
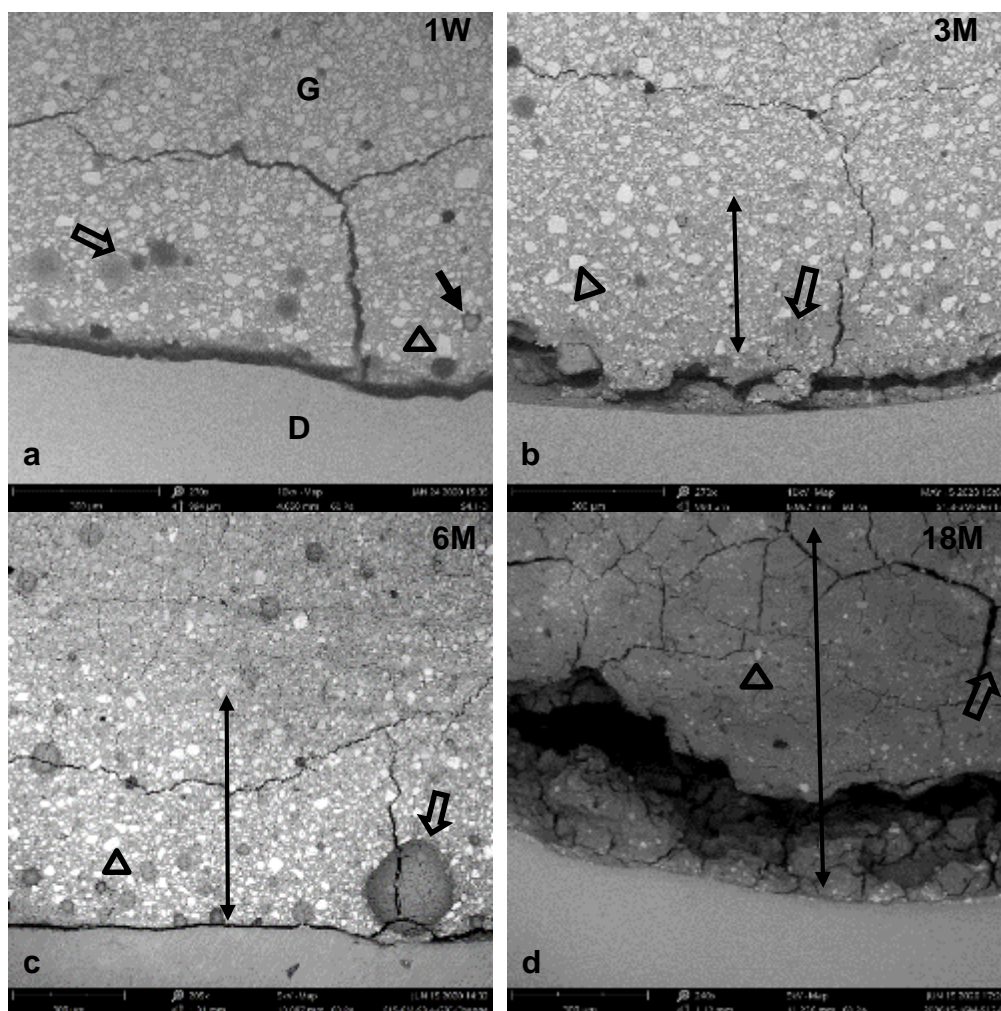
Figure 19 SEM backscatter images show GIC changes in contrast thickness (connected arrows) at the pulpal wall dentine at 1 week (a), 3 months (b) 6 months (c) and 18 months (d). The GIC at 18 months is almost washed out of large particles (triangles). Pores with (black arrows) or without spherical bodies (empty arrows) of different sizes with cracks inside the GIC bulk were seen. Scale bars= 300 μm.

Even though the GIC-enamel interface was mostly intact in both new and old samples, this intact attachment was accompanied by cracks in the GIC or in the enamel tissue close to the interface. In both cases, the cracks were cohesive, and the GIC-tooth interfaces were safe. Change of enamel at the GIC-enamel interfaces was not seen throughout the study (Fig. 20). However, the GIC attached to enamel that faced outside, the outer GIC restoration, showed signs of change in contrast thickness, which was clearly seen in 18 months immersed samples.
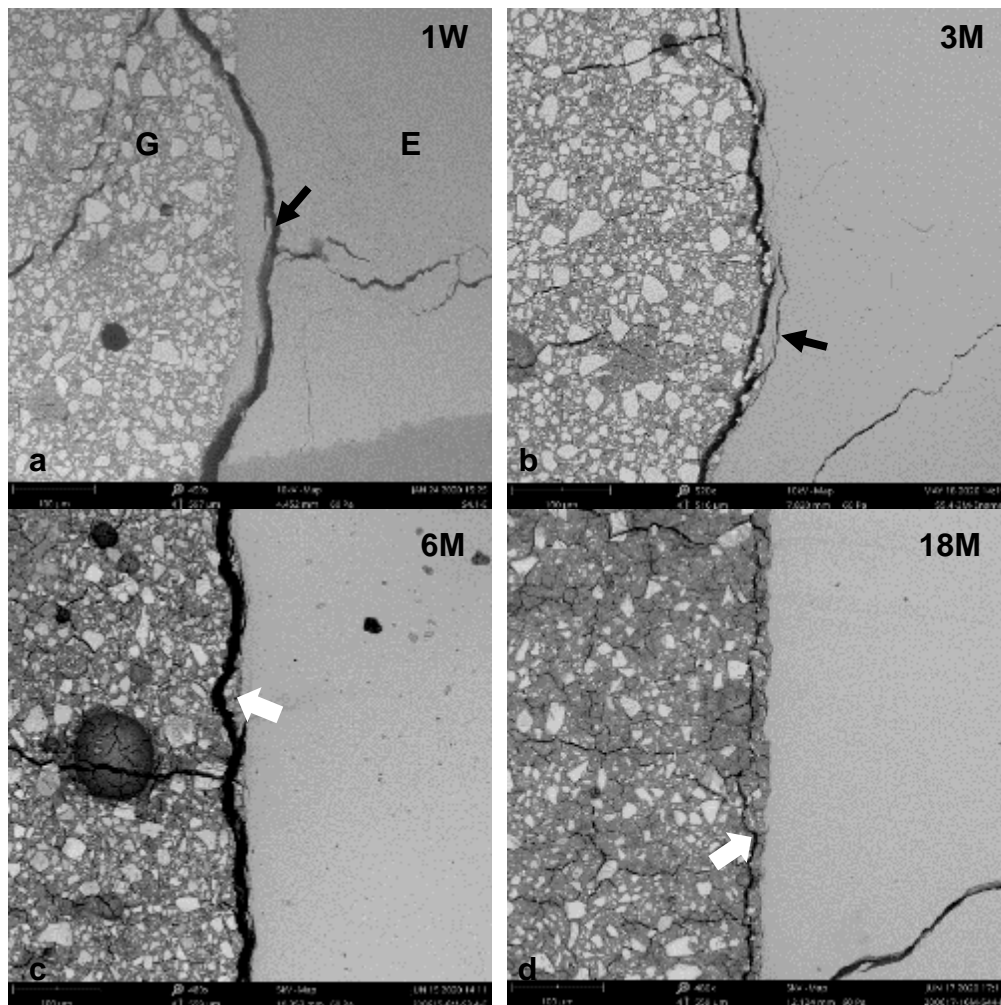
Figure 20 SEM images show GIC-enamel attachment. Enamel is continuous with GIC. Cohesive failure of enamel (black arrow) in 1 week and 3 months (a, b) and cohesive failure of GIC (white arrow) in 6 and 18 month immersed samples (c and d) are seen. Cracks and pores are spread in the samples. Scale bars= 100 μm.

Similarly, the GIC-dentine interface was intact and continuous but less than that of GIC-enamel interfaces. GIC-dentine interfaces were cracked mixed and cohesively with few adhesive cracks. The GIC was cracking cohesively, but no sample showed cohesive cracking of dentine in this study. The GIC in contact with dentine changed in contrast thickness per time period, mostly at

the pulpal wall of the cavity. This change was clearly seen in 6 and 18 month immersed samples (Fig. 19).

The dentine, on the other hand, revealed changes of density at the interface with GIC at all the time points. The changes in dentine were highly apparent in 18 month samples. Figure 21 shows the changes in dentine at the interface. Dentine changes in 1 week, 3 and 6 month samples were 15-20µm at the interface, and started to increase with time (18 months) to reach more than 150-400µm, especially in the pulpal dentine The change was also seen in the axial dentine, but less in depth in comparison to the pulpal dentine change.
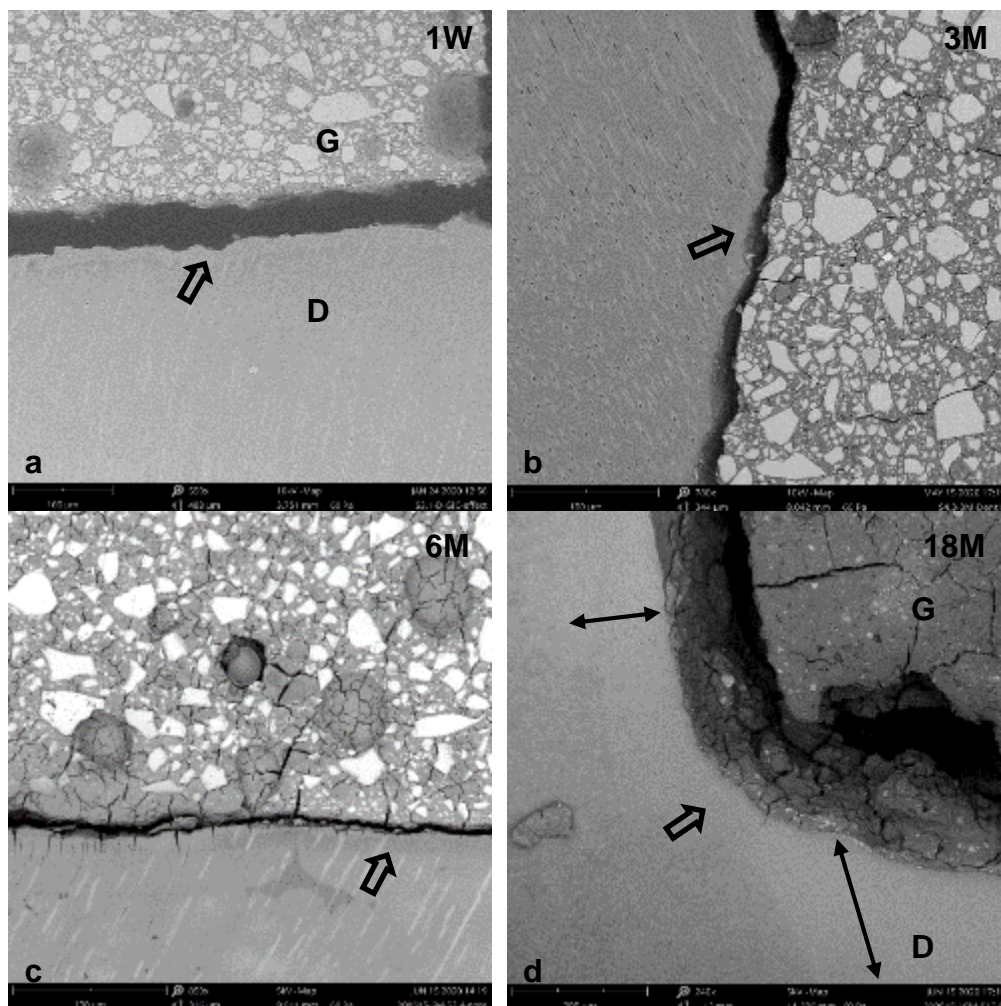
Figure 21 SEM images show dentine change in density (arrows) at 1 week (a), 3 months (b), 6 months (c), and 18 months (d). The dentine change is small in a, b and c, but drastically increased at 18 months (connected arrows), especially at the pulpal dentine. The GIC is still covering the dentine at the interface despite the crack (d). Pores and cracks are seen in the samples. Scale bars in a, b and c= 100 µm, and in d= 300 µm.

Beside the changes in dentine, all the groups revealed layer-like structures at their GIC-dentine interfaces, located exactly between the etched surface of dentine by the GIC and the GIC itself in 1 week, 3 and 6 month samples. This layer was broken and fragmented in most of the samples and had the same color appearance as spherical bodies inside GIC pores, except in an 18 months sample, where it was intact and had its own brighter appearance differentiating it from the surroundings (Fig. 22).
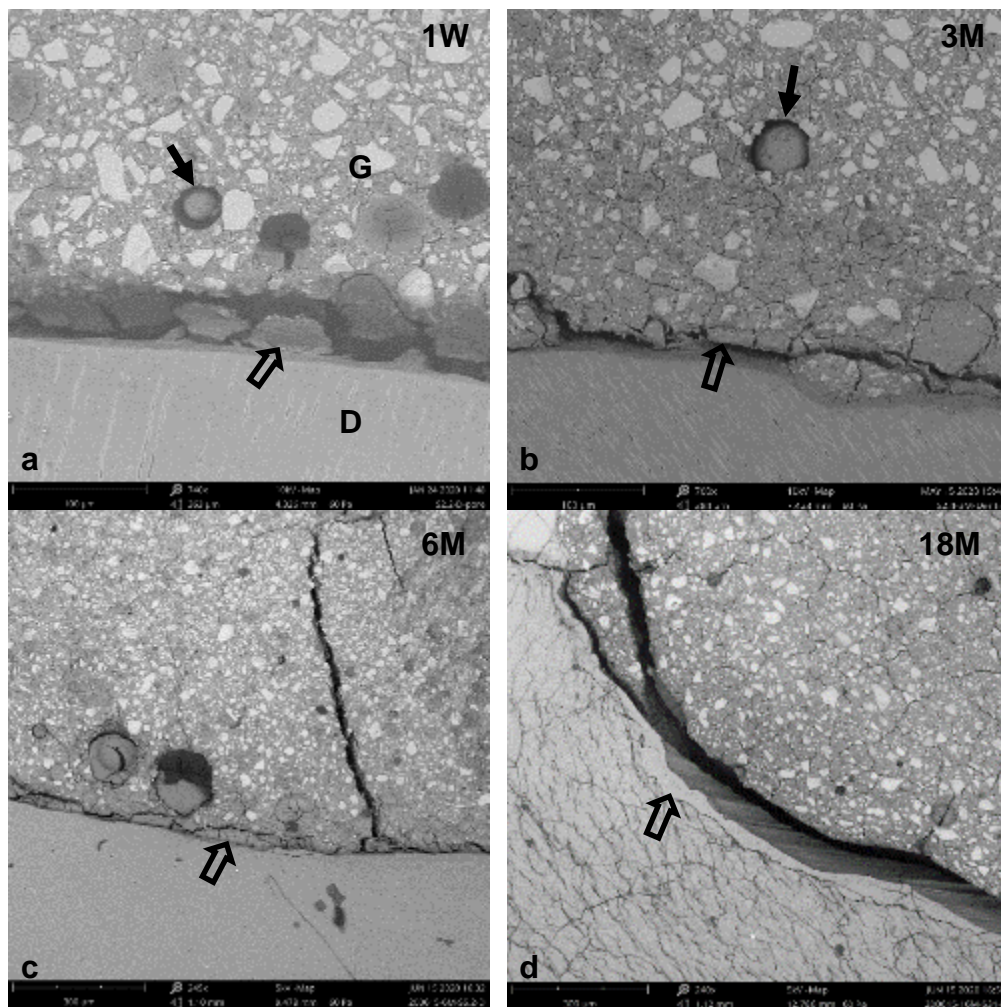
Figure 22 SEM images show interaction interphase layer (IIL, empty arrows) in contact with dentine, at 1 week (a), 3 months (b) 6 months (c) and 18 months (d). The IIL are fragmented at all time points except at 18 months. Spherical bodies inside pores (black arrows). Scale bars a and b= 100, c and d= 300 μm.

In 18 month samples, no spherical bodies were seen to compare their color to the layer at the GIC-dentine interface. The layer and spherical bodies inside GIC pores did not appear in the GIC-enamel regions, including the interface in the same samples.
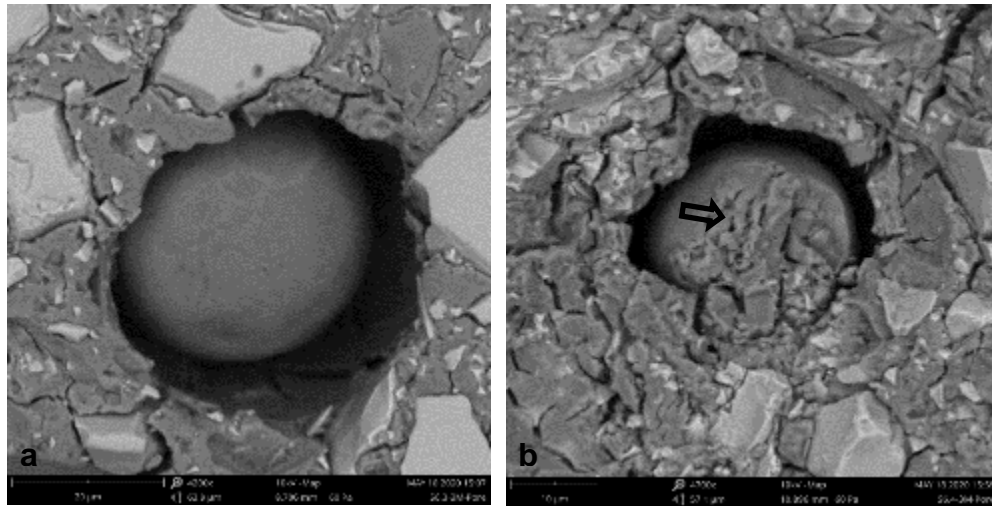
Figure 23 SEM images show spherical bodies inside pores in the GIC at 3 months, where the spherical body is intact (a), and when its surface is eroded (arrow) (b). Scale bars a= 20 μm and b= 10 μm.

Spherical bodies inside pores at the GIC regions in contact with dentine were shaped according to the interior contour of the pores. They were mostly spherical in shape and had semi-smooth surfaces, as in Figure 23.a. They appeared as shrunk spheres and stayed inside the pore without completely filling it. The spheres cores internally seemed to have hard structures, so that when eroded superficially, the material within the cores was visible (Fig. 23.b).

3.2.6 Energy Dispersive X-ray spectroscopy (EDX)

With EDX, the GIC-tooth substrate interfaces were mapped through color coding of the ion elements present in both GIC and tooth substrates. GIC contained F, Na, Mg, Al, Si, P, Ca, La and Sr in its composition as spectral peaks of those elements were raised in the sample spectrum. Here we presented 6 elements (F, Al, Ca, P, Sr, and La) for EDX mapping, of which some of them, i.e., Ca, P and F, are also present in tooth substrates.

In both 1 week and 3 month samples, no obvious changes were mapped in both GIC- enamel and dentine interfaces, whereas after 3 months' immersion, changes in the GIC-dentine interfaces were depicted. Particularly in the 18 month samples, Ca and P on the GIC interface and Sr, Al, and La on the dentine side were increased (Figs. 24-27).
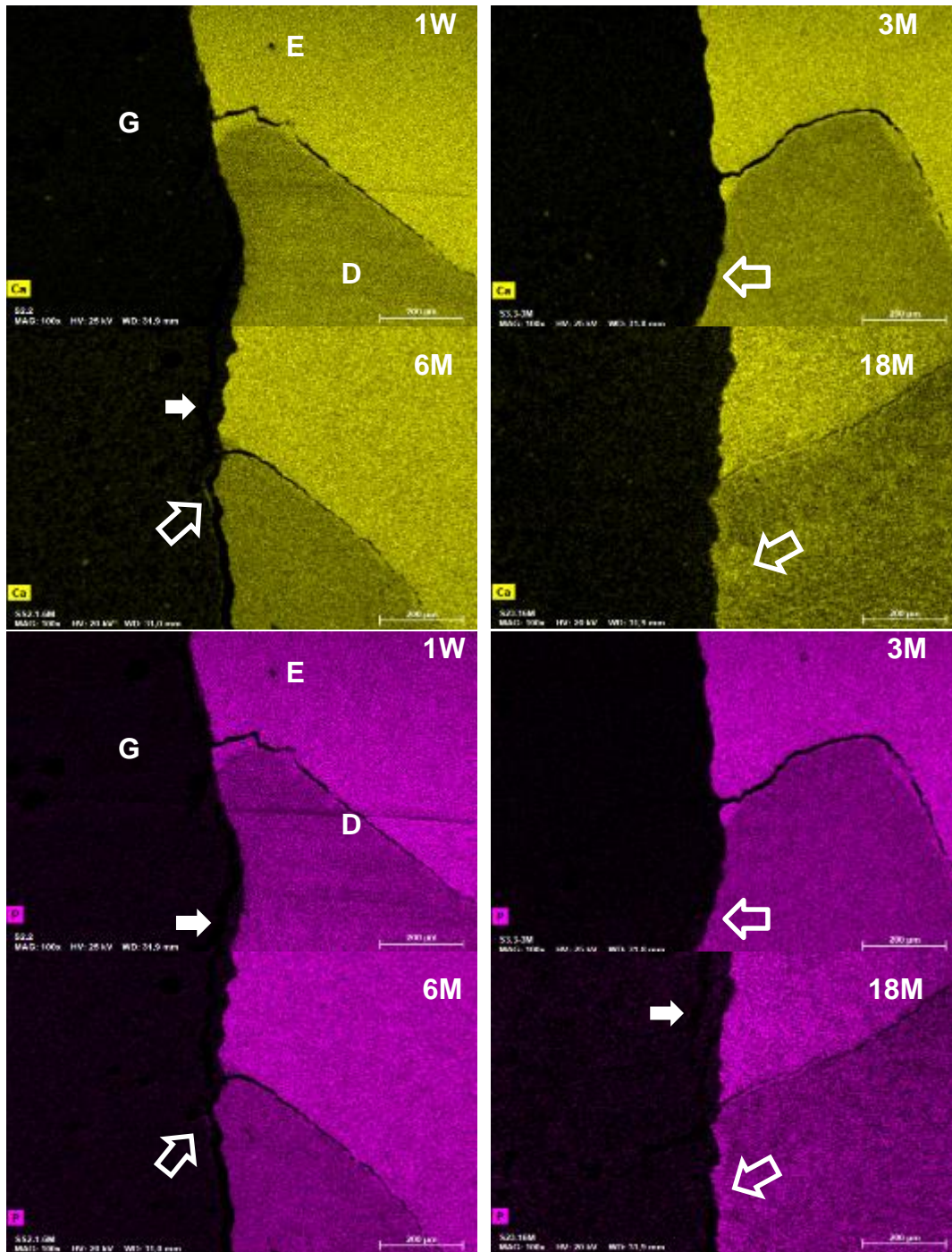
Figure 24 EDX elemental mapping of EDJ region in the 1 week, 3, 6 and 18 month samples for Ca (upper 2 rows) and P (lower 2 rows). No mineral density changes were visible in or around the GIC-tooth substrate interfaces in 1 week samples, whereas afterwards mineral density changes were seen (empty arrows) at GIC-dentine interfaces. Enamel contains more Ca and less P than dentine, and showed no mineral change at the interface with GIC. GIC cracked cohesively at GIC-tooth interfaces (white arrows). Scale bars= 200 μm.
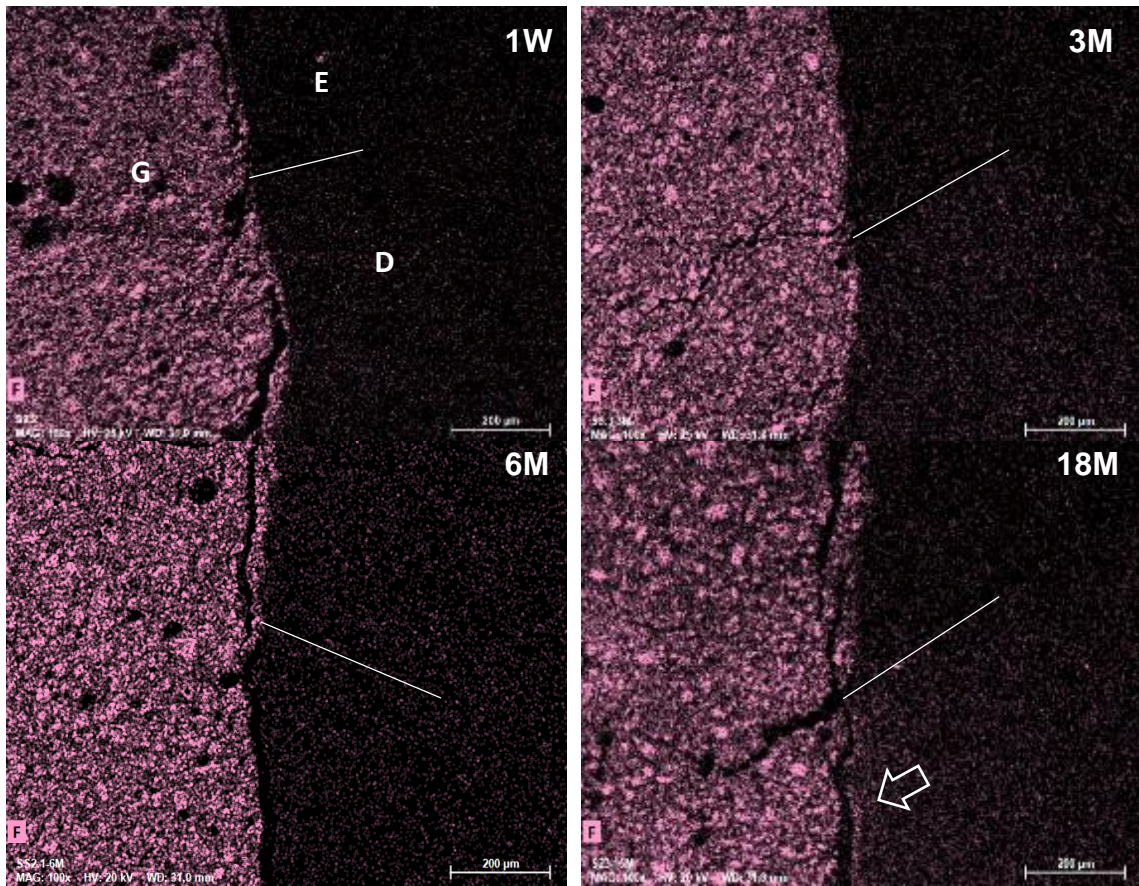
Figure 25 EDX elemental mapping of EDJ region in the 1 week (W), 3, 6 and 18 month (M) samples for F. No mineral density changes were visible in or around the GIC-tooth substrate interfaces in 1 week, 3 and 6 month samples, whereas afterwards mineral density changes were seen (empty arrow) in dentine at the interface. Enamel showed no sign of mineral change. White lines= EDJ. Scale bars= 200 µm.
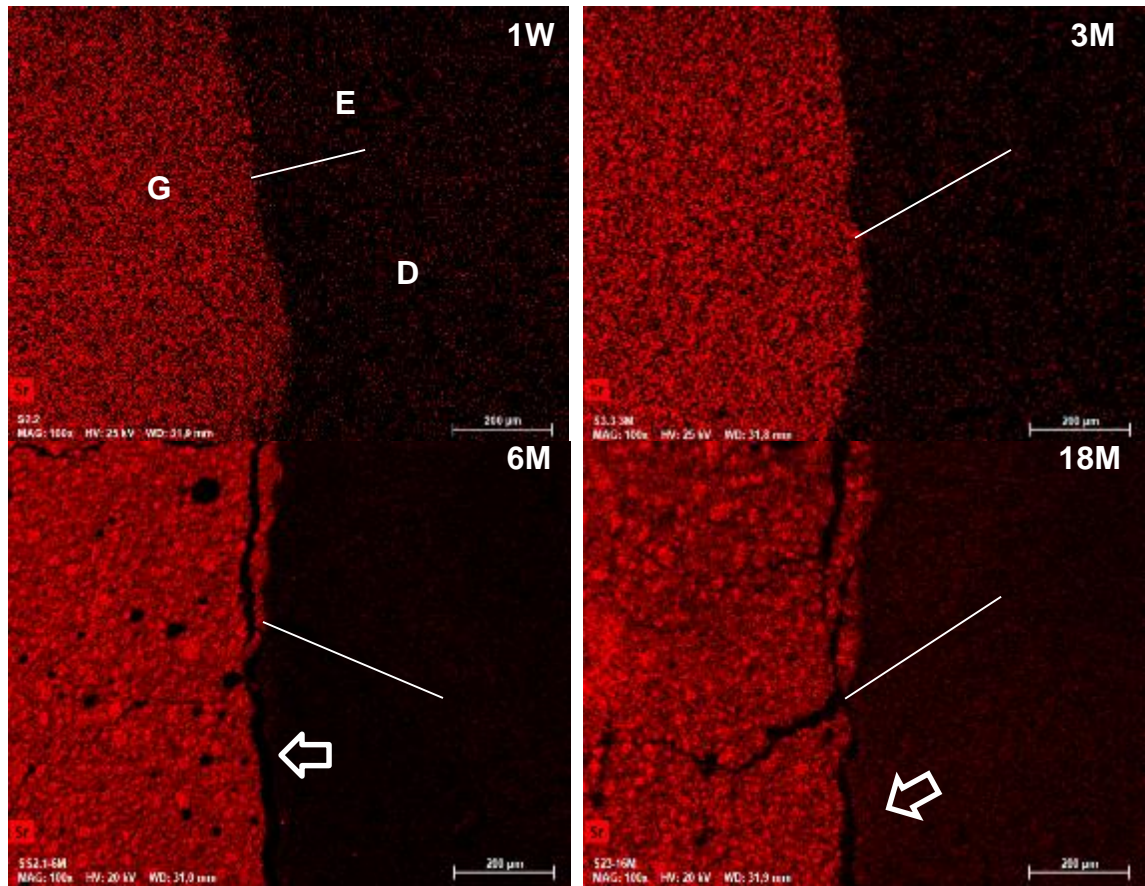
Figure 26 EDX elemental mapping of EDJ region in the 1 week (W), 3, 6 and 18 month (M) samples for Sr. No mineral density changes were visible in or around the GIC-tooth substrate interfaces in 1 week and 3 month samples, whereas afterwards mineral density changes were seen (empty arrows) in dentine at the interface. Enamel showed no sign of mineral change. White lines= EDJ. Scale bars= 200 µm.
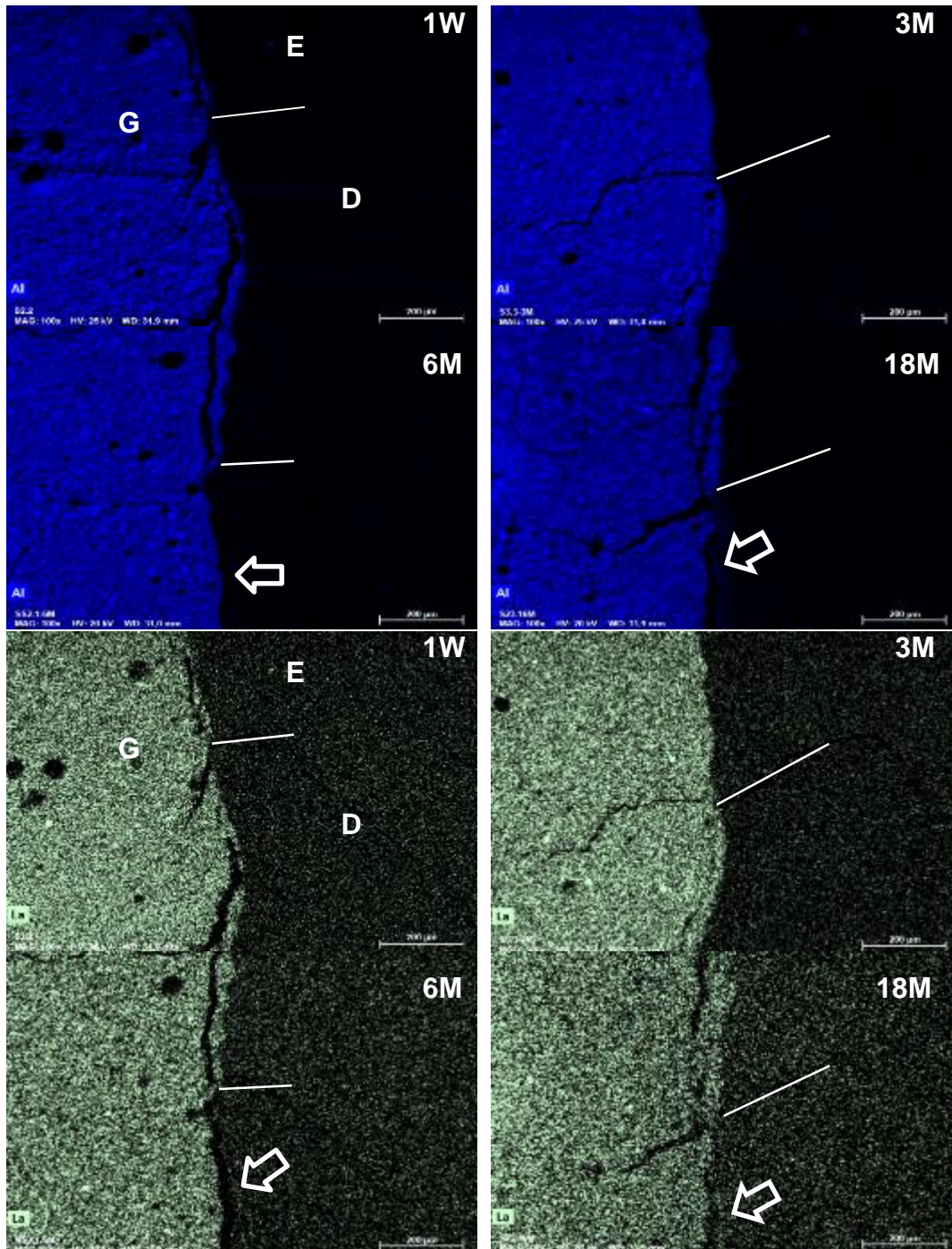
Figure 27 EDX elemental mapping of EDJ region in the 1 week (W), 3, 6 and 18 month (M) samples for Al (upper 2 rows) and La (lower 2 rows). No mineral density changes were visible in or around the GIC-tooth substrate interfaces in 1 week and 3 month samples, whereas afterwards mineral density changes were seen (empty arrows) in dentine at the interface, particularly in 18 month samples. White lines= EDJ. Scale bars= 200 µm.

.

GIC-Dentine at the pulpal region

EDX mapping showed higher dentine change (mineral density) in the pulpal wall than the axial walls of the cavity. A thin rim of changes appeared at the GIC and dentine interfaces in 3 and 6 months axial walls, whereas dentine change at the pulpal cavity walls reached 150-250µm (Fig. 28).
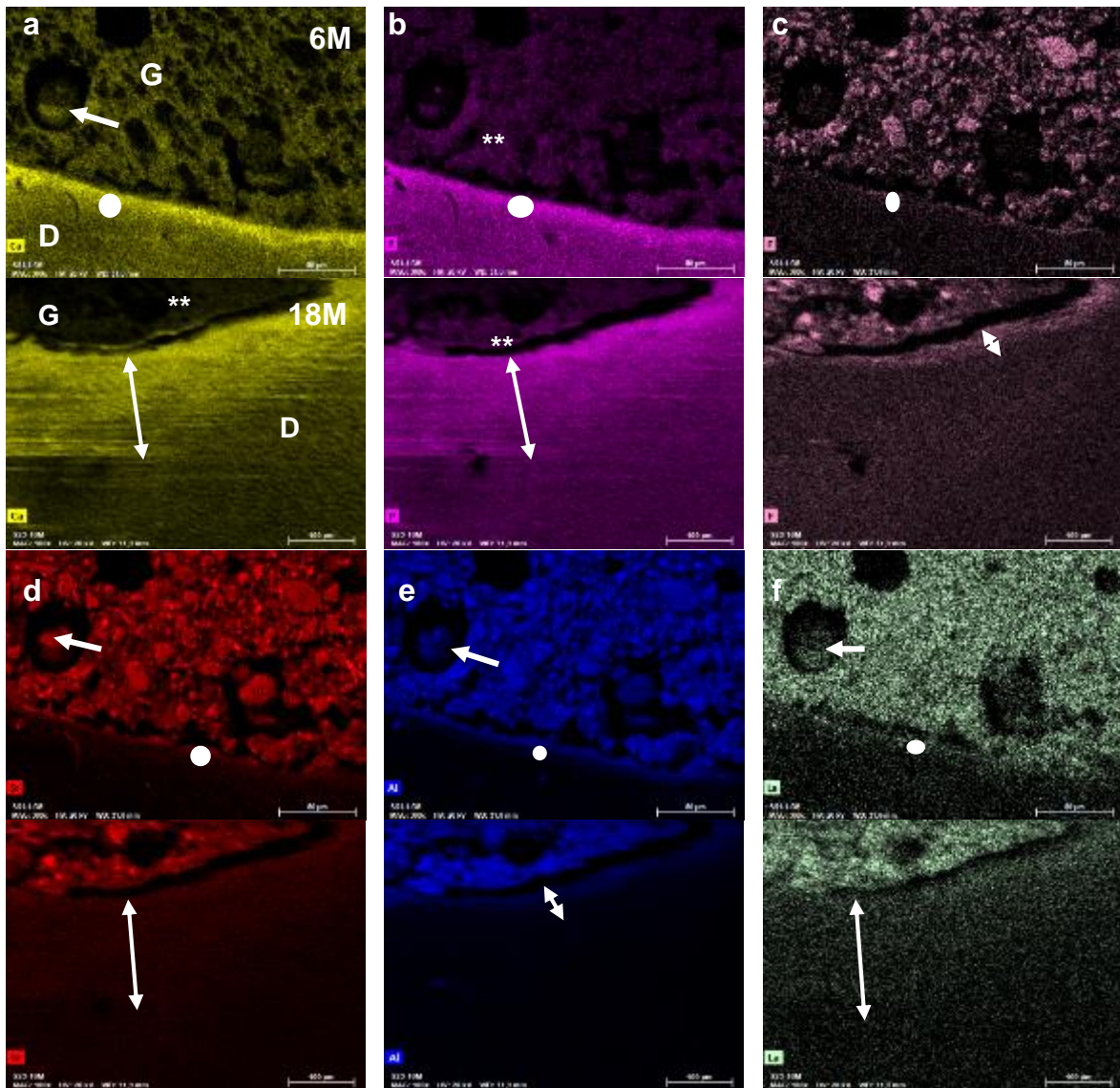
Figure 28 EDX elemental mapping of pulpal wall region in the 6 and 18 month samples for Ca (a), P (b), F (c), Sr (d), Al (e), and La (f). Changes of mineral density in GIC (*), as well as dentine at 6 months (white circles) and 18 months (connected arrows) were obvious in or around the GIC-tooth substrate interfaces. GIC contains pores, some of which have spherical bodies inside (white arrow), and their composition is explained later in this chapter. All elements were increased slightly at the dentine interphase, particularly in the 18 month samples, which contain artifacts (shift) seen in Ca and P images. Scale bars= 80 and 100 µm

EDX-point analysis of dentine-enamel change

In order to quantify the weight percentage (wt%) of every element, point analysis of dentine and enamel was performed at the EDJ at different areas (10, 50, 100, 150, and 200μm) away from GIC-tooth interface. The GIC used in this study was Sr based cement and also contained La, which are usually not present in the tooth substrates. In general, F, Al, Sr, La were increased in wt% toward the GIC-tooth substrate interfaces at all the time points as shown in the tables below. Dentine exhibited higher wt% of the elements than enamel, except for F, Na and Mg where they were higher in enamel than dentine in the 18 months water immersed samples.

Si and La were leached less into the tooth substrates in comparison to other elements, however their level at the 18 months' time period was elevated at the interface (10 μm). Although Silicon is one of the main components of GIC glass composition, it was not detected in the one week samples.

Table 7 EDX-point scan for element distribution (wt%) at dentine interface at 10, 50, 100, and 200 μm with GIC after 1 week immersion.

Dentine	F	Na	Mg	Al	P	Ca	Sr	La
10	2.53	1.04	0.28	0.56	8.91	20.14	0.39	0.00
50	1.82	0.70	0.46	0.23	10.74	26.48	0.32	0.00
100	1.74	0.79	0.36	0.08	10.17	25.27	0.31	0.05
200	2.54	0.89	0.61	0.36	7.76	17.24	0.17	0.00

Table 8 EDX-point scan for element distribution (wt%) at enamel interface at 10, 50, 100, and 200 μm with GIC after 1 week immersion.

Enamel	F	Na	Mg	Al	P	Ca	Sr	La
10	1.50	1.16	0.53	0.36	9.80	21.38	0.09	0.05
50	1.55	1.26	0.36	0.19	11.50	24.47	0.33	0.02
100	1.34	0.96	0.13	0.08	12.32	28.52	0.09	0.02
200	0.90	0.80	0.17	0.11	13.34	31.11	0.06	0.00

Both Ca and P, which are the main component of tooth hydroxyapatite structures were not detected in a trend (Tab. 7-12). They were reduced 10-50 µm away from the interface and then elevated in the 100 µm away from the interface, and so on. Although the wt% ratios of these two elements decreased at the interface, the values were close to other point scans away from the interface in the 18 months group (Tab. 13 and 14).

Table 9 EDX-point scan for element distribution (wt%) at dentine interface at 10, 50, 100, 150 and 200 µm with GIC after 3 months' immersion

Dentine	F	Na	Mg	Al	Si	P	Ca	Sr	La
10	2.73	1.38	0.71	0.54	0.01	10.30	23.15	0.81	0.04
50	2.68	1.61	1.04	0.69	0.06	11.21	20.37	0.50	0.04
100	3.53	1.78	0.89	0.91	0.03	8.77	15.78	0.01	0.02
150	2.50	1.45	0.76	0.84	0.02	10.89	21.77	0.50	0.02
200	2.09	1.27	0.80	0.56	0.02	12.54	27.10	0.95	0.05

Table 10 EDX-point scan for element distribution (wt%) at enamel interface at 10, 50, 100, 150 and 200 µm with GIC after 3 months' immersion.

Enamel	F	Na	Mg	Al	Si	P	Ca	Sr	La
10	1.42	1.58	0.40	0.11	0.03	12.83	26.58	0.26	0.00
50	1.25	1.32	0.32	0.08	0.01	12.01	27.31	0.17	0.00
100	1.01	1.48	0.33	0.10	0.01	12.65	27.03	0.13	0.01
150	0.82	1.05	0.28	0.09	0.01	11.72	28.28	0.11	0.04
200	1.44	1.84	0.43	0.11	0.03	12.95	25.02	0.03	0.01

Table 11 EDX-point scan for element distribution (wt%) at dentine interface at 10, 50, 100, 150 and 200 μm with GIC after 6 months' immersion.

Dentine	F	Na	Mg	Al	Si	P	Ca	Sr	La
10	1.01	0.77	0.29	0.07	0.01	13.97	32.04	1.43	0.00
50	0.84	0.73	0.30	0.20	0.03	13.20	36.85	0.47	0.04
100	0.87	0.59	0.26	0.11	0.00	15.45	36.03	0.98	0.01
150	0.60	0.52	0.28	0.07	0.00	16.19	36.34	0.99	0.13
200	0.34	0.88	0.28	0.24	0.00	15.45	37.69	0.76	0.01

Table 12 EDX-point scan for element distribution (wt%) at enamel interface at 10, 50, 100, 150 and 200 μm with GIC after 6 months' immersion.

Enamel	F	Na	Mg	Al	Si	P	Ca	Sr	La
10	2.62	1.15	0.66	0.27	0.06	6.66	17.69	0.74	0.10
50	1.90	0.80	0.70	0.20	0.00	6.56	15.09	0.23	0.12
100	2.23	1.25	0.77	0.20	0.01	8.33	16.15	0.73	0.20
150	1.86	1.05	0.76	0.17	0.02	7.53	17.68	0.50	0.07
200	1.16	0.39	0.47	0.10	0.02	8.50	19.82	0.47	0.04

Table 13 EDX-point scan for element distribution (wt%) at dentine interface at 10, 50, 100, 150 and 200 μm with GIC after 18 months' immersion.

Dentine	F	Na	Mg	Al	Si	P	Ca	Sr	La
10 M	2.30	1.15	0.39	1.31	0.09	14.08	30.48	2.92	0.74
50 M	2.28	1.12	0.41	0.80	0.05	14.19	33.82	2.39	0.23
100 M	3.18	1.63	0.50	0.68	0.04	11.53	26.18	1.85	0.10
150 M	1.53	1.02	0.32	0.49	0.02	16.52	37.55	2.68	0.14
200 M	1.87	0.64	0.25	0.26	0.01	15.87	38.52	2.73	0.10

Table 14 EDX-point scan for element distribution (wt%) at enamel interface at 10, 50, 100, 150 and 200 μm with GIC after 18 months' immersion.

Enamel	F	Na	Mg	Al	Si	P	Ca	Sr	La
10 M	4.58	2.13	0.71	1.06	0.06	6.54	10.20	1.29	0.09
50 M	5.01	2.17	0.69	0.90	0.05	5.21	7.20	0.92	0.16
100 M	4.26	2.28	0.75	0.71	0.04	5.47	8.15	0.94	0.08
150 M	2.45	2.29	0.84	0.69	0.06	6.06	9.47	1.03	0.05
200 M	2.37	2.24	0.85	0.68	0.06	6.53	10.26	1.08	0.07

EDX-point analysis of the interaction interphase layer

The interaction interphase layer was scanned in a quantitative manner using an EDX-point scan to differentiate its composition from the surrounding dental tissue. The wt% results of the elements that appeared in this IIL region (P1 in Fig. 29) and away from it (P2= 100 and P3= 500 μm) are presented in Table 15. At the IIL, P1, most of the ions were increased in comparison to the other two points away from it. However, this was not quite true for Ca and P, which showed a slightly lower wt% than the other two points away from the IIL. What is worth mentioning is that this sample was immersed in water for 18 months and showed a high level of Si and La at IIL.
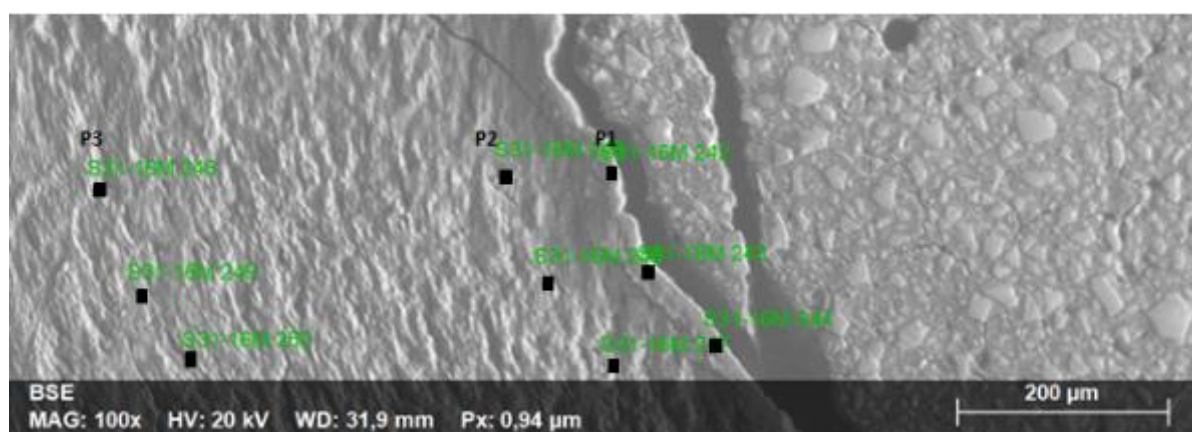
Figure 29 Backscattered image of the interaction interphase layer showing EDX point scan analysis at the IIL (P1= 10 μm) and away from it (P2= 100 μm and P3= 500 μm). Scale bars = 200 μm.

Table 15 EDX-point scan of elements (wt%) at the interaction interphase layer (P1) and away from it at 100 μm (P2) and 500 μm (P3).

	F	Na	Mg	Al	Si	P	Ca	Sr	La
P 1	2.90	1.19	0.50	1.36	0.10	12.62	27.62	3.01	0.52
P 2	2.74	1.43	0.42	0.61	0.04	12.31	28.60	2.22	0.12
P 3	2.27	1.18	0.44	0.18	0.01	13.94	33.12	2.05	0.07

EDX observation of changes at the dentinal GIC restoration

All the different techniques illustrated a change at the outer and dentinal GIC restoration. The outer GIC was in direct contact with the storage solution. However, the dentinal GIC restoration was in direct contact with the pulpal wall of the cavity, the dentine. Therefore, GIC changes at the base of the cavity were assessed using EDX object scans and compared to the middle (where GIC was not changed) of the GIC restoration (Fig. 30) to calculate the wt% of interesting elements.

In the 1 week, 6 months and 18 month samples, Al and Si were reduced, whereas Ca and P were increased at the interface. Fluoride, which is higher in GIC than in tooth structure, was decreased in the 1 week and 6 month samples and increased in the 18 month samples at the GIC-dentine interfaces. Sr and La, were decreased after 1 week, increased at 6 months immersion at the GIC-dentine interface, but then decreased at 18 months immersion' (Tab. 16, 17, 18). Because of the drastic change in the bulk of GIC after 18 months' immersion, regions of interest were selected at the areas where the GIC looked normal in the middle of restoration and abnormal at the dentinal GIC restoration.
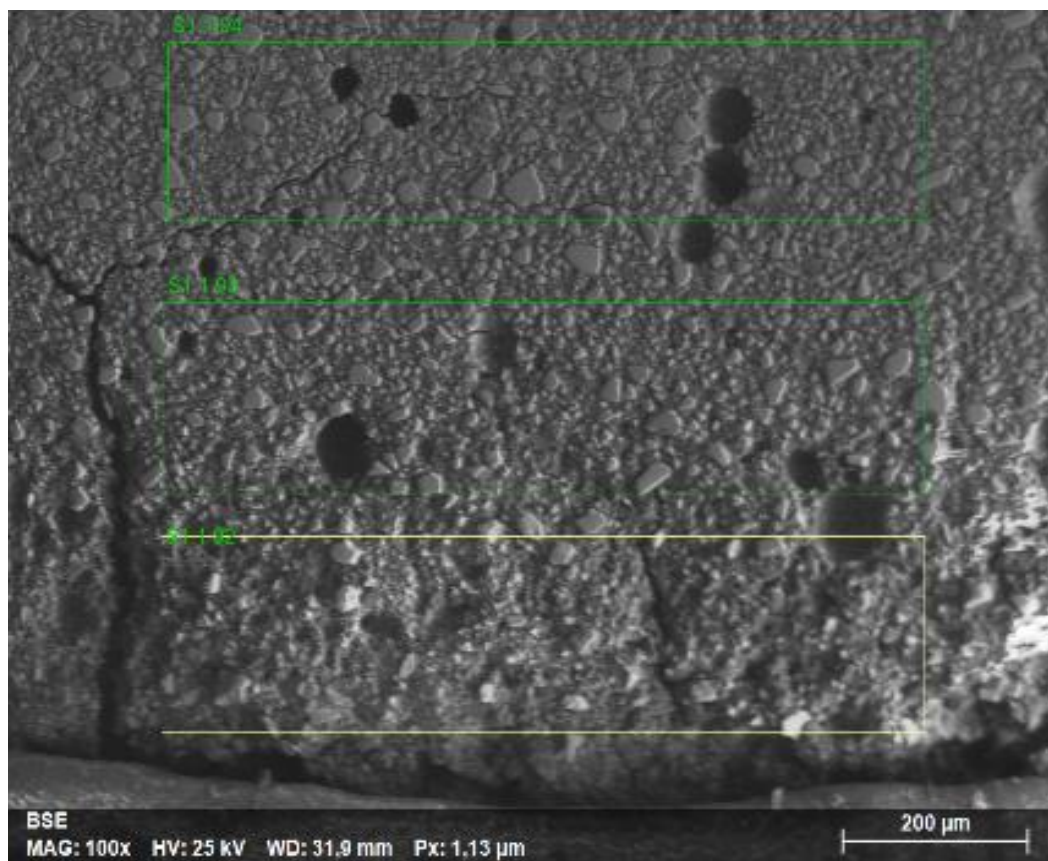
Figure 30 SEM image shows EDX-object analysis (regions) of changes in the GIC restoration at the pulpal wall of the cavity and GIC in the middle of restoration after 1 week immersion. Signs of GIC erosion are seen in the part in contact with dentine. Scale bars= 200 μm.

Additionally, GIC attached to axial dentine was also compared to the dentinal GIC restoration side. In the axial GIC, there was more of F, Al, Si, Sr and La than Pulpal GIC, which only had higher Ca and P (Tab. 18). GIC-dentine interaction at the axial wall was less active than GIC-dentine at the pulpal wall. GIC adjacent to the axial wall preserved more of the ions and took less Ca and P when compared to pulpal GIC.

Table 16 EDX-object analysis of changes in the GIC restoration via elements (wt%) in 1 week samples, 200, 400 and 600 μm away from the dentine.

	F	Na	Mg	Al	Si	P	Ca	Sr	La
200	9.02	2.05	0.65	10.57	5.81	1.70	0.71	2.22	2.77
400	10.39	2.28	0.71	11.50	7.15	1.57	0.39	2.83	2.94
600	9.67	2.29	0.50	12.13	8.29	1.66	0.23	8.41	3.78

53

Table 17 EDX-object analysis of changes in the GIC restoration via elements (wt%) in 6 month samples, 200 and 600 μm away from the dentine.

	F	Na	Mg	Al	Si	P	Ca	Sr	La
200	6.55	1.41	0.00	9.13	6.98	2.39	5.74	10.49	4.94
600	9.18	1.77	0.32	10.42	8.48	1.57	2.93	8.92	2.83

Table 18 EDX-object analysis of changes in the GIC restoration via elements (wt%) at 18 month samples, in axial dentine and 400 and 2000 μm away from pulpal dentine.

	F	Na	Mg	Al	Si	P	Ca	Sr	La
400	10.87	1.36	0.74	6.51	2.75	1.19	0.71	3.46	0.80
Axial	12.97	1.54	0.72	6.78	3.30	1.10	0.62	4.62	0.92
2000	10.23	2.05	0.63	7.08	4.49	0.98	0.47	5.64	1.15

Pores and spherical bodies in GIC

In order to show the difference between the pore inclusions, the GIC matrix and particles spread in the GIC, some samples with pores occupied by spherical bodies were mapped and point analyzed (Fig. 31). In the 18 month samples, no spherical bodies were seen in the pores, and thus no analysis is available for those samples.

According to the spectrum gained from those points, in P1 the spherical body showed a sharp peak of Si and a low peak of Al. In P2, the particle, both Si and Al peaks were similar, with the Al peak a bit higher, whereas in P3 the Al peak was higher than the Si peak. The F peak was higher in P2 and P3 than P1. See Figure 32 for the spectrum peaks taken from a 6 months sample.
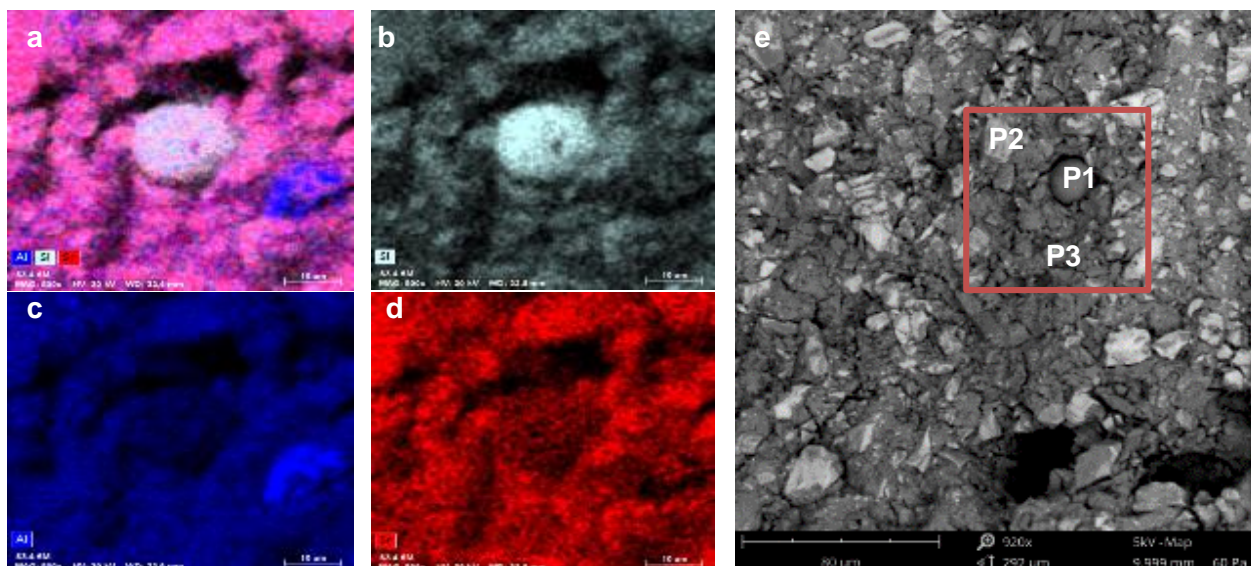
Figure 31 EDX elemental mapping of the spherical body region for Al, Si and Sr (a), the sphere that is completely Si (b), and the surroundings of the pore that contain Al (c) and Sr (d). SEM-backscattered image (e) of the GIC pore containing spherical body (P1) in 6 months immersed sample with GIC particle (P2) and Matrix (P3). P1 was highly made of Si. P2 and 3 contained less Si (b). Scale bars in mapping and SEM images= 10 and 80 μm.
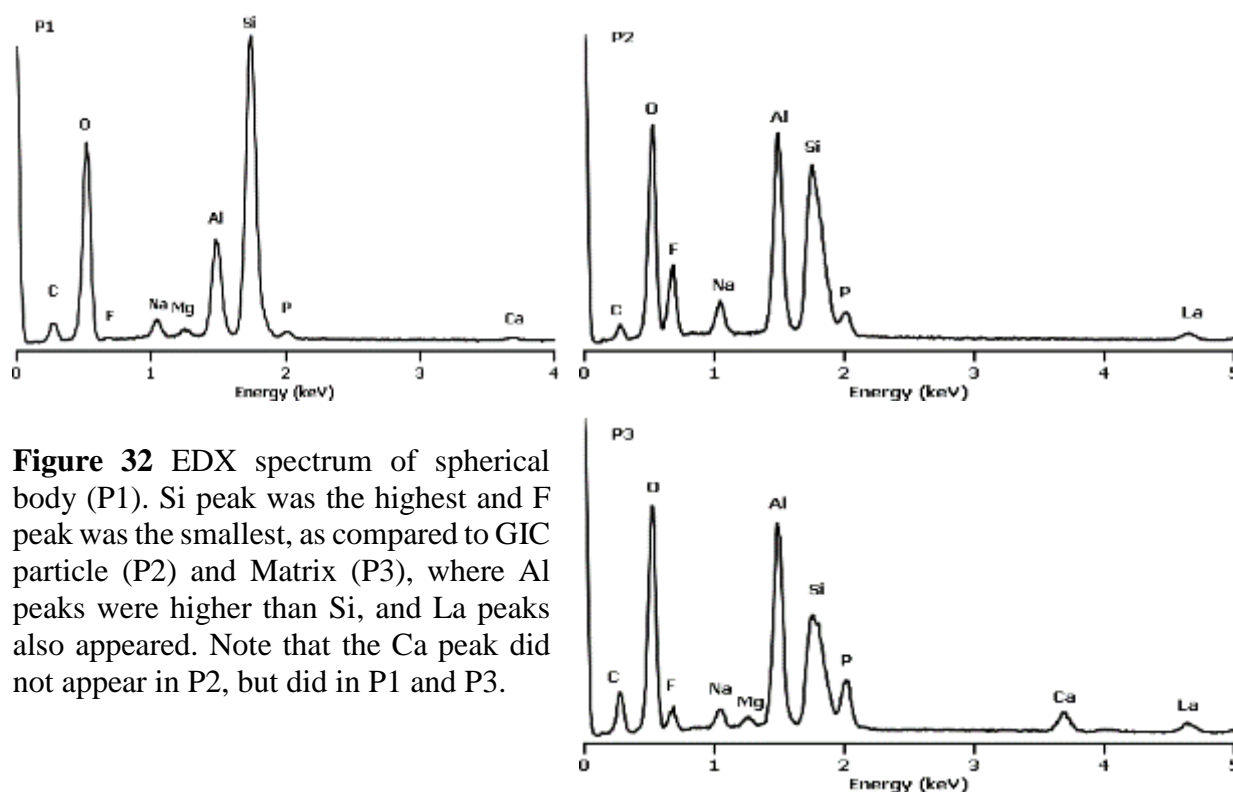
Figure 32 EDX spectrum of spherical body (P1). Si peak was the highest and F peak was the smallest, as compared to GIC particle (P2) and Matrix (P3), where Al peaks were higher than Si, and La peaks also appeared. Note that the Ca peak did not appear in P2, but did in P1 and P3.

What was seen in the spectrums is presented in Table 21 for the 6 months sample. SiO_2 had a tall peak in the P1 spectrum and thus had a higher wt% than the other elements in P2 and P3. This was also seen in 1 week and 3 month samples too (Tab. 19 and 20).

55

Table 19 Elemental analysis (wt%) of the spherical body (P1) with GIC particle (P2) and surrounding matrix (P3) in 1 week samples.

Wt.%	F	Na	Al	Si	P	Ca	Sr	La
P1	1.68	1.73	10.01	26.73	1.63	0.54	1.61	0.07
P2	3.08	3.95	19.55	9.66	5.05	0.39	10.24	5.20
P3	4.44	1.95	15.53	11.02	3.63	0.96	17.47	6.11

Table 20 Elemental analysis (wt%) of the spherical body (P1) with GIC particle (P2) and surrounding matrix (P3) in 3 month samples.

Wt%	F	Na	Al	Si	P	Ca	Sr	La
P1	1.15	1.56	13.61	19.48	6.40	2.84	5.68	1.20
P2	13.96	3.75	15.82	12.16	2.28	0.03	10.11	4.02
P3	4.79	2.22	16.08	11.37	3.38	1.72	21.79	6.48

Table 21 Elemental analysis (wt%) of the spherical body (P1) with GIC particle (P2) and surrounding matrix (P3) in 6 month samples.

Wt%	F	Na	Al	Si	P	Ca	Sr	La
P1	1.63	2.42	7.21	18.96	0.60	0.40	1.93	0.05
P2	18.18	3.07	10.23	6.67	1.58	0.04	11.45	2.03
P3	6.79	1.64	9.45	3.92	2.73	1.53	8.48	2.44

3.3 GIC-tooth interface resin replicas

GIC was well attached to the tooth substrates and formed IIL. With the application of all the 2D and 3D techniques, no visual change was observed at the GIC-enamel interface, whereas the GIC-dentine interface saw the formation of an IIL. In order to check the resistance of this IIL to acidity, some samples were acid etched, impressions taken and replicas were reproduced for comparison (Fig. 33). A higher magnification of the IIL from the replica (Fig. 33.d) revealed the shape of the bulge area, which to some extent resembled the prickles or speckled features that appeared on the IIL in the CLSM images (Fig. 17.a). This layer remained higher than the neighboring GIC and dentine tissue after acid attack.
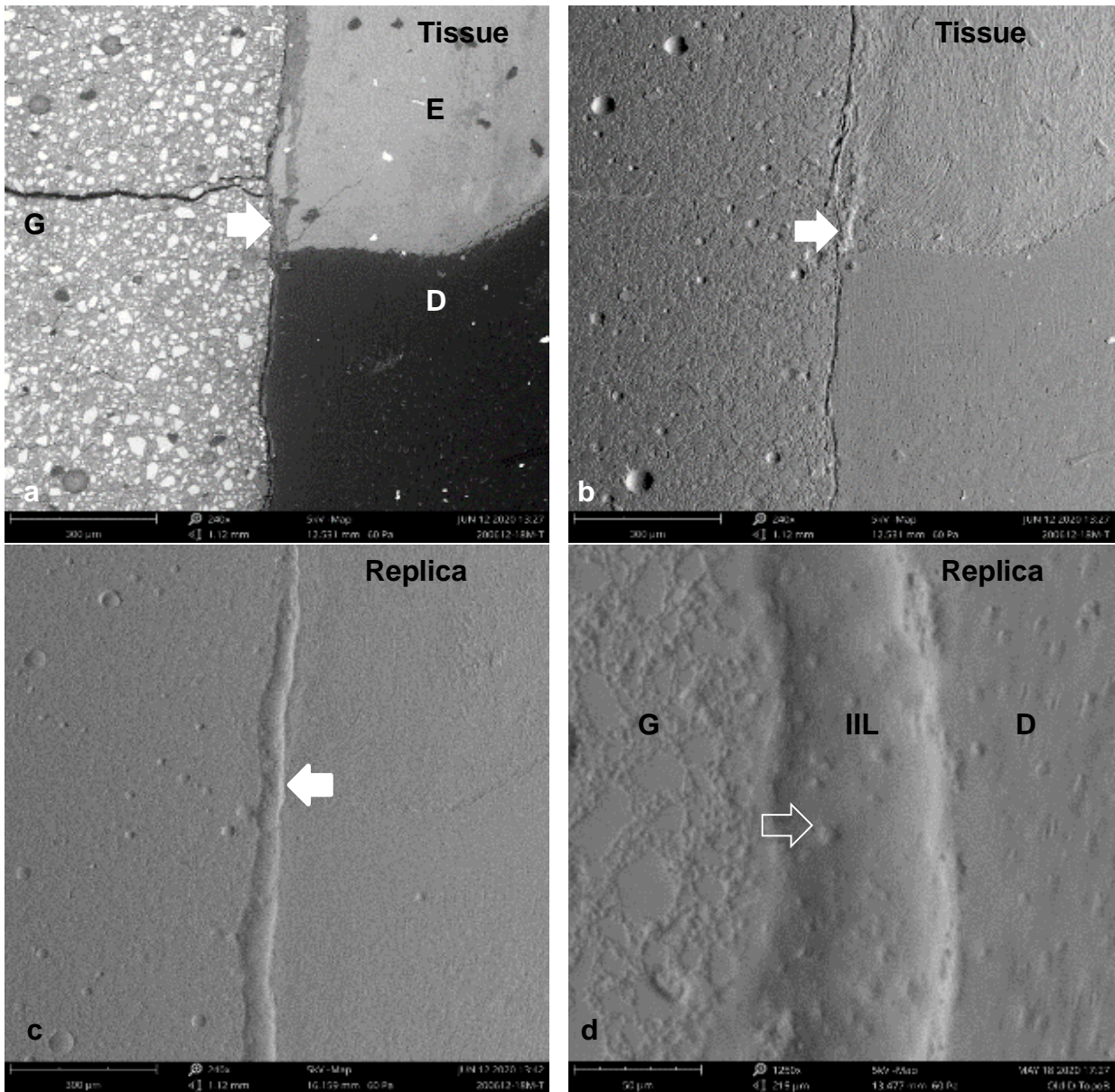
Figure 33 Backscattered (a) and Topo B detector images of the tissue sample (b) and its replica (c and d) for SEM imaging and GIC-tooth interface analysis in 18 months sample. Remnants of the IIL (arrows) are clearly seen on the enamel in (a, b) in comparison to the replica (c). The topography of IIL appears as a bulge over the sample surface with a speckled appearance (empty arrow) after acid etching. Scale bars= 300 μm in (a, b, and c) and = 50 μm in (d).

In the real dehydrated sample, remnants of the layer were seen. The remnants had mostly stayed and were seen in enamel part, as proven by Topo B image - see the shadow of the remnants enamel part (Fig. 33.a, and b). However, in the replica, the IIL looked intact and continuous along the GIC-tooth interfaces (Fig. 33.c).
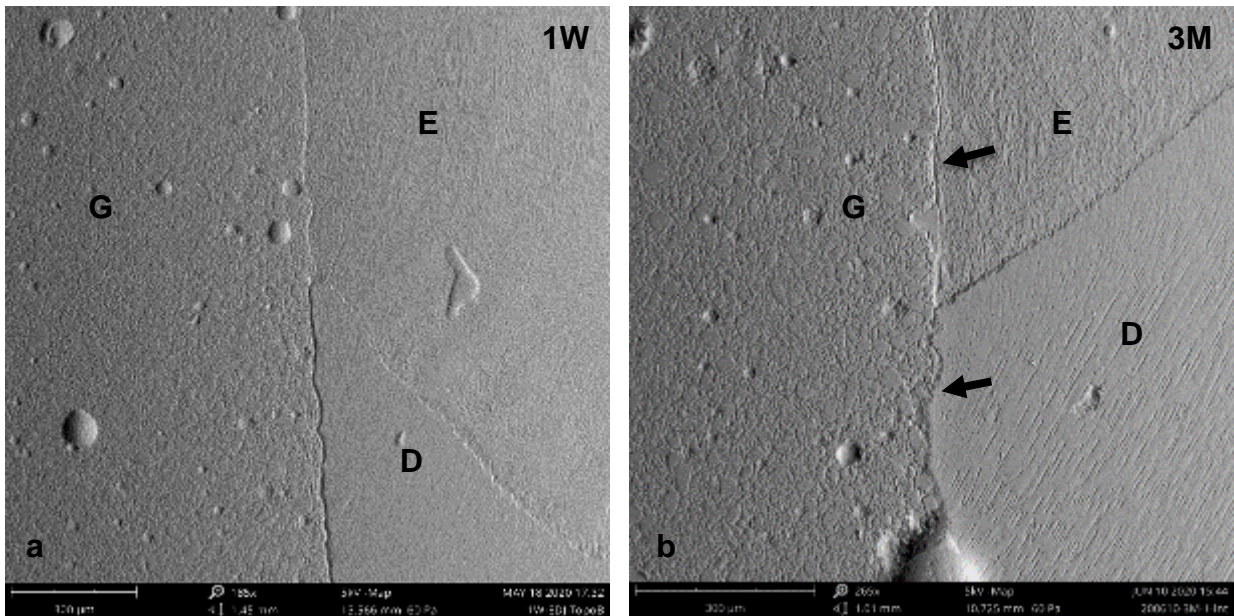
Figure 34 SEM-Topo B detector images of replicas from samples after 1 week show no change at the GIC-tooth substrate interfaces (a), but after 3 months (b) the GIC-tooth interfaces show slight changes (arrows) particularly in dentine where the GIC-dentine interface is slightly elevated (c). Scale bars= 300 µm.

Through the replicas, the IIL was revealed at both the enamel and dentine interfaces with GIC. The IIL seemed to develop after around 3 months of contact between the GIC and dentine, forming a slight bulge (Fig. 34.b). With time a layer was formed at the GIC-enamel interface, as seen after 18 months storage, which became wider and higher, especially at the dentine part. Stability of this layer to acid attack was confirmed as it remained higher than the surrounding GIC and tooth substrates (Fig. 33.c and d). The bulged layer had a shadow to the left, since the Topo B detector source illuminated the region from the right side. Therefore, any high points on the sample surface would exhibit shadows formed to their left, while low regions, concavity or pores had their shadows to their right sides.

The axial dentine showed a thin layer in comparison to the wide layer formed at the pulpal side of the cavity between the GIC and dentine (Fig. 35). This region showed GIC change in contrast in the all previous techniques, and more ionic exchange in EDX analysis. However, examining the same region from the dehydrated tissue samples where replicas were made from did not reveal the same layer structures seen in replicas, but rather some IIL remnant structures that shifted from the interface, as they were not stable enough, or yet to set (Fig. 36.b).
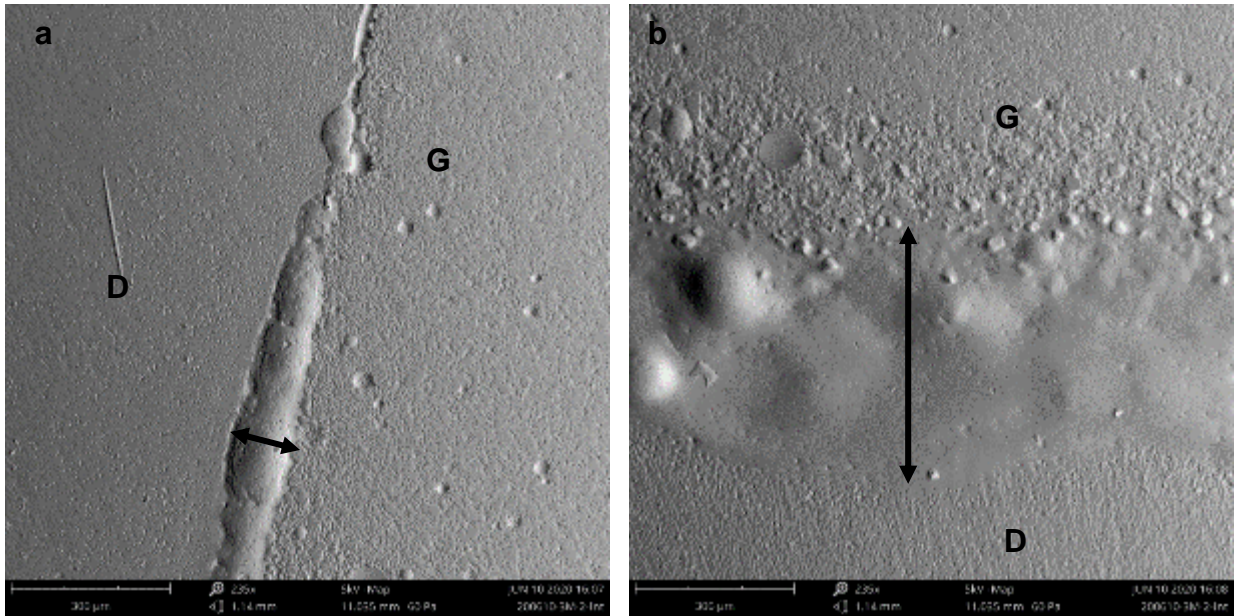
Figure 35 SEM-Topo B detector images of the replica from a 3 months sample show changes (bulge or elevation) at the GIC-dentine interfaces. The width of the change in axial dentine was less (a) than that in the pulpal wall of the cavity (b). This pulpal region corresponded well with images that showed GIC change in the other included techniques. Scale bars= 300 μm.

In a 3 months dehydrated tissue sample, the remnant of the layer was scarcely seen at the GIC-tooth interfaces. In 6 month samples, the interface exhibited a layer-like structure, which had the same color as in 18 month samples but shifted from the GIC-tooth interfaces to the sides. It might be that the sol-gel phase of GIC maturation was not hard enough and it shifted during the setting or dehydration processes that followed the impression process. In 18 months dried samples, the layer was partially there at the GIC-tooth interfaces. It resembled the images seen in CLSM (Fig. 18) and SEM (Fig. 22.c), where the layer might experience tension forces that ruptured it. The color of this layer remnant was darker than the GIC and brighter than the dentine (Fig. 36).

The width of the IIL ranged between 30-100±50 μm in this study, since the remnants of the IIL on the real tissue samples showed a thick diameter of the IIL at the interface, mainly in the GIC-dentine part (~150 μm) when compared to the GIC-enamel interface (~100 μm), as in Figure 36.c, whereas the IIL diameter in the replicas ranged from 30-100 μm, with dentine displaying a thicker IIL than the enamel. It was also discerned that the IIL became wider in thickness, starting from the EDJ toward the pulpal cavity (Fig. 33.c).
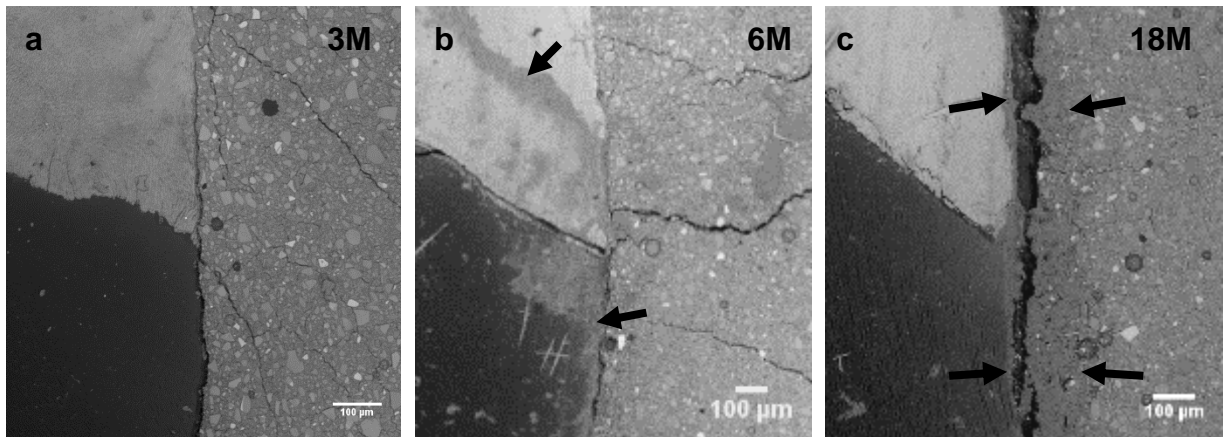
Figure 36 SEM-backscattered images of the tissue samples, from which replicas were made, and dehydrated for GIC-tooth interface analysis after 3 months (a), 6 months (b) and 18 months (c). Notice the IIL remnants (arrow) spread on the sample surface in (b), whereas they remained at the interface region, on the GIC and on the tooth substrate surfaces in (c), which appears as a broken or ruptured layer. Scale bars= 100 μm.

4 Discussion

The present work highlights the main findings typical of GIC in contact with enamel and dentine, and explores the changes observed over time using multiple 2D and 3D material characterization techniques. When freshly mixed GIC is applied to dentine discs and is immediately removed, the ability of GIC to erode the hard tissue surface within seconds is observed. This is important as it forms the basis for adhesion of GIC. Self-etching has been an attribute of GIC from the onset and it has a crucial role in increasing mechanical interlocking (57). Overall, the present study shows clearly that GIC exhibits excellent and durable bonding to tooth structure, as both enamel and dentine rarely showed detachment at the GIC-tooth substrate interfaces. A curious, often overlooked observation within the GIC porosity was the frequent presence of spherical bodies, located inside voids close to the GIC-dentine interface. Overwhelmingly, water-storage led to observable changes in the outer 300 μm of GIC, both internally in dentinal GIC, and externally in outer GIC restoration. Further changes were seen in the axial dentine walls of the cavity. Within a few weeks following application, and always increasing with time (up to 18 months), GIC exchanges ions with the tooth substrates. In many cases, interaction interphase layers (IILs) appeared at the interface with tooth substrates. The following sections survey the different observations and their consequences.

4.1 Time-evolving changes observed in GIC

This work highlights a dynamic of GIC restorations, whereby the density and chemical composition continuously change over time. Previous studies have examined GIC and its effect on tooth substrates; however few have compared changes in GIC between the occlusal and pulpal zones of the restoration (see recent review 52). The current study clearly showed a marked change of contrast in the outer and dentinal GIC margins. The changes in outer GIC (occlusal regions) are likely to be due to direct contact with the water-based storage medium. A similar change in contrast suggestive of reduced density was observed near the dentinal GIC margins (Figs. 4, 6, 13). Indeed, the permeability of dentine and ionic exchange with the immersion liquid led to leaching of components of the GIC restoration near the dentine. The contrast change of dentinal GIC in this work resembles images published in a previous study (84). Those authors reported that dentinal GIC restoration exhibits lower mechanical properties than inner bulk GIC regions in samples stored wet for 1 year. They postulated that the reduced mechanical properties are associated with material dissolution and diffusion of ions out of GIC. Indeed, the EDX and μCT results of the present study proved that significant components of the GIC leach out.

Interestingly, a previous time-lapse CLSM study offers explanations and observations of the primary reactions of GIC with dentine and enamel (85). Those authors reported the movement of water from dentine into the GIC after setting, which changed the dentinal GIC. The µCT data in the present work (Fig. 6) clearly depict a loss of substance in the GIC, which is a result of slow dissolution. Images presented in a different previous X-ray microtomography study, where authors applied minimal invasive dentistry on carious lesions overlooked the changes clearly observed in images of GIC fillings in contact with the outer environment after 3 weeks of storage in simulated body fluid (86). Overall, water storage of GIC fillings leads to gradients in the outer GIC in contact with the environment.

The current study also found that the density changes of dentinal GIC were higher than those observed on the outer GIC restoration, a finding recurring at all time points. With time, the GIC density at the pulpal side continued to decrease to a point where it appeared completely washed out of large particles, up to 200-400 µm away from the pulpal dentine interface. EDX-quantifications in such regions detected reduced F, Al, Si, Mg and increased Ca and P, when compared to the bulk of GIC following 1 week of immersion. It must therefore be concluded that both GIC and dentine continue to leach ions and that the interaction interzone region is active in terms of chemical reaction for many months (52). Additional proof of this is seen in the sol-gel appearance of the IIL in replicas, suggestive of ongoing chemical activity (Fig. 35).

High activity of the GIC in the pulpal region might have a relation with the permeability of dentine, specifically the density, accessibility and orientation of the dentinal tubules. The tubules near the pulp chamber have a wider diameter than tubules on the axial wall close to the enamel-dentine junction (3). A previous study showed that when tubules are cut, they leave different opening orifices with regions within the same tooth showing significantly different morphologies from each other (87). All these previous works match the findings reported in the current study well, in that change in contrast observed using both 2D and 3D techniques was not found in enamel but was found in dentine. Exposure to water (e.g., though direct contact or through tubules) promotes GIC component dissolution and ion exchange with the environment.

4.1.1 Integrity of GIC-tooth substrate attachment

The present study confirmed the existence of a good GIC-tooth attachment zone (52). Cracks, when present, were mostly seen away from the interface region, appearing as cohesive and mixed failures in the GIC as well as the cohesive failure of enamel (Table 6). Note that no mechanical tests were applied to any samples in this work. Water has an elusive effect: GIC is a hydrophilic

material and stays intact in an 80% relative humidity environment; increases or decreases in humidity lead to changes in the GIC structure, with swelling and disintegration when fully saturated with water, or shrinkage and cracking when dehydrated (52).

Enamel showed an intact continuous attachment with GIC, which occasionally exhibited cohesive cracking. Examination of all time points showed that enamel only failed adhesively once, which was in an 18 months water immersed sample. The attachment between enamel and GIC is reported to be a true ionic reaction (38), which might explain why enamel adheres well to GIC. Cohesive cracks suggest that GIC establishes a good attachment to the tooth substrate because the bonding force is higher than the cohesive strength of GIC. For the product used here, namely Ketac Fil, the strength values are known to be 5MPa with enamel and 2.5MPa with dentine (88, 89). Some studies reported that GIC was not adapted well to enamel (90, 91), unless pretreated with a cavity conditioner, but this was not the case in the present work. Importantly, the results of the present study appear to be as good as previous studies that examined the GIC-enamel attachment region when enamel was pretreated (85, 92, 93). Reportedly, pretreatment of enamel helps to increase GIC adhesion by creating irregularities that increase the surface area for chemical interaction and mechanical interlocking (58). Presumably, this was achieved by the strict protocol used in the current study (see sample preparation section). The GIC-dentine attachment was not as intact and continuous as the attachment with enamel (94). As seen in the Results section, various types of cracks were observed at the GIC-dentine interface. Usually mixed and cohesive cracks were seen, with only a few adhesive failures. The results are presented in Table 6 and show that mixed>cohesive>adhesive failures. This differs from studies which assessed GIC failure modes and found more cohesive failures than mixed and adhesive failures (52). This difference from reports in the literature might be due to the larger size of the regions studied in the current work. Clearly those new findings make it possible to identify more and varied types of cracks.

With increasing water-storage times, adhesive failures were encountered more frequently. At 18 months of immersion, a similar prevalence of adhesive and cohesive failures were noted. This may be due to GIC dissolution, which also explains the changes in GIC filling density. Other authors reported that cohesive failures were twice as frequent as adhesive failures, but only for shorter storage times (52, 95). A possible explanation for the observations of fewer cracks near the adhesion site with the tooth substrate might relate to a protective effect that good bonding may have, specifically between GIC and the substrate. Thus, only with increasing time and further dissolution do adhesive failures play a more dominant role. Dentine showed more cracks than enamel in the SEM (Figs. 20, 21, 22), presumably due to more extensive water loss and consequent

high stresses (96, 97, 98). Thus, the difference between enamel and dentine in structure is a main cause for cracking, regardless of if there is any bonding with GIC. Note also that dentine only has 45 vol% of mineral, as compared with 92% mineral in enamel (Section 1.1), which adheres to GIC through hydrogen bonds. Thus, dentine is less ideal as a substrate when compared to enamel, where adhesion with GIC develops via ionic bonds (94).

Previous studies that used CLSM or cryo-SEM avoiding sample dehydration prior to imaging also did not report any cracks (52). In general, in the present work, wet samples imaged with optical microscopy, as well as non-destructive 3D techniques, exhibited fewer cracks and a more integrated interface between tooth and GIC, when compared with the dehydrated samples studied in the SEM in vacuum.

4.1.2 Porosity of GIC

In addition to cracks, the bulk of GIC exhibits numerous pores. Porosity is defined as the presence of empty spaces inside the bulk, and is occasionally identified as "voids," "air bubbles," or "air inclusions" (52). Porosity weakens GIC, reducing strength and increasing the chances of fracture (52, 99). The present work did not quantify porosity in GIC, however, it appears to be non-uniform, with frequent observations of clusters near the inner filing margins (e.g. in GIC adjacent to dentine, Fig. 6). It often concentrates near the base of the filling, possibly as a consequence of trapped air in the filling placement procedures. Interestingly, there are reports of decreasing pore sizes with storage time (100). Several studies even reported improvement of GIC strength after long storage times suggesting that ongoing GIC setting and chemical activity (99, 101) lead to the formation of spherical bodies that close up some of the porosity. Curiously, such cement maturation may lead to long-term increased GIC compressive strength (102).

In the current study, pores in the GIC-enamel contact zone were always empty, lacking any spherical bodies. This is different from observations in pores near GIC-dentine interfaces, many of which were occupied by spherical bodies. The results in the present work therefore corroborate reports in a previous study (102). Note that spherical bodies are always localized within pores close to the attachment between GIC and water-immersed dentine. There was a difference between the spherical bodies seen in the current study and those reported previously (102). Those same authors reported that the spherical bodies were rich in silicon (Si), an element found in glass (SiO_2), which is one of the main components of GIC cements. The spherical body cores in the present study were not hollow; their cores were filled with material, as seen in Fig. 23. Similar to literature reports, the SEM-EDX results of the present study (Figs. 31, 32) clearly identified spherical bodies

already at 1 week, and with increased prevalence at 3 and 6 months of immersion. It would appear that these spherical bodies are made of a silica phase that has 3 times higher Si concentrations than the GIC matrix. The GIC used in the present work (Ketac Fil) is Sr based, yet surprisingly, the EDX elemental analysis revealed increased Ca in particular in the spherical bodies, when compared with the GIC matrix (Tables 19-21). This suggests that there is significant movement of ions at GIC-dentine interface.

4.2 Changes observed in tooth substrates at the interface with GIC

The contrast within enamel appeared to be rather constant with most 2D and 3D techniques with only phase contrast enhanced synchrotron data revealing a slight change in enamel density in zones in contact with GIC following 18 months of immersion. Clearly, the denser enamel structure, highly loaded with Ca with little organic material (as compared with dentine), makes ionic exchange difficult and slow. This is probably the reason that the lower sensitivity imaging techniques were unable to detect any structural changes in enamel. It is important to note that different ions have different X-ray absorption levels depending on their mass attenuation coefficients, which can be detected by 3D X-ray methods (103). Elements such as Sr and La from the GIC were not detected in enamel, but were detected in dentine (see EDX point analysis). Only EDX was therefore able to show the ongoing chemical reactions that led to the diffusion of ions from the GIC into the enamel tissue - in particular, small quantities of F, Al, Sr and La diffuse up to 200 µm into enamel (Tables 7-14). The displacement of even small quantities of these elements also produces a change in the phase contrast density, as observed by PCE-CT. These findings match previous studies that used EDX to identify an increase of elements from GIC (F, Al and Sr) in the enamel surfaces attached to the cement (104, 105).

A change in contrast and density was much easier to observe by several methods in dentine at the interface with GIC. Interestingly, pulpal dentine was more prone to change than axial dentine, suggesting that the more open tubules play an important role. Changes in density exceeded 200µm from the outer surface (Figs. 13.a, 19.d, 28). The dentine density change might have a relation with dentine location and dentinal tubule direction (3, 87). The density changes near the pulp horns take on a funnel shape that follows the trajectories of the dentinal tubules in native tissue (Fig. 11). This change in contrast, wide at the base of the cavity and narrow at the top of the pulp chamber, was also reported in other studies (86). This suggests that the present experiment mirrors the dynamics that are typical for GIC.

Within 7 days following restoration, dentine exhibited density changes at the interfaces with GIC. The density changes increased with time, reaching the greatest effect following 18 months of water immersion. The density changes were seen by SEM (Fig. 21) and CLSM (Fig. 16) and were also reflected in changes of X-ray attenuation detected by μCT and PCE-CT (Figs. 7, 13-15). EDX mapping however, due to its high noise to signal ratio, requires greater % changes for reliable detection. It is for this reason that EDX was unable to reveal changes in dentine at 1 week of water immersion. We therefore conclude that small changes occur very swiftly in dentine, in the hours and days after placement, and that only a combination of methods was able to detect this at the interface after short exposure times. Etching and demineralization are likely to stimulate and enhance ion diffusion into the tissue. Due to dentine etching/erosion, Ca and P are released into contact with GIC. That is why both Ca and P were elevated at the bottom of GIC restorations in contact with dentine. Elements prevalent in GIC, such as Sr and La, were decreased on the pulpal filling aspect as compared to other regions of the filling. The changes in density of dentine observed in the present work resemble reports in a previous study (106), which combined TEM and EDX to analyze the attachment zone between a modified GIC and dentine. Those authors, however, focused only on the first few μm (<10). In any case, all studies consistently show that Ca and P are high in the first few microns and are reduced in dentine distant to GIC, due to the diffusion of ions from GIC to the dentine surface.

The present study revealed higher elemental changes in pulpal dentine as compared to axial dentine, as observed by EDX, SEM and μCT (Figs. 7, 21.d, 24-28). These results can be compared with a previous X-ray microtomography study that quantified the linear attenuation coefficient (LAC) change (107). Within 3 weeks of liquid immersion, those authors observed remineralization of carious dental lesions that were in contact with GIC. In pulpal dentine, remineralization was higher than in axial dentine, extending from the GIC-dentine interface towards the pulp chamber. In axial dentine only a thin rim of mineralization was observed on different sides of the cavity.

4.3 Observations in the interaction interphase layer (IIL)

Near enamel, there were only faint signs of the formation of an IIL following 3 months or longer hydration immersion times. The IIL lined enamel near the interface region (Fig. 36). A recurring observation was the appearance of a clear ridge, consistently and easily detected in replicas of the GIC-enamel interfaces. For example, at 3 months, direct observations of the tooth showed no IIL (Fig. 36.a), but in the replica, a small elevation of enamel was clearly observed at the interface with GIC (Fig. 34.b). In contrast, the 18 month stored samples all exhibited well-developed IIL in

direct observations, which was also clearly visible as a ridge, elevated above the sample surface in replica topographies, revealing a structure that was higher than adjacent enamel and GIC after acid etching (Fig. 33). Such observations of a structure, probably a gel, which is not directly visible by electron microscopy, correspond well with previous studies - for example, a study of GIC-enamel resistance against acid attacks. Those authors demonstrated that the IIL remained intact when compared to the dissolved surroundings; enamel and GIC were eroded after acid etching (93, 108). Clinically, the IIL and the ions it accumulates near the interface - particularly F (as identified by EDX) - are important for prevention of secondary caries.

Differently to enamel, dentine is far more permeable, easily contributing to the percolation of water, dye and fluorescent materials with diffusion across its interface with GIC. This apparently supports the development of an interaction interphase layer rather swiftly, with the exchange of mobile ions (52). Ion accumulation at the GIC-dentine interface developed into an IIL, which became more evident with time (Figs.16a, 29). In the current study, IIL revealed higher intensity (density) than the neighboring dentine and GIC (Fig. 17). Some researchers evaluated the effects of GIC on dentine by CLSM using fluorescein and rhodamine-B dyes and found an IIL layer at the GIC-dentine interface that was rich in dyes (79). When both the fluorescent and rhodamine-B images were superimposed, it showed a higher fluorescence intensity when compared to the surroundings.

The present work revealed the location of the developed IIL. The tooth samples retained the remnants of the IIL on both sides of the interface including both the tooth substrates and GIC surfaces (Fig. 36). The replica of the same region revealed an intact acid resistant IIL that formed at the same region of IIL remnants in the tissue (Fig. 33). Therefore, the IIL might emerge from the continuous chemical reaction between the GIC and tooth substrates at the interface containing both GIC and dental hard tissue parts. The thickness of the IIL in the current study was 30 to 100µm, examined after 18 months of water storage. However, in recent review (52), the thickness of the IIL was reported to be 1 to 15 µm, which formed after 1-10 days of storage.

5 Outlook and future study directions

µCT studies paved the way to quantify 3D characteristics of GIC down to the micrometer length scale. However the small differences in density between materials and the minute dimensions of the interfaces render the task difficult. PCE-CT using synchrotron radiation facilities provided additional 3D insights using tomographic methods based on edge-enhanced radiography. Such measurements with accentuated interphases may in turn reveal details regarding intact GIC restorations obtained in a clinically relevant setting. Future work with smaller samples with higher magnifications may reveal nanometer domains of interest using those 3D techniques.

SEM is a reliable source for the evaluation of GIC-tooth interface morphologies; however, it is generally destructive and requires dehydration that is likely to change the real structural relations of the samples. Therefore, using complementary techniques where samples can be examined wet, with no dehydration, is recommended. Other options include FIB-SEM and cryo-based TEM where the hydration state of the sample may be preserved.

Most studies in the literature tested only limited time spans, so that stability and dynamic changes are poorly described. New studies mapping material attributes over time, ideally for more than 3 months, are still missing, in particular due to the impressive clinical success of GIC. Also, new methods that protect the GIC from cracking and wearing during sample preparation are needed. To minimize the variability between samples, using bovine teeth might be an option. This would make it possible to prepare multiple samples from the same tooth to be examined at different time points.

One limitation of this study is that only one type of conventional GIC was investigated, whereby each sample served as a control. Another limitation is that the age of extracted teeth was largely unknown. Thus, further studies should focus on different GIC types, matching control groups and balancing type and age of teeth.

5.1 Conclusions

The current in vitro study evaluated the morphological features of GIC, and of untreated tooth substrates including the interface between them, over a 18 month period with different 2D and 3D techniques. The main observations are summarized in the following points:

1. GIC was self-etching and eroded the dentine surface within a few seconds.

2. GIC exhibited cracks of different forms, mostly of a cohesive and mixed nature. Mixed GIC contains pores of different sizes and some of the pores in the vicinity of the GIC-dentine interface become occupied with spherical bodies. SEM-EDX showed that those spherical bodies contained high amounts of silicon.

3. GIC changed dramatically over time in both contrast and density, particularly the dentinal GIC, where the filling comes into contact with pulpal dentine, and at the outer GIC, the occlusal region of the restoration in contact with water. The change observed means that GIC is bioactive material and reacts continuously with its surroundings.

4. GIC-tooth substrate interfaces were intact, and interaction interphase layers (IILs) were formed between the GIC and enamel and dentine at the interface. The IIL represents continuous reactions, diffusion and ion exchange between GIC and tooth substrates.

5. The IIL had a prickled (speckled) appearance, which was seen by CLSM and SEM. However, neither low nor high 3D techniques were able to reliably depict it.

6. Changes in dentine density/composition adjacent to GIC were greater than enamel and they increased over time. Both 2D and 3D techniques were capable of detecting the dentine changes, whereas the effects in enamel were detected only by EDX and PCE-CT using synchrotron radiation.

Therefore, the first hypothesis can be rejected as this work shows the reactivity of GIC with tooth substrates over time, but mostly with dentine rather than enamel, whereas the second hypothesis is totally accepted, as this in vitro study approves the added value of combined 2D and 3D material characterization methods to study clinically important restorative materials such as GIC in contact with enamel and dentine in both hydrated and non-hydrated situations.

6 References

1 Sakaguchi RL, Powers JM. Craig's restorative dental materials. St. Louis, Mo.: Elsevier/Mosby; 2012.

2 Berkovitz BKB, Holland GR, Moxham BJ, Berkovitz BKB. Oral anatomy, embryology and histology. Edinburgh; New York: Mosby;2002.

3 Avery JK, Chiego DJ. Essentials of oral histology and embryology : a clinical approach. St. Louis; London: Mosby; 2006.

4 Berkovitz BKB, Moxham BJ, Linden RWA, Sloan AJ. Master Dentistry Volume 3 Oral Biology : Oral Anatomy, Histology, Physiology and Biochemistry. Elsevier Health Sciences; 2010.

5 Elderton RJ. The dentition and dental care. Oxford: Heinemann Medical Books; 1990.

6 Ferguson DB, Shuttleworth A, Whittaker DK. Oral bioscience. Churchill Livingstone Edinburgh; 1999.

7 Dorozhkin S. Calcium orthophosphates. Journal of Materials Science. 2007;42(4):1061-95.

8 An B, Wang R, Zhang D. Role of crystal arrangement on the mechanical performance of enamel. Acta biomaterialia. 2012;8(10):3784-93.

9 Lussi A. Erosive tooth wear - a multifactorial condition of growing concern and increasing knowledge. Monographs in oral science. 2006;20:1-8.

10 Addy M. Tooth wear and sensitivity : clinical advances in restorative dentistry. 2000.

11 Ratih DN, Palamara JEA, Messer HH. Dentinal fluid flow and cuspal displacement in response to resin composite restorative procedures. DENTAL Dental Materials. 2007;23(11):1405-11.

12 Guyton AC, Hall JE. Textbook of medical physiology. Philadelphia: Elsevier Saunders; 2006.

13 Zaslansky P, Friesem AA, Weiner S. Structure and mechanical properties of the soft zone separating bulk dentin and enamel in crowns of human teeth: Insight into tooth function. J Struct Biol. 2006;153(2):188-99.

14 Wilson AD. Glass-ionomer cement--origins, development and future. Clin Mater. 1991;7(4):275-82.

15 Wilson NH, Mjor IA. The teaching of Class I and Class II direct composite restorations in 20 European dental schools. Journal of dentistry. 2000;28(1):15-21.

16 Peng CF, Yang Y, Zhao YM, Liu H, Xu Z, Zhao DH, Qin M. Long-term treatment outcomes in immature permanent teeth by revascularisation using MTA and GIC as canal-sealing materials: a retrospective study. International journal of paediatric dentistry. 2017;27(6):454-62.

17 Thomas B, Gupta K. In vitro biocompatibility of hydroxyapatite-added GIC: An SEM study using human periodontal ligament fibroblasts. Journal of Esthetic and Restorative Dentistry. 2017;29(6):435-41.

18 Nedeljkovic I, De Munck J, Slomka V, Van Meerbeek B, Teughels W, Van Landuyt KL. Lack of Buffering by Composites Promotes Shift to More Cariogenic Bacteria. Journal of dental research. 2016;95(8):875-81.

19 Pereira JR, da Rosa RA, So MVR, Afonso D, Kuga MC, Honorio HM, do Valle AL, Vidotti HA. Push-out bond strength of fiber posts to root dentin using glass ionomer and resin modified glass ionomer cements. Journal of Applied Oral Science. 2014;22(5):390-6.

20 Lorenzetti CC, Bortolatto JF, Ramos ATPR, Shinohara AL, Saad JRC, Kuga MC. The effectiveness of glass ionomer cement as a fiber post cementation system in endodontically treated teeth. Microscopy research and technique. 2019;82(7):1191-7.

21 Marcusson A, Norevall LI, Persson M. White spot reduction when using glass ionomer cement for bonding in orthodontics: A longitudinal and comparative study. European journal of orthodontics. 1997;19(3):233-42.

22 European C, Directorate General for H, Consumers. The safety of dental amalgam and alternative dental restoration materials for patients and users. 2015.

23 Beauchamp J, Caufield PW, Crall JJ, Donly K, Feigal R, Gooch B, Ismail A, Kohn W, Siegal M, Simonsen R, Frantsve-Hawley J. Evidence-based clinical recommendations for the use of pit-and-fissure sealants - A report of the American Dental Association Council on Scientific Affairs. Journal of the American Dental Association. 2008;139(3):257-68.

24 American Academy of Pediatric Dentistry. Clinical Affairs Committee - Restorative Dentistry S. Guideline on pediatric restorative dentistry. Pediatric dentistry. 2012;34(5).

25 Nicholson JW. Adhesion of glass-ionomer cements to teeth: A review. Int J Adhes Adhes. 2016;69:33-8.

26 Banerjee A, Frencken JE, Schwendicke F, Innes NPT. Contemporary operative caries management: consensus recommendations on minimally invasive caries removal. British dental journal. 2017;223(3):215-22.

27 Tonmukayakul U, Arrow P. Cost-effectiveness analysis of the atraumatic restorative treatment-based approach to managing early childhood caries. Community Dent Oral Epidemiol. 2017;45(1):92-100.

28 Sidhu SK. Glass-Ionomers in Dentistry. Cham: Springer International Publishing; 2016. https://doi.org/10.1007/978-3-319-22626-2

29 Aboush YE, Torabzadeh H. Clinical performance of Class II restorations in which resin composite is laminated over resin-modified glass-ionomer. Operative dentistry. 2000;25(5):367-73.

30 Wilson AD, Nicholson JW. Acid-Base Cements: Their Biomedical and Industrial Applications. 2005. ISBN: 0-521-37222-4r

31 Mount GJ. An atlas of glass-ionomer cements: a clinician's guide. 2003. ISBN 0-203-21545-1

32 Albers HF. Tooth-colored restoratives: principles and techniques. Hamilton, Canada: BC Derek; 2002.

33 Wilson AD, Kent BE. The glass-ionomer cement, a new translucent dental filling material. JCTB Journal of Applied Chemistry and Biotechnology. 1971;21(11):313.

34 Khoroushi M, Keshani F. A review of glass-ionomers: From conventional glass-ionomer to bioactive glass-ionomer. Dental Research Journal. 2013;10(4):411-20.

35 Lin Y, Smedskjaer MM, Mauro JC. Structure, properties, and fabrication of calcium aluminate-based glasses. International Journal of Applied Glass Science. 2019;10(4):488-501.

36 Braden M. Polymeric Dental Materials. 1997. 978-3-642-64450-4

37 Shahid S, Hassan U, Billington RW, Hill RG, Anderson P. Glass ionomer cements: Effect of strontium substitution on esthetics, radiopacity and fluoride release. Dental Materials. 2014;30(3):308-13.

38 Beech DR. A spectroscopic study of the interaction between human tooth enamel and polyacrylic acid (polycarboxylate cement). Archives of Oral Biology Archives of Oral Biology. 1972;17(5):907-11.

39 Fennell B, Hill RG. The influence of poly(acrylic acid) molar mass and concentration on the properties of polyalkenoate cements Part I Compressive strength. JOURNAL OF MATERIALS SCIENCE. 2001;36:5193-202.

40 Sidhu SK, Nicholson JW. A Review of Glass-Ionomer Cements for Clinical Dentistry. Journal of functional biomaterials. 2016;7(3).

41 Stephen C, Alan DW. Reactions in Glass Ionomer Cements: V. Effect of Incorporating Tartaric Acid in the Cement Liquid. Journal of dental research. 1976;55(6):1023-31.

42 Prosser HJ, Richards CP, Wilson AD. NMR spectroscopy of dental materials. II. The role of tartaric acid in glass-ionomer cements. J Biomed Mater Res Journal of Biomedical Materials Research. 1982;16(4):431-45.

43 Stephen C, Alan DW. Reactions in Glass Ionomer Cements: III. The Precipitation Reaction. Journal of dental research. 1974;53(6):1420-4.

44 Crisp S, Wilson AD. Reactions in glass ionomer cements: I. Decomposition of the powder. Journal of dental research. 1974;53(6):1408-13.

45 Barry TI, Clinton DJ, Wilson AD. The structure of a glass-ionomer cement and its relationship to the setting process. Journal of dental research. 1979;58(3):1072-9.

46 Crisp S, Wilson AD. Reactions in glass ionomer cements: III. The precipitation reaction. Journal of dental research. 1974;53(6):1420-4.

47 Mount GJ, Hume WR. Preservation and restoration of tooth structure. 2005.

48 Wasson EA, Nicholson JW. New Aspects of the Setting of Glass-Ionomer Cements. Journal of dental research. 1993;72(2):481-3.

49 Wilson AD, Prosser HJ. Biocompatibility of the glass ionomer cement. J Dent Assoc S Afr. 1982;37(12):872-9.

50 Pires R, Nunes TG, Abrahams I, Hawkes GE, Morais CM, Fernandez C. Stray-field imaging and multinuclear magnetic resonance spectroscopy studies on the setting of a commercial glass-ionomer cement. J Mater Sci Mater Med. 2004;15(3):201-8.

51 Almuhaiza M. Glass-ionomer Cements in Restorative Dentistry: A Critical Appraisal. The journal of contemporary dental practice. 2016;17(4):331-6.

52 Mustafa HA, Soares AP, Paris S, Elhennawy K, Zaslansky P. The forgotten merits of GIC restorations: a systematic review. Clinical oral investigations. 2020;24(7):2189-201.

53 Ullah R, Zafar MS. Oral and dental delivery of fluoride: A review. Fluoride. 2015;48(3):195-204.

54 Seppä L, Korhonen A, Nuutinen A. Inhibitory effect on S. mutans by fluoride-treated conventional and resin-reinforced glass ionomer cements. European journal of oral sciences. 1995;103(3):182-5.

55 Davidson CL, Mjör IA. Advances in Glass-Ionomer Cements: Quintessence Publishing Co, Inc; 1999.

56 Ellis J, Jackson AM, Scott BP, Wilson AD. Adhesion of carboxylate cements to hydroxyapatite. Biomaterials Biomaterials. 1990;11(6):379-84.

57 Lin A, McIntyre NS, Davidson RD. Studies on the adhesion of glass-ionomer cements to dentin. Journal of dental research. 1992;71(11):1836-41.

58 Glasspoole EA, Erickson RL, Davidson CL. Effect of surface treatments on the bond strength of glass ionomers to enamel. Dental materials : official publication of the Academy of Dental Materials. 2002;18(6):454-62.

59 Yoshida Y, Van Meerbeek B, Nakayama Y, Snauwaert J, Hellemans L, Lambrechts P, Vanherle G, Wakasa K. Evidence of chemical bonding at biomaterial-hard tissue interfaces. Journal of dental research. 2000;79(2):709-14.

60 Peumans M, De Munck J, Mine A, Van Meerbeek B. Clinical effectiveness of contemporary adhesives for the restoration of non-carious cervical lesions. A systematic review. Dental materials : official publication of the Academy of Dental Materials. 2014;30(10):1089-103.

61 Schwendicke F, Gostemeyer G, Blunck U, Paris S, Hsu LY, Tu YK. Directly Placed Restorative Materials: Review and Network Meta-analysis. Journal of dental research. 2016;95(6):613-22.

62 Sennou HE, Lebugle AA, Gregoire GL. X-ray photoelectron spectroscopy study of the dentin-glass ionomer cement interface. Dental materials : official publication of the Academy of Dental Materials. 1999;15(4):229-37.

63 Trairatvorakul C, Kladkaew S, Songsiripradabboon S (2008) Active management of incipient caries and choice of materials. J Den t Res 87:228 - 232.

64 Wu YH, Hutton JE, Marshall GW. In vitro enamel demineralization and the marginal gap of simulated cast restorations with three different cements. Journal of prosthodontics: official journal of the American College of Prosthodontists. 1997;6(2):96-103.

65 Lin A, McIntyre NS, Davidson RD. Studies on the adhesion of glass-ionomer cements to dentin. Journal of dental research. 1992;71(11):1836-41.

66 Abdalla AI. Morphological interface between hybrid ionomers and dentin with and without smear-layer removal. Journal of oral rehabilitation. 2000;27(9):808-14.

67 Yip HK, Tay FR, Ngo HC, Smales RJ, Pashley DH. Bonding of contemporary glass ionomer cements to dentin. Dental materials: official publication of the Academy of Dental Materials. 2001;17(5):456-70.

68 Coutinho E, Cardoso MV, De Munck J, Neves AA, Van Landuyt KL, Poitevin A, Peumans M, Lambrechts P, Van Meerbeek B. Bonding effectiveness and interfacial characterization of a nano-filled resin-modified glass-ionomer. Dental materials: official publication of the Academy of Dental Materials. 2009;25(11):1347-57.

69 Sidhu SK, Pilecki P, Sherriff M, Watson TF. Crack closure on rehydration of glass-ionomer materials. European journal of oral sciences. 2004;112(5):465-9.

70 Sauro S, Watson T, Moscardo AP, Luzi A, Feitosa VP, Banerjee A. The effect of dentine pre-treatment using bioglass and/or polyacrylic acid on the interfacial characteristics of resin-modified glass ionomer cements. Journal of dentistry. 2018;73:32-9.

71 Zakizadeh P, Marshall SJ, Hoover CI, Peters OA, Noblett WC, Gansky SA, Goodis HE. A novel approach in assessment of coronal leakage of intraorifice barriers: a saliva leakage and micro-computed tomographic evaluation. Journal of endodontics. 2008;34(7):871-5.

72 Oglakci B, Kazak M, Donmez N, Dalkilic EE, Koymen SS. The use of a liner under different bulk-fill resin composites: 3D GAP formation analysis by x-ray microcomputed tomography. Journal of applied oral science : revista FOB. 2020;28:e20190042.

73 Coutinho E, Yoshida Y, Inoue S, Fukuda R, Snauwaert J, Nakayama Y, De Munck J, Lambrechts P, Suzuki K, Van Meerbeek B. Gel phase formation at resin-modified glass-ionomer/tooth interfaces. Journal of dental research. 2007;86(7):656-61.

74 Falsafi A, Mitra SB, Oxman JD, Ton TT, Bui HT. Mechanisms of setting reactions and interfacial behavior of a nano-filled resin-modified glass ionomer. Dental materials. 2014;30(6):632-43.

75 Ryan AK, Mitchell CA, Orr JF. Fracture mechanics analysis of the dentine-luting cement interface. Proceedings of the Institution of Mechanical Engineers Part H, Journal of engineering in medicine. 2002;216(4):271-6.

76 Gjorgievska E, Nicholson JW, Grcev AT. Ion migration from fluoride-releasing dental restorative materials into dental hard tissues. J Mater Sci-Mater M. 2012;23(7):1811-21.

77 Mitra SB, Lee CY, Bui HT, Tantbirojn D, Rusin RP. Long-term adhesion and mechanism of bonding of a paste-liquid resin-modified glass-ionomer. Dental materials: official publication of the Academy of Dental Materials. 2009;25(4):459-66.

78 Papagiannoulis L, Kakaboura A, Eliades G. In vivo vs in vitro anticariogenic behavior of glass-ionomer and resin composite restorative materials. Dental materials : official publication of the Academy of Dental Materials. 2002;18(8):561-9.

79 Atmeh AR, Chong EZ, Richard G, Festy F, Watson TF. Dentin-cement Interfacial Interaction: Calcium Silicates and Polyalkenoates. Journal of dental research. 2012;91(5):454-9.

80 Toledano M, Osorio R, Osorio E, Cabello I, Toledano-Osorio M, Aguilera FS. In vitro mechanical stimulation facilitates stress dissipation and sealing ability at the conventional glass ionomer cement-dentin interface. Journal of dentistry. 2018;73:61-9.

81 Knight GM, McIntyre JM, Craig GG, Mulyani. Electron probe microanalysis of ion exchange of selected elements between dentine and adhesive restorative materials. Australian dental journal. 2007;52(2):128-32.

82 Knight GM, McIntyre JM, Craig GG, Mulyani, Zilm PS, Gully NJ. An in vitro investigation of marginal dentine caries abutting composite resin and glass ionomer cement restorations. Australian dental journal. 2007;52(3):187-92.

83 Tay FR, Smales RJ, Ngo H, Wei SH, Pashley DH. Effect of different conditioning protocols on adhesion of a GIC to dentin. The journal of adhesive dentistry. 2001;3(2):153-67.

84 Zoergiebel J, Ilie N. An in vitro study on the maturation of conventional glass ionomer cements and their interface to dentin. Acta biomaterialia. 2013;9(12):9529-37.

85 Watson TF, Pagliari D, Sidhu SK, Naasan MA. Confocal microscopic observation of structural changes in glass-ionomer cements and tooth interfaces. Biomaterials. 1998;19(6):581-8.

86 Zain S, Davis GR, Hill R, Anderson P, Baysan A. Mineral exchange within restorative materials following incomplete carious lesion removal using 3D non-destructive XMT subtraction methodology. JJOD Journal of Dentistry. 2020;99.

87 Hariri I, Sadr A, Shimada Y, Tagami J, Sumi Y. Effects of structural orientation of enamel and dentine on light attenuation and local refractive index: an optical coherence tomography study. Journal of dentistry. 2012;40(5):387-96.

88 Watson TF, Billington RW, Williams JA. The interfacial region of the tooth/glass ionomer restoration: a confocal optical microscope study. American journal of dentistry. 1991;4(6):303-10.

89 Pereira LC, Nunes MC, Dibb RG, Powers JM, Roulet JF, Navarro MF. Mechanical properties and bond strength of glass-ionomer cements. The journal of adhesive dentistry. 2002;4(1):73-80.

90 Birkenfeld LH, Schulman A. Enhanced retention of glass-ionomer sealant by enamel etching: a microleakage and scanning electron microscopic study. Quintessence international (Berlin, Germany : 1985). 1999;30(10):712-8.

91 Yilmaz Y, Gurbuz T, Kocogullari ME. The influence of various conditioner agents on the interdiffusion zone and microleakage of a glass Ionomer cement with a high viscosity in primary teeth. Operative dentistry. 2005;30(1):105-12.

92 Hosoya Y, Garcia-Godoy F. Bonding mechanism of Ketac-Molar Aplicap and Fuji IX GP to enamel and dentin. American journal of dentistry. 1998;11(5):235-9.

93 Ngo H, Mount GJ, Peters MC. A study of glass-ionomer cement and its interface with enamel and dentin using a low-temperature, high-resolution scanning electron microscopic technique. Quintessence international (Berlin, Germany : 1985). 1997;28(1):63-9.

94 Perdigão J. Current perspectives on dental adhesion: (1) Dentin adhesion not there yet. Japanese Dental Science Review Japanese Dental Science Review. 2020.

95 Kaup M, Dammann CH, Schafer E, Dammaschke T. Shear bond strength of Biodentine, ProRoot MTA, glass ionomer cement and composite resin on human dentine ex vivo. Head & Face Medicine. 2015;11:14.

96 Shemesh H, Lindtnen T, Portoles CA, Zaslansky P. Dehydration Induces Cracking in Root Dentin Irrespective of Instrumentation: A Two-dimensional and Three-dimensional Study. J Endodont. 2018;44(1):120-5.

97 Forien JB, Fleck C, Cloetens P, Duda G, Fratzl P, Zolotoyabko E, Zaslansky P. Compressive Residual Strains in Mineral Nanoparticles as a Possible Origin of Enhanced Crack Resistance in Human Tooth Dentin. Nano Lett. 2015;15(6):3729-34.

98 Forien JB, Zizak I, Fleck C, Petersen A, Fratzl P, Zolotoyabko E, Zaslansky P. Water-Mediated Collagen and Mineral Nanoparticle Interactions Guide Functional Deformation of Human Tooth Dentin. Chem Mater. 2016;28(10):3416-27.

99 Lohbauer U, Frankenberger R, Krämer N, Petschelt A. Time-dependent strength and fatigue resistance of dental direct restorative materials. Journal of Materials Science: Materials in Medicine Journal of Materials Science: Materials in Medicine. 2003;14(12):1047-53.

100 Benetti AR, Jacobsen J, Lehnhoff B, Momsen NCR, Okhrimenko DV, Telling MTF, Kardjilov N, Strobl M, Seydel T, Manke I, Bordallo HN. How mobile are protons in the structure of dental glass ionomer cements? Sci Rep-Uk. 2015;5.

101 Hill RG. The fracture properties of glass polyalkenoate cements as a function of cement age. JOURNAL OF MATERIALS SCIENCE. 1993;28(14):3851.

102 Yiu CK, Tay FR, King NM, Pashley DH, Sidhu SK, Neo JC, Toledano M. Wong SL. Interaction of glass-ionomer cements with moist dentin. Journal of dental research. 2004;83(4):283-9.

103 Burcu A, Salih ZE. The Mass Attenuation Coefficients, Electronic, Atomic, and Molecular Cross Sections, Effective Atomic Numbers, and Electron Densities for Compounds of Some Biomedically Important Elements at 59.5keV. STNI Science and Technology of Nuclear Installations. 2014;1-8.

104 Kantrong N, Mongkontunpimon W, Supameteeworakul S, Wongkhantee S. Differential induction of surface chemical compositional change on tooth structure by glass ionomer restorative materials. Odontology. 2020.

105 Paiva LFS, Fidalgo TKD, Maia LC. Mineral content of ionomer cements and preventive effect of these cements against white spot lesions around restorations. Brazilian oral research. 2014;28(4):266-74.

106 Tay FR, Sano H, Tagami J, Hashimoto M, Moulding KM, Yiu C, Pashley DH. Ultrastructural study of a glass ionomer-based, all-in-one adhesive. Journal of dentistry. 2001;29(7):489-98.

107 Davis GR, Evershed ANZ, Mills D. Quantitative high contrast X-ray microtomography for dental research. JJOD Journal of Dentistry. 2013;41(5):475-82.

108 Milicich G. A resin impression SEM technique for examining the glass-ionomer cement chemical fusion zone. J Microsc. 2005;217(Pt 1):44-8.

7 Statutory Declaration

"I, **Hawshan Abdulrahman Mustafa**, by personally signing this document in lieu of an oath, hereby affirm that I prepared the submitted dissertation on the topic:'' **Structural characterization of interaction zone between glass ionomer cement and enamel and dentine in human teeth**'', in German ''**Strukturelle Charakterisierung der Wechselwirkungszone zwischen Glasionomer Zement und Schmelz und Dentin in menschlichen Zähnen**'', independently and without the support of third parties, and that I used no other sources and aids than those stated.

All parts, which are based on the publications or presentations of other authors, either in letter or in spirit, are specified as such in accordance with the citing guidelines. The sections on methodology (in particular regarding practical work, laboratory regulations, statistical processing) and results (in particular regarding Figures, charts and tables) are exclusively my responsibility.

Furthermore, I declare that I have correctly marked all of the data, the analyses, and the conclusions generated from data obtained in collaboration with other persons, and that I have correctly marked my own contribution and the contributions of other persons (cf. declaration of contribution). I have correctly marked all texts or parts of texts that were generated in collaboration with other persons.

My contributions to any publications to this dissertation correspond to those stated in the below joint declaration made together with the supervisor. All publications created within the scope of the dissertation comply with the guidelines of the ICMJE (International Committee of Medical Journal Editors; www.icmje.org) on authorship. In addition, I declare that I shall comply with the regulations of Charité – Universitätsmedizin Berlin on ensuring good scientific practice.

I declare that I have not yet submitted this dissertation in identical or similar form to another Faculty.

The significance of this statutory declaration and the consequences of a false statutory declaration under criminal law (Sections 156, 161 of the German Criminal Code) are known to me."

Date   Signature

Declaration of your own contribution to the publications

Hawshan Abdulrahman Mustafa, Ana Prates Soares, Sebastian Paris, Karim Elhennawy, Paul Zaslansky. The forgotten merits of GIC restorations: a systematic review. Clinical oral investigations. 2020;24(7):2189-201. Published 08.06.2020.

Hawshan Abdulrahman Mustafa initiated the paper idea and elaborated the main concepts and design of the publication. He performed the literature search using multiple searching engines and collected the data as (figure 1) in the paper. He was one of the two evaluators that extracted and analyzed the data. The main characteristics analyzed in this systematic review are presented in figure 2 (the schematic), which was drew by Hawshan. The results were collected and summarized in (table 1) in the publication. Hawshan Abdulrahman Mustafa prepared the primary draft of the manuscript independently. The final draft was accepted after serial adjustment and discussion sessions. Afterwards, he personally submitted the final draft of manuscript into the journal. During the submission time, Hawshan Abdulrahman Mustafa prepared all the answers to the reviewer's questions and comments and provided the necessary supplements to the manuscript after agreement from all the co-authors. Finally, the paper was accepted in 8 May 2020 and published in 8 June 2020.

_____

Signature, date and stamp of first supervising university professor / lecturer

_____

Signature of doctoral candidate

8 Curriculum vitae

My curriculum vitae does not appear in the electronic version of my paper for reasons of data protection.

9 Publication list

Papers

Hawshan Abdulrahman Mustafa, Ana Soares, Karim Elhennawy, Paul Zaslansky (**2020**). The forgotten merits of GIC restorations: a systematic review. Clinical Oral Investigations. Impact factor: 2.812

Leona Bauer, **Hawshan Abdulrahman Mustafa**, Paul Zaslansky, Ioanna Mantouvalou (**2020**). Chemical mapping of teeth in 2D and 3D: X-ray fluorescence reveals hidden details in dentine surrounding fillings. Acta Biomaterialia. Impact factor: 6.319.

Katrein Sauer, Alexander Rack, **Hawshan Abdulrahman Mustafa**, Mario Thiele, Ron Shahar, Paul Zaslansky (**2019**). Microstructure and texture contributing to damage resistance of the anosteocytic hinge-bone in the cleithrum of *Esox lucius*. International Journal of Materials Research. Impact factor: 0.851

Poster presentation

Hawshan A. Mustafa, Farah Raja, Tony Worthington, Richard Martin, Delia Brauer (**2017**). Antimicrobial efficacy of strontium and zinc glass ionomer cements against clinically relevant bacteria. 4th Euro BioMAT - European Symposium and Exhibition on Biomaterials and Related Areas, Weimar, Germany.

Xiaohui Chen, **Hawshan A. Mustafa**, David Gillam, Robert Hill (**2014**). SEM Evaluation of Tubular Occluding Properties of Selected Desensitizing Toothpastes. IADR, 92nd General Session, Cape Town, South Africa.

Xiaohui Chen, David Gillam, **Hawshan A. Mustafa**, Robert Hill (**2014**). Dentine Tubule Occlusion of a Novel Self-assembling Peptide Containing Gel. IADR, 92nd General Session, Cape Town, South Africa.

10 Acknowledgments

Thanks to the Almighty GOD for giving me the strength to start and carry out this PhD project.

I would like to express my gratitude towards my supervisors, Professor Sebastian Paris and Dr. Paul Zaslansky, for their continuous guidance, encouragement and help during the entire study.

I would also like to express my deepest appreciation to Dr. Herbert Renz, the technicians for their support during laboratory procedures and all my colleagues who helped me throughout this study.

Special thanks and appreciation to my beloved parents (Ashti and Abdulrahman) and brothers (Dr. Karwan, Dr. Shakhawan, Zrian and Tekoshan) for believing in me and supporting me during these years.

I would sincerely like to thank my scholarship sponsors, The DAAD, for giving me this opportunity to pursue my PhD in Germany and Charité that supported my graduation time.

Last but certainly not least, my wife (Fenk Al-Askari), last couple of years have been challenging, and it would not have been possible to complete this study without your help and patience. Thank you for being by my side. I cannot find words to express my gratefulness for you my darling and a very special thanks is due to our cute and brilliant son (Nali), for giving meaning to our hard life.

11 Statistics certificate

CHARITÉ

CharitéCentrum für Human- und Gesundheitswissenschaften

Charité | Campus Charité Mitte | 10117 Berlin

Institut für Biometrie und Klinische Epidemiologie (iBikE)

Direktor: Prof. Dr. Frank Konietschke

Postantschrift:
Charitéplatz 1 | 10117 Berlin
Besucheranschrift:
Reinhardtstr. 58 | 10117 Berlin

Surame, Name: Mustafa, Hawshan

Email: hawshan.mustafa@charite.de

Immatriculation Number: 9172101

Thesis Advisor: Dr. Paul Zaslansky

Institution / Clinic: CC03 - Centrum für Zahn-, Mund- und

Kieferheilkunde

Tel. +49 (0)30 450 562171
frank.konietschke@charite.de
https://biometrie.charite.de/

iBikE

Certification

I hereby certify that Mr. Hawshan Mustafa has received a statistical consultation on a PhD project with me, within the Service Unit Biometry of the Institute of Biometry and Clinical Epidemiology (iBikE). The following consultation dates were attended:

- Appointment 1: 19.4.2022

The following key advice regarding meaningful analysis and interpretation of data was given during the consultation:

- *The focus should be on the clear descriptive analysis and presentation of the data, where measures of both central tendency (e.g. mean, median) and of dispersion (e.g. standard deviation, interquartile range) should be used.*

- *The applied statistical methods, just as the sample the calculations were based on should be clearly indicated in the Results section, e.g. in tables.*

- *The presentation of data might profit from the use of differences instead of absolute values, e.g. to show trends over time. Moreover this would take the dependencies of the data better into account.*

- *Overall the dependencies between the individual observations have to be taken into account for all applied analyses, as e.g. linear and polynomial regression are both based on the assumption of independent observations.*

This certificate does not guarantee the correct implementation of the suggestions made in the consultation, the correct performance of the recommended statistical procedures, nor the correct presentation and interpretation of the results. The responsibility for this rests solely with the doctoral student. The Institute of Biometry and Clinical Epidemiology assumes no liability for this.

Date: 19.4.2022

Name of consultant: Annette Aigner, PhD